Targeting Cancer Stem Cells in Mucoepidermoid Carcinoma

By

April Adams

A dissertation submitted in partial fulfillment
of the requirements for the degree of
Doctor of Philosophy
(Cancer Biology)
in the University of Michigan
2016

Doctoral Committee:

Professor Jacques E. Nör, Chair
Professor Maria G. Castro
Professor Peter Polverini
Professor Stephen J. Weiss
Professor Max S. Wicha

ACKNOWLEDGEMENTS

My profound gratitude and many thanks to my advisor, Dr. Jacques E. Nör, for his constant support, guidance, and extraordinary mentorship.

My gratitude to the members of my dissertation committee: Dr. Maria Castro, Dr. Peter Polverini, Dr. Stephen Weiss, and Dr. Max Wicha, for sacrificing time and energy to intellectually direct and guide my work.

Thank you to the many members of the Nör laboratory for their continual support, expertise, encouragement, and guidance. A special thank you to Dr. Kristy Warner who supported and contributed significantly to my research.

Thank you to the University of Michigan Flow Cytometry Core staff and director for their technical expertise and patience in analyzing and sorting my samples.

Thank you to the University of Michigan School of Dentistry Histology Core for effectively processing my tissue samples.

A special thank you to the University of Michigan Cancer Center clinicians and patients who graciously donated tissue to our laboratory.

Thank you to Dr. Shaomeng Wang for letting us use his drug, MI-773, to study in salivary gland mucoepidermoid carcinoma.

This work was supported by funding R01DE021139 and P50 - CA - 97248 from the NIH.

Finally, a special thanks to my family for their love and support.

PREFACE

A version of CHAPTER II, Salivary gland cancer stem cells, was accepted for publication in Oral Oncology and was published online June 28, 2013. The authors are as follows: April Adams, Kristy Warner, Jacques E. Nör.

A version of CHAPTER III, “ALDH/CD44 identifies uniquely tumorigenic cancer stem cells in salivary gland mucoepidermoid carcinomas”, is accepted in Oncotarget and was published online September 22, 2015. The list of authors is as follows: April Adams, Kristy Warner, Alexander T. Pearson, Zhaocheng Zhang, Hong Sun Kim, Daiki Mochizuki, Gregory Basura, Joseph Helman, Andrea Mantesso, Rogério M. Castilho, Max S. Wicha, Jacques E. Nör.

A version of CHAPER IV, “Therapeutic ablation of cancer stem cells by MDM2 inhibition in salivary gland mucoepidermoid carcinoma”, will be submitted to Cancer Research. The list of authors is as follows: April Adams, Kristy Warner, Felipè Nör, Christie Rodriguez Ramirez, Zhaocheng Zhang, Sam Kerk, Gregory J. Basura, Joseph Helman, Shaomeng Wang, Jacques E. Nör.

TABLE OF CONTENTS

LIST OF TABLES

CHAPTER III

LIST OF FIGURES

CHAPTER II

CHAPTER III

CHAPTER IV

ABSTRACT

Salivary gland mucoepidermoid carcinoma is rare but causes significant morbidity in patients who are diagnosed. Slow, persistent growth as well as resistance to chemotherapy treatment has greatly hindered the response of these tumors to conventional therapies. Emerging research has identified a population of highly tumorigenic cells, termed cancer stem cells, which possess stem cell-like properties of multipotency, self-renewal, and unique tumorigenic potential compared to non-cancer stem cells. Importantly, cancer stem cells have been shown to be resistant to chemotherapy and radiation therapies. Selective targeting of stem cell associated pathways could prevent therapy resistance.

Here, we investigated the presence of cancer stem cell markers ALDH, CD44, CD24, and CD10 and the tumorigenic potential of human mucoepidermoid carcinoma (HMC) cells sorted for these stem cell markers in *in-vitro* salisphere formation and *in-vivo* xenograft growth models. FACS-sorted $ALDH^{high}CD44^{high}$ cells preferentially formed salispheres in primary and secondary ultra-low attachment, serum-free culture compared to $ALDH^{low}CD44^{low}$ cells suggesting that $ALDH^{high}CD44^{high}$ cells are capable of self-renewal. Importantly, $ALDH^{high}CD44^{high}$ sorted cells consistently formed primary and secondary tumors compared to $ALDH^{low}CD44^{low}$ cells when implanted *in-vivo*, each tumor replicating the original ALDH/CD44 sub-populations suggesting that $ALDH^{high}CD44^{high}$ cells are capable of tumorigenicity and multipotency. Together, these

results suggest that $ALDH^{high}CD44^{high}$ cells identify a population of uniquely tumorigenic cancer stem cells.

In an effort to identify a therapeutic to target the $ALDH^{high}CD44^{high}$ cells, we used the MDM2/p53 small molecule inhibitor, MI-773, and treated human mucoepidermoid carcinoma cells using low doses of the drug. We found a significant reduction of $ALDH^{high}CD44^{high}$ cells *in-vitro* as well as *in-vivo*. Importantly, we also noted an increase in p21 expression and decrease in Bmi-1 expression suggesting that accumulation of p53 in the cell by inhibiting MDM2 greatly affects self-renewal and differentiation associated protein. Treatment of human mucoepidermoid carcinoma cells with MI-773 also induced apoptosis and cell-cycle arrest both *in-vitro* and *in-vivo*. Together, these results demonstrate the presence of highly tumorigenic cancer stem cells in salivary gland mucoepidermoid carcinoma. Further, we propose the use of MDM2 inhibitors in the selective ablation of cancer stem cells as a therapeutic target for the treatment of salivary gland mucoepidermoid carcinomas.

CHAPTER I

Introduction

Salivary gland cancer is rare, accounting for approximately 2-6.5% of all head and neck cancers, with 3,300 new cases each year (1-3). The most common form of salivary gland cancer, mucoepidermoid carcinoma (MEC), represents about 30-35% of all malignant salivary gland tumors (3-10). Treatment of mucoepidermoid carcinomas consists of surgical resection, radiation treatment, and neck dissection. While effective for lower grade tumors, conventional treatments for high-grade or recurrent tumors are often ineffective leading to significant facial disfigurement and morbidity. Importantly, mucoepidermoid carcinomas are resistant to conventional chemotherapy, thereby limiting treatment options for patients with advanced disease.

Increased understanding of the pathobiology of mucoepidermoid carcinomas has been limited by the lack of cell line and xenograft models. Previous work published in our laboratory by Warner and colleagues unveiled the generation of stable human mucoepidermoid carcinoma (HMC) cells lines capable of forming tumors in immunodeficient (SCID) mice (11). One of the three cell lines, UM-HMC-1, was generated from a stage IVa, intermediate grade tumor taken from the minor salivary gland of the buccal mucosa of the patient. The other two cell lines, UM-HMC-3A and UM-HMC-3B, were generated from a patient with a stage IVb, intermediate grade tumor. The UM-HMC-3A cells were generated from a recurrent tumor found in the left hard palate while the UM-HMC-3B cells were generated from the lymph node

metastasis in the same patient. Importantly, all three cells lines have been genotyped as well as passaged up to 100 times *in-vitro* and are capable of forming tumors *in-vivo*. With appropriate models and resources to begin research on salivary gland mucoepidermoid carcinomas, we first sought to learn how mucoepidermoid carcinoma tumors are generated and maintained as well as identify targetable pathways associated with cancer aggressiveness.

Emerging research has identified the presence of a population of cells termed, cancer stem cells, that display stem cell-like properties. Interestingly, cancer stem cells display unique tumorigenicity as well as an ability to self-renew and differentiate into non-cancer stem cells (further elaboration of salivary gland cancers and the properties of cancer stem cells is provided in Chapter II). Cancer stem cells are frequently isolated using FACS sorting for surface or enzymatic markers such as ALDH, CD44, and CD24. Importantly, studies have shown that cancer stem cells defined by these specific marker combinations are resistant to conventional chemotherapy and radiation treatments due to slower proliferation rates and expression of transporter proteins (12-18). Survival of cancer stem cells following treatment allows for reconstitution and recurrence of the tumor leading to disease relapse and patient morbidity. While the identification and isolation of cancer stem cells have been found to be critical in correctly treating many cancer types, cancer stem cells have not been identified or isolated in salivary gland mucoepidermoid carcinomas.

Due to the resistance of cancer stem cells (CSCs) to conventional treatment, much research has been dedicated to the identification of cancer stem cell-targeted therapies with the hypothesis that combined chemotherapy and CSC-targeted therapies

will eliminate all cells from the tumor and prevent tumor recurrence and disease relapse. Drugs targeting the Notch, Wnt, Hedgehog, IL-6, and PI3K/AKT pathways have been investigated for therapeutic effectiveness against cancer stem cells in several different cancer types, however, the efficiency of these drugs is often limiting by the lack of specificity towards the targeted pathway (19-22). One pathway that has yet to be investigated in the context of cancer stem cell function is that of the tumor suppressor protein, p53. While much research has focused on the role of p53 in cell cycle regulation and the induction of apoptosis, research in induced-pluripotent stem (iPS) cells also identified p53 as a key player in embryonic stem cell function. Several studies reported that by knock down or reducing the levels of p53 within the cell that the efficiency of reprogramming differentiated cells to iPS cells was greatly enhanced (23-27). In the context of cancer, researchers also found that elimination of p53 leads to the expansion of malignant progenitor cells and the development of mixed lineage tumors (28).

p53 is predominately regulated by mouse double minute 2 (MDM2) which functions as a E3 ubiquitin ligase marking p53 for degradation, can also bind p53 blocking its transactivation domain. MDM2 is frequently overexpressed in cancer and serves as an oncogene in many cancers due to its function in inhibiting p53. Ideally, inhibition of MDM2 binding to p53 in the cancer cell would prevent the blockage and degradation of p53 thereby releasing it into the cell to induce cell cycle arrest and apoptosis. Many small molecule inhibitors have been developed to interrupt MDM2/p53 binding, however, lack of specificity or ineffective clinical translatability are significant challenges to targeting this interaction (29-33). MI-773, developed in Dr. Shaomeng

Wang's laboratory at the University of Michigan, shows enhanced binding specificity when compared to the p53 and MDM2 inhibitor gold standard, Nutlin-3a (34). In several cancer types, MI-773 was effective in inducing apoptosis and drastically reducing tumor volume. Importantly, MI-773 was effective in cell with both wild-type and mutant p53 (35). As p53 plays an important role in stem cell biology, the potential role of p53 activation as a consequence of MDM2 inhibition in the ablation of cancer stem cells is an intriguing question. Considering salivary gland cancers frequently contain wild-type p53, MDM2 inhibition is an interesting therapeutic to study in this cancer type (36-40). However, no research has been done studying MDM2 inhibitors in the context of salivary gland cancer or more specifically, in the context of salivary gland cancer stem cell biology.

The central hypothesis of this work is that a subpopulation of highly tumorigenic cancer stem cells defines the pathobiology of salivary gland mucoepidermoid carcinomas. To address our hypothesis, this project seeks to both define the role of cancer stem cell in the initiation of mucoepidermoid carcinoma and to determine the therapeutic efficacy of MDM2 inhibition via MI-773 on cancer stem cell function in salivary gland mucoepidermoid carcinoma.

References

1. Speight PM, Barrett AW. Salivary gland tumors. Oral Dis 2002;8:229–40.

2. Spiro RH. Salivary neoplasms: overview of a 35-year experience with 2807 patients. Head Neck Surg 1986;8:177–84.

3. Gillespie MB, Albergotti WG, Eisele DW. Recurrent salivary gland cancer. Curr Treat Options Oncol 2012;13:58–70.

4. Eversole LR, Sabes WR, Rovin S. Aggressive growth and neoplastic potential of odontogenic cysts: with special reference to central epidermoid and mucoepidermoid carcinomas. Cancer 1975;35:270–82.

5. Ezsias A, Sugar AW, Milling MA, Ashley KF. Central mucoepidermoid carcinoma in a child. J Oral Maxillofac Surg 1994;52:512–5.

6. Ellis GL, Auclair PL. Tumors of the salivary glands—Atlas of tumor pathology. In: Fascicle 17 Washington: Armed Forces Institute of, Pathology; 1996.

7. Gingell JC, Beckerman T, Levy BA, Snider LA. Central mucoepidermoid carcinoma. Review of the literature and report of a case associated with an apical periodontal cyst. Oral Surg Oral Med Oral Pathol 1984;57:436–40.

8. Ito FA, Ito K, Vargas PA, de Almeida OP, Lopes MA. Salivary gland tumors in a brazilian population: a retrospective study of 496 cases. Int J Oral Maxillofac Surg 2005;34:533–6.

9. Luna MA. Salivary mucoepidermoid carcinoma: revisited. Adv Anat Pathol 2006;13:293–307.

10. Pires FR, de Almeida OP, de Araujo VC, Kolawski LP. Prognostic factors in head and neck mucoepidermoid carcinoma. Arch Otolaryngol Head Neck Surg 2004;130:174–80.

11. Warner KA, Adams A, Bernardi L, Nor C, Finkel KA, Zhang Z, et al. Characterization of tumorigenic cell lines from the recurrence and lymph node metastasis of a human salivary mucoepidermoid carcinoma. Oral Oncol 2013;49:1059-1066.

12. Cheng L, Ramesh AV, Flesken-Nikitin A, Choi J, Nikitin AY. Mouse models for cancer stem cell research. Toxicol Pathol 2010;38:62–71.

13. Dontu G, Abdallah WM, Foley JM, Jackson KW, Clarke MF. Kawamura, et al. In vitro propagation and transcriptional profiling of human mam- mary stem/ progenitor cells. Genes Dev 2003;17:1253–70.
14. Reynolds BA, Weiss S. Clonal and population analyses demonstrate that an EGF-responsive mamma- lian embryonic CNS precursor is a stem cell. Dev Biol 1996;175:1–13.

15. Diehn M, Cho RW, Clarke MF. Therapeutic implications of the cancer stem cell hypothesis. Semin Radiat Oncol 2009;19:78–86.

16. Diehn M, Cho RW, Lobo NA, Kalisky T, Dorie MJ, Kulp AN, et al. Association of reactive oxygen species levels and radioresistance in cancer stem cells. Nature 2009;458:780–3.

17. Hambardzumyan D, Squatrito M, Holland EC. Radiation resistance and stem- like cells in brain tumors. Cancer Cell 2006;10:454–6.

18. Shafee N, Smith CR, Wei S, Kim Y, Mills GB, Hortobagyi, et al. Cancer stem cells contribute to cisplatin resistance in Brca1/p53-mediated mouse mammary tumors. Cancer Res 2008;68:3243–50.

19. Takabe N, Harris PJ, Warren RQ, Ivy SP. Targeting cancer stem cells by inhibiting Wnt, Notch, and Hedgehog pathways. Nat Rev Clin Oncol 2011;8:97-106.

20. Krishnamurthy S, Warner KA, Dong Z, Imai A, Nör C, Ward BB, et al. Endothelial interleukin-6 de nes the tumorigenic potential of primary human cancer stem cells. Stem Cells 2014;32:2845-57.

21. Li X, Lewis MT, Huang J, Gutierrez C, Osborne CK, Wu MF, et al. Intrinsic resistance of tumorigenic breast cancer cells to chemotherapy. J Natl Cancer Inst 2008;100:672-9.

22. Kolev VN, Wright QG, Vidal CM, Ring JE, Shapiro IM, Ricono J, et al. PI3K/mTOR dual inhibitor VS-5584 preferentially targets cancer stem cells. Cancer Res 2015 ;75:446-55.

23. Marión RM, Strati K, Li H, Murga M, Blanco R, Ortega S, et al. A p53-mediated DNA damage response limits reprogramming to ensure iPS cell genomic integrity. Nature 2009;460:1149-53.

24. Hong H, Takahashi K, Ichisaka T, Aoi T, Kanagawa O, Nakagawa M et al. Suppression of induced pluripotent stem cell generation by thep53-p21 pathway. Nature 2009;460:1132-5.

25. Utikal J, Polo JM, Stadtfeld M, Maherali N, Kulalert W, Walsh RM, et al. Immortalization eliminates a roadblock during cellular reprogramming into iPS cells. Nature 2009;460:1145-8.

26. Li H, Collado M, Villasante A, Strati K, Ortega S, Cañamero M, et al. The Ink4/Arf locus is a barrier for iPS cell reprogramming. Nature 2009;460:1136-9.
27. Kawamura T, Suzuki J, Wang YV, Menendez S, Morera LB, Raya A, et al. Linking the p53 tumour suppressor pathway to somatic cell reprogramming. Nature 2009;460:1140-4.

28. Tschaharganeh DF, Xue W, Calvisi DF, Evert M, Michurina TV, Dow LE, et al. p53-dependent Nestin regulation links tumor suppression to cellular plasticity in liver cancer. Cell 2014;158:579-92.

29. Vassilev LT, Vu BT, Graves B, Carvajal D, Podlaski F, Filipovic Z, et al. In vivo activation of the p53 pathway by small-molecule antagonists of MDM2. Science 2004;303:844–8.

30. Shangary S, Qin D, McEachern D, Liu M, Miller RS, Qiu S, et al. Temporal activation of p53 by a specific MDM2 inhibitor is selectively toxic to tumors and leads to complete tumor growth inhibition. Proc Natl Acad Sci U S A 2008;105:3933–8.

31. Vassilev LT. p53 Activation by small molecules: application in oncology. J Med Chem 2005;48:4491–9.

32. Vassilev LT. MDM2 inhibitors for cancer therapy. Trends Mol Med 2007;13:23–31.

33. Carry JC, Garcia-Echeverria C. Inhibitors of the p53/hdm2 protein-protein interaction- Path to the clinic. Bioorg Med Chem Letters 2013; 23:2480–5.

34. Wang S, Sun W, Zhao Y, McEachern D, Meaux I, Barrière C, et al. SAR405838: an optimized inhibitor of MDM2-p53 interaction that induces complete and durable tumor regression. Cancer Res 2014;74:5855-65.

35. Hoffman-Luca CG, Yang CY, Lu J, Ziazadeh D, McEachern D, Debussche L, et al. Significant Differences in the Development of Acquired Resistance to the MDM2 Inhibitor SAR405838 between In Vitro and In Vivo Drug Treatment. PLoS One 2015;10:e0128807.

36. Gomes CC, Diniz MG, Orsine LA, Duarte AP, Fonseca-Silva T, Conn BI, et al. Assessment of TP53 mutations in benign and malignant salivary gland neoplasms. PLoS One 2012;7:e41261.

37. Augello C, Gregorio V, Bazan V, Cammareri P, Agnese V, Cascio S, et al. TP53 and p16INK4A, but not H-KI-Ras, are involved in tumorigenesis and progression of pleomorphic adenomas. J Cell Physiol 2006;207: 654–9.

38. Kishi M, Nakamura M, Nishimine M, Ikuta M, Kirita T, Konishi N. Genetic and epigenetic alteration profiles for multiple genes in salivary gland carcinomas. Oral Oncol 2005;41:161–9.

39. Kiyoshima T, Shima K, Kobayashi I, Matsuo K, Okamura K, Komatsu S, et al. Expression of p53 tumor suppressor gene in adenoid cystic and mucoepidermoid carcinomas of the salivary glands. Oral Oncol 2001;37:315–22.

40. Weber A, Langhanki L, Schutz A, Gerstner A, Bootz F, Wittekind C, et al. Expression profiles of p53, p63, and p73 in benign salivary gland tumors. Virchows Arch 2002;441:428–36.

CHAPTER II

Salivary Gland Cancer Stem Cells

Abstract

Emerging evidence suggests the existence of a tumorigenic population of cancer cells that demonstrate stem cell-like properties such as self-renewal and multipotency. These cells, termed cancer stem cells (CSC), are able to both initiate and maintain tumor formation and progression. Studies have shown that CSC are resistant to traditional chemotherapy treatments preventing complete eradication of the tumor cell population. Following treatment, CSC are able to re-initiate tumor growth leading to patient relapse. Salivary gland cancers are relatively rare but constitute a highly significant public health issue due to the lack of effective treatments. In particular, patients with mucoepidermoid carcinoma or adenoid cystic carcinoma, the two most common salivary malignancies, have poor long-term survival rates due to the lack of response to current therapies. Considering the role of CSC in resistance to therapy in other tumor types, it is possible that this unique sub-population of cells is involved in resistance of salivary gland tumors to treatment. Characterization of CSC can lead to better understanding of the pathobiology of salivary gland malignancies as well as to the development of more effective therapies. Here, we make a brief overview of the state-of-the-science in salivary gland cancer, and discuss possible implications of the cancer stem cell hypothesis to the treatment of salivary gland malignancies.

Introduction

Salivary gland cancer is a relatively rare yet deadly disease. On average, 3,300 new cases are diagnosed every year in the USA. Due to limited mechanistic understanding of the disease and lack of effective regimens for chemotherapy, surgery is still the main treatment option of these patients. As a consequence, treatment for these tumor is generally accompanied by significant morbidity and debilitating facial disfigurement. Malignant tumors are generally fatal. This is reflected in the 5-year survival rate that drops drastically from 78% for stage I tumors to 25%, 21%, and 23% for stages II-IV, respectively (1). Of much concern is the fact that the survival of patients has not improved over the last 3 decades, which is in contrast with the significant improvement in survival observed in other glandular tumors. Such data suggest that focused research efforts on the understanding of the pathobiology of these tumors could lead to significant improvements in patient survival and quality of life.

Mounting evidence supports the existence of a sub-population of tumorigenic cells that possess stem cell-like characteristics in many tumor types (*e.g.* breast cancer, pancreatic cancer, head and neck squamous cell carcinomas). These cells, termed cancer stem cells (CSC), are capable of self-renewal and also to differentiate into cells that constitute the bulk of the tumor. Cancer stem cells are resilient cells that play a major role in resistance to chemotherapy and radiation therapy in other cancer types (2-4). While such studies are unveiling the mechanisms of resistance to therapy in other malignancies, very little is known about the resistance of salivary gland tumors. Indeed, one of the most pressing clinical issues in salivary gland cancer is the poor response to therapy (5). It is certainly possible that low proliferation rates contribute to resistance to

therapy in a group of salivary gland tumors but another possibility is that cancer stem cells play a role in the resistance to therapy observed in these tumors. Characterization of stem cells in these tumors might lead to the identification of novel pathways that could be targeted to sensitize these tumors to chemotherapy.

Salivary Gland Structure and Function

Salivary glands play an essential role in protection and maintenance of health in the oral cavity, lubrication of food, taste of food, and speech. Saliva is produced in secretory cells called acini. There are three different types of acini and each is characterized by the composition of the cell secretions. Serous cells release saliva that is abundant in several proteins but lacks mucin protein. Mucous cells secrete saliva-containing mucin proteins (6). Seromucous cells secrete a combination of both mucous and serous saliva. Once the saliva is secreted from these cells, it is transported through intercalated ducts, small excretory ducts, and then through a larger excretory duct that opens into the mouth (6). Excretory ducts are lined with columnar epithelium, cuboidal cells surround the intercalated ducts, and columnar cells make up the striated duct. As the saliva passes through these ducts, additional proteins, such as Immunoglobulin A and lysozyme, from the ductal cells are secreted into the saliva. Myoepithelial cells contract and help secretory cells release the saliva while promoting salivary flow through the ducts.

Salivary glands are subdivided into the major and minor glands. The major salivary glands consist of three pairs of glands that are located around the oral cavity. The largest are the parotid glands that are located in directly below the ears along the jaw. Saliva is exported from the gland directly across from the crowns of the second

maxillary molars via Stensen's duct, a 5 cm duct connecting the gland to the oral cavity. Secretions from the parotid glands are exclusively serous. The sublingual gland is located underneath the floor of the mouth and are the smallest of the major salivary glands. These glands open to the oral cavity via 8-20 excretory ducts and secrete only mucous saliva (6). The submandibular glands are also located in the floor of the month but are adjacent to the mandibular bone. Saliva is secreted via the Warthon's duct that opens into the floor of the mouth. This gland secrets seromucous saliva but contains a higher percentage of serous acini then mucous acini. The oral cavity also contains 600-1,000 minor salivary glands that can be found on the tongue, inside of the cheek, lips, floor of the mouth, and the hard palate (6). Secretions from these glands are predominately mucous with the exception of von Ebner's glands, which are exclusively serous.

Salivary Gland Cancer

Salivary gland cancers are rare accounting for 2-6.5% of all head and neck cancers with annual incidence of 2.2-3.0 cases per 100,000 people in the United States (7-9). Tumors can originate in either the major or minor salivary glands. Approximately 80% of these tumors arise in the parotid gland, 15% arise in the submandibular gland, and 5% arise in the minor and sublingual salivary glands (10). Males have a 51% higher rate of incidence over females, although both tend to develop the cancer within the fifth decade of life (11). While little is known about the pathogenesis of salivary gland cancers, research has shown that radiation exposure is a risk factor and suggests that occupation exposures, viruses, UV light, alcohol, and tobacco may also be involved (12-14). As much as 75% of salivary masses are benign. However, presentation of both

malignant and benign tumors is similar making diagnosis and treatment very challenging. Malignant salivary gland tumors are markedly heterogeneous including 24 histologic subtypes, generating significant challenges in diagnosis, prognosis, and treatment (9). The following discussion is centered on mucoepidermoid carcinomas and adenoid cystic carcinomas (Figure II.1), the two most common salivary gland malignancies.

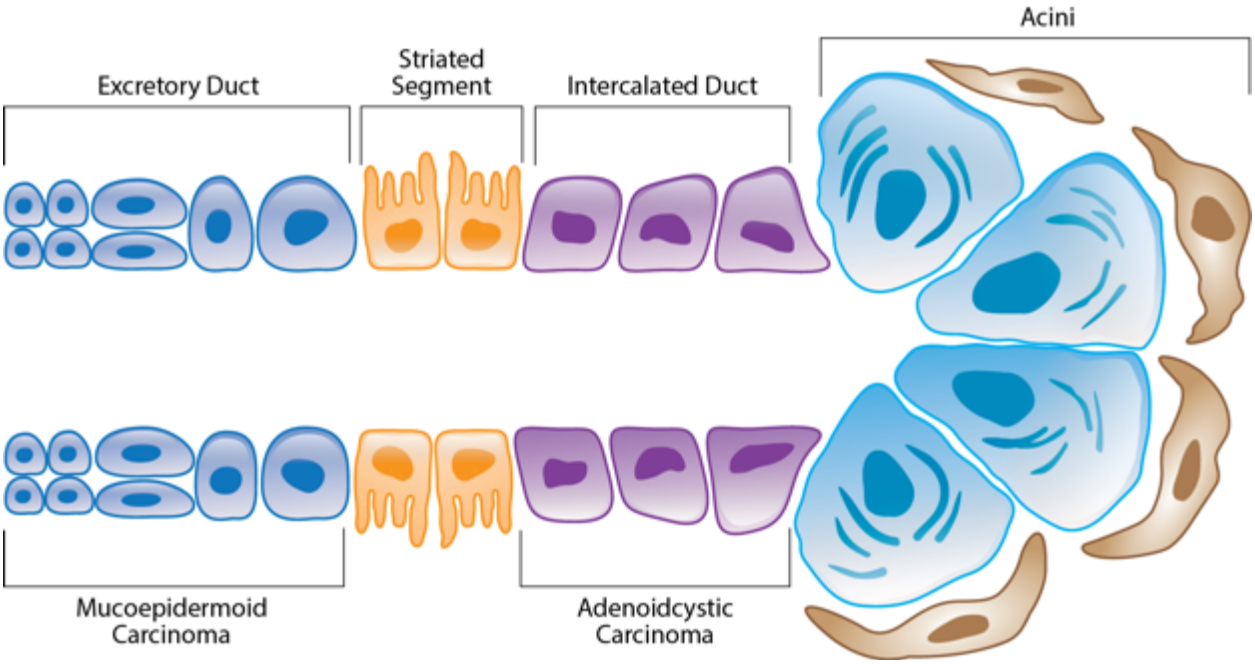

Figure II.1. Schematic representation of a salivary gland indicating putative areas of origin for mucoepidermoid carcinomas and adenoid cystic carcinomas. Adapted by authors from Bell et al. Salivary gland cancers: biology and molecular targets for therapy. Curr Oncol Rep 2012;14(2):166–174.

Mucoepidermoid Carcinoma

Mucoepidermoid carcinoma (MEC) is the most common salivary gland malignancy and represents approximately 5-15% of all salivary gland tumors and 30-35% of all malignant salivary gland tumors (8,15-21). These tumors occur in both the major and minor salivary gland glands and are mostly comprised of epidermoid, mucous, and intermediate cells types. The epidermoid cells are polygonal in shape and

characterized by keratinization and intercellular bridges. Mucous cells very in size but all stain positively for mucin proteins. Intermediate cells are thought to functions as progenitor cells for epidermoid and mucous cells and are often basal-like in appearance. Mucoepidermoid carcinomas also contain a variety of other cell types including squamous, clear, columnar, and other uncommon cell types (22-28). They are extralobular tumors and are believed to originate in the excretory duct (22,24).

Diagnosis of mucoepidermoid carcinoma is based on the presence of both, histological and cytogenetic abnormalities. These tumors are categorized into three grades depending on the amount of cyst formation, the degree of cytological mutation, and the relative number of epidermoid, mucous, and intermediate cell types. Low-grade tumors tend to have a minimal amount of cytological mutation, a high population of mucous cell, and noticeable cyst formation. High-grade tumors contain large areas of intermediate and squamous cells that demonstrate increased mitotic activity. Intermediate-grade tumors manifest a combination of both low and high-grade characteristics. Additional unfavorable histologic factors include perineural invasion, necrosis, increased mitotic rate, angiolymphatic invasion, anaplasia, infiltrative growth pattern, and the presence of a cystic component (27) However, this grading system is often variable making reproducibility difficult (28). Low and intermediate-grade tumors are treated using surgical resection while treatment for high-grade tumors includes neck dissection and radiation therapy (27). While surgical removal and radiation is often successful, a significant number of patients have a recurrence of the disease years later (29). For these patients, few treatments options are available as mucoepidermoid carcinomas are highly chemo-resistant (12). As a result, chemotherapy is used for

patient palliation, although ineffective for actual treatment (30). Improved understanding of the pathobiology of the disease leading to rationally designed targeted therapies are necessary to improve the outcome of patients with mucoepidermoid carcinoma.

The most common cytogenetic abnormality in mucoepidermoid carcinoma is a recurrent translocation between chromosomes 11 and 19 creating the CRTC1-MAML2 fusion protein. This translocation is found in 38-81% of mucoepidermoid carcinomas and is expressed in all cell types. CREB-regulated transcription coactivator 1 (CRTC1) protein activates transcription mediated by cAMP response element-binding (CREB) protein (26,31). CREB activated genes regulate cell differentiation and proliferation (32). Abnormal expression of these genes has been shown to lead to cancer development (32). MAML2 is a coactivator for Notch transcriptional activity that regulates cellular differentiation and proliferation (32-33). In the fusion protein, the intracellular Notch-binding domain of MAML2 is replaced by the CREB binding domain of CRTC1 (12).

Many studies have shown that presence of CRTC-MAML2 translocation has prognostic and diagnostic value (12). Patients with tumors expressing CRTC1-MAML2 have a greater overall survival as well as a lower risk of recurrence and metastasis when compared with fusion-negative tumors (34-35). However, there is a subset of high-grade tumors that express CRTC1-MAML2. Studies by Anzick and colleagues found that in these high-grade tumors expressing CRTC1-MAML2 and additional deletion or hypermethylation of CDKN2A was often found suggesting that the presence or absence of both of these abnormalities may serve as a better diagnostic marker (36). The role this chimeric protein plays in the pathogenesis of mucoepidermoid carcinoma is not known, however, research suggests that this mutation occurs early on during

tumor initiation (12,27). Studies have shown that this translocation also appears in a subset of Warthin's tumors and may be linked to the development of these tumors to malignant MEC tumors(34-35, 37).

Adenoid Cystic Carcinoma

Adenoid cystic carcinoma (ACC) is the second most common malignant salivary gland cancer accounting for 10-25% of patients (37-40). Tumors can occur in both parotid and submandibular glands as well as the minor salivary glands but are believed to arise from the intercalated duct reserve cells found in each of these glands (22,41). Adenoid cystic carcinoma is histologically a biphasic cancer indicating that it is composed of both epithelial and myoepithelial cells (22, 42-43). Although growth of these tumors is slow, the long-term prognosis of these patients is poor. The 5-year survival rates are very favorable at 70-90% (39). However, the 15 and 20-year survival rates are rather poor at 35-40% and 10% respectively (39-40, 43). Patients with distant metastasis have a 5-year survival rate as low as 20% (38). Overall low survival is primarily due to the persistence of tumor growth, late recurrence after initial treatment, perineural invasion, hematogenous spread and invasion to distant and neighboring tissues (44-47).

Diagnosis and determination of tumor grade is based solely on the predominance of one of three histologic growth patterns. The cribriform pattern is easily characterized as having numerous pseudocysts giving a "Swiss cheese" like appearance. These pseudocysts are mostly made of myoepithelial cells. Ductal areas within this pattern are composed of basophilic mucoid material. Tumor cells are cuboidal in shape and are small in size. The tubular pattern has similar shaped tumors cells, however, they

constitute small ducts in this case. The inside of these ducts is lined with both basal myoepithelial cells and luminal ductal cells. Tumors containing a solid growth pattern demonstrate large islands of tumors cells with no appearance of cysts of tubules. These areas have higher rates of mitosis, necrosis, and variability in cellular shape. Predominance of tubular and cribriform growth patterns is associated with less aggressive progression and overall longer survival time (27, 40, 43). Tumors consisting of >30% solid pattern have the highest grading, and are associated with increased aggressiveness and lower survival (43). Though regional metastasis is rare, solid tumors have a greater likelihood of metastasizing to the lymph nodes (43). Biomarkers of epithelial to mesenchymal transition (EMT) such as Snail1 and Slug have also emerged as being associated with increased tumor aggressiveness and may be useful in diagnosing adenoid cystic carcinoma (39,40). As all grades are considered aggressive, all ACC patients are treated with surgery and radiation (43). Chemotherapy treatment has low response rate. However, improved understanding of the biology of adenoid cystic carcinomas is leading to clinical trials using targeted therapies known to work in other cancer types (43).

The most common cytological abnormality is a translocation between chromosomes 6 and 9 resulting in the MYB-NFIB fusion protein (48). This translocation occurs in 33-100% of primary ACC samples and expression is not correlated with aggressiveness or grade(31, 48-49). Human nuclear factor 1 (NFI) transcription factor contains domains that enable dimerization and DNA-binding. MYB is a transcription factor that regulates genes involved in proliferation, differentiation, and apoptosis. The t(6;9) translocation typically results in loss of exon 15 in the MYB protein, a site shown

to bind micro-RNAs, which in turn negatively regulate expression of MYB (48). This leads to overexpression of the fusion protein and overexpression of MYB-induced genes, which are involved in cell cycle control, angiogenesis, and apoptosis (48).

Recent work has shown that c-Kit and epidermal growth factor (EGF) tyrosine kinase receptors are also over expressed in adenoid cystic carcinoma (50-55). Although it is uncertain the exact mechanism by which overexpression of c-Kit influences cancer growth and progression, it has been suggested that it may influence various genetic and epigenetic processes. EGFR overexpression is commonly found in cancer and promotes cancer development through inhibition of apoptosis and stimulation of angiogenesis (10). Imatinib methylate has been successfully used to inhibit tyrosine kinase receptors in other cancers such as chronic myelogenous leukemia and gastrointestinal stromal tumors (56-58). However, little or no response has been observed in adenoid cystic carcinoma (59). Further studies in c-Kit and EGFR may have uncovered the reason for this lack of response. Work by the Bell laboratory demonstrated that expression of c-Kit is found in the inner ductal cells but negative in the myoepithelial cells. Interestingly, the myoepithelial cells showed strong expression of EGFR while the ductal cells showed very little expression. This difference in expression between cell types could lead to complex patterns of drug response. Further research will be necessary to determine the full therapeutic potential of these targets (27).

Cancer Stem Cell Hypothesis

The cancer stem cell hypothesis states that tumors are initiated and maintained by a subpopulation of tumorigenic cells capable of continuous self-renewal and

differentiation. The idea that stem cells could initiate cancer progression was first suggested over 150 years ago (60-61). However, evidence supporting this hypothesis was not shown until Lapidot and colleagues identified a population of stem-like acute myeloid leukemic cells with enhanced ability to engraft non-obese diabetic severe combined immune-deficient (NOD/SCID) mice (62). Implantation of these CD34+CD38- stem cells effectively recapitulated patient tumors whereas CD34+CD38+ and CD34- cells showed no such ability. Using limiting dilution assays, they showed that approximately 1 in 250,000 cells is a stem cell that can initiate leukemia. This ability was sustained in serial transplantation into secondary mice. The Clarke laboratory further validated this hypothesis in solid tumors. Implantation of CD44+/CD24-Lin- breast cancer cells into NOD/SCID mice also accurately reproduced the original primary tumor heterogeneity using as few as 100 cells (63). Isolation using aldehyde dehydrogenase 1 (ALDH1) activity further enriched this cancer stem cell population (64). Cancer stem cells have since been identified in pancreatic, brain, ovarian, colorectal, head and neck, and liver cancer (65-96).

Further characterization of cancer stem cells has identified several properties commonly seen in normal tissue stem cells. Both normal and cancer stem cells are able to undergo self-renewal through asymmetric cell divisions, demonstrate multi-lineage differentiation, show active expression of telomerase as well as increased expression of membrane transporter proteins, and upregulation of anti-apoptotic pathways (97-100). While normal and cancer stem cells share common characteristics, the term cancer stem cell does not necessarily refer to the cell of origin. Currently there are two hypotheses that describe the role of CSC in cancer development (Figure II.2). The

original hypothesis states that the first oncogenic hit occurs in normal adult stem cells that are then able to differentiate into neoplastic cells. Additional mutations occur as the differentiated stem cells divide to form the bulk tumor. An alternative hypothesis states that normal differentiated cells, called tumor-initiating cells (T-IC), undergo oncogenic mutation and acquire stem cell-like properties enabling them to differentiate and self-renew. These cells are then able to differentiate into the bulk tumor cells. However, work by the Weinberg laboratory suggests that this differentiation is reversible (101). Upon depletion of the tumor-initiating cells population, differentiated cells are able to de-differentiate via epithelial to mesenchymal transition (EMT) pathway (102).

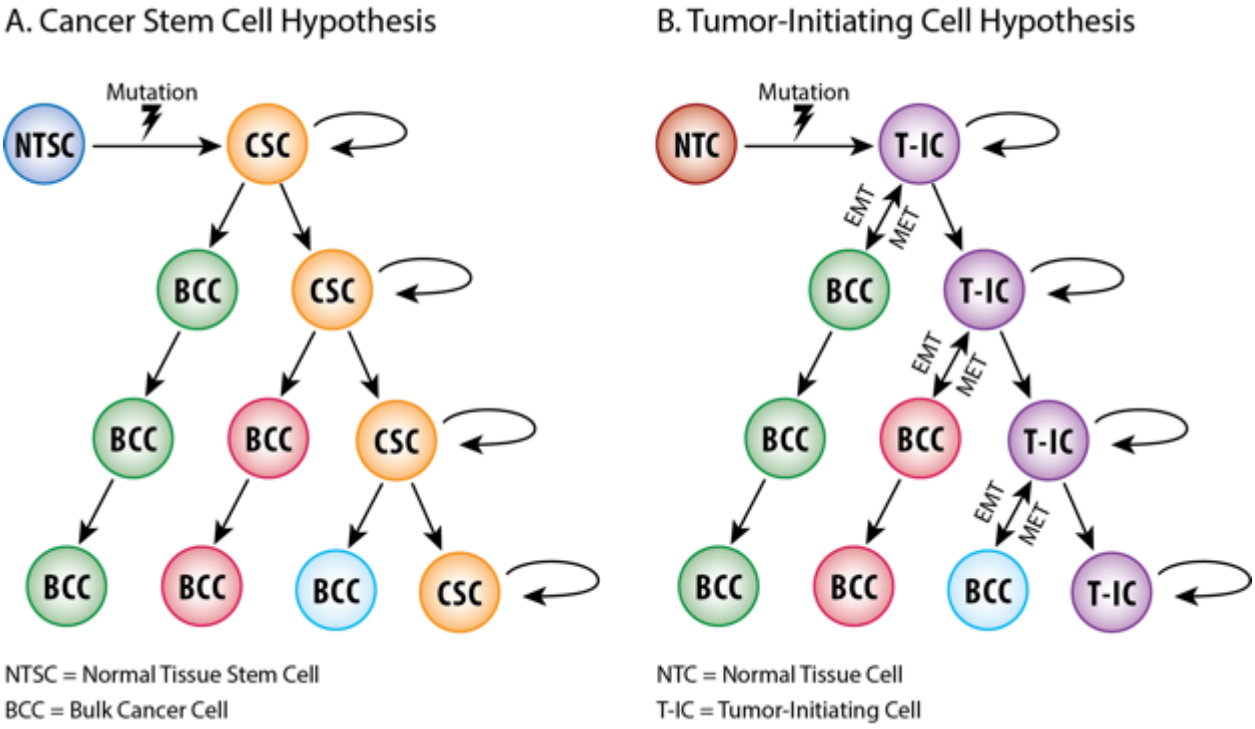

Figure II.2. Schematic representation of two prevailing hypotheses for tumorigenesis, i.e. the cancer stem cell hypothesis and the tumor-initiating cell hypothesis. Adapted by authors from Reya et al. Stem cells, cancer, and cancer stem cells. Nature 2001;414(6859):105–111.

In addition to tumor initiation, cancer stem cells play an important role in tumor relapse and resistance to chemotherapy. Several studies have shown that this

population of cells is resistant to traditional chemotherapeutic and radiation treatments (3-4, 103-106). For example, studies have shown that pancreatic cancer stem cells are enriched after treatment with gemcitabine and play a major role in tumor growth and metastasis (65, 107). Survival and enrichment of these stem cells allows for re-initiation of tumor growth resulting in patient relapse. Cancer stem cell survival can be attributed to several unique attributes. These cells are typically in G_0 making them relatively quiescent and endowing them with resistance to chemotherapeutic agents that act in a cell cycle-dependent manner (108). Studies have also shown that cancer stem cells upregulate DNA damage repair proteins, anti-apoptotic proteins, and transporter proteins such as ABCG2 (109-115). For such reasons, the cancer stem cells hypothesis is intriguing in the context of salivary gland tumors, which are not responsive to chemotherapy treatments. Further understanding of pathways involved in cancer stem cell resistance could lead to development of treatments that target this subpopulation of cells thereby sensitizing salivary gland tumors to therapies that eliminate the bulk tumor population.

Emerging research also suggests that the stem cell niche and surrounding microenvironment enables cancer stem cells to survive chemo and radiation treatments as well as to sustain self-renewal and progression of the cancer. The concept of a stem cell niche was first suggested by the Morrison laboratory and is defined as a tissue microenvironment that is capable of taking up and maintaining the function of stem cells (116). A substantial amount of evidence suggests that surrounding cells in the microenvironment are capable of signaling and promoting cancer growth via immune and stromal cell signaling (117). Work by several groups suggests that signaling from

the microenvironment specifically acts to maintain and promote survival and self-renewal of the CSC in the stem cell niche. Macrophages play a critical role in the onset of inflammation and the recruitment of other immune cells. These cells have also been shown to activate epithelial cells via NF-kB signaling, increase expression of genes associated with pluripotency thereby maintaining undifferentiated state of the cancer, and increase microvasculature production providing tumors with essential nutrients (118-121). Endothelial cells have also been shown to play a similar role in the tumor microenvironment. Studies in head and neck cancer have shown that cancer stem cell survival and self-renewal is increased when exposed to the growth factor milieu secreted adjacent endothelial cells (93). Fibroblasts have also been shown to be an important component of the microenvironment that helps maintain cancer stem cells. Under normal conditions, fibroblasts function to promote wound healing. In cancer, however, tumor-associated fibroblasts promote both invasion and angiogenesis as well as secrete factors that promote stemness of cancer stem cells (122). Development of targeted therapies that disrupt the microenvironment in these stem cells niches could inhibit survival and self-renewal properties of cancer stem cells.

Head and Neck Cancer Stem Cells

Increasing evidence indicates that the cancer stem cells play an important role in the pathogenesis and progression of head and neck squamous cell carcinomas (HNSCC). While novel treatments have improved the quality of life of patients diagnosed with this cancer, overall survival rates have remained largely unchanged in the last few decades, particularly in patients with advanced disease (123-125). Distant metastasis, loco-regional disease recurrence, and lack of response to chemotherapy

are the primary challenges facing these patients (126-130). As cancer stem cells have been implicated in each of these same challenges, further understanding of the biology of these cells in the context of HNSCC could lead to targeted treatments that benefit patients.

Cancer stem cells were first isolated in HNSCC by Prince and colleagues in 2007 (88). In these experiments, cells sorted for CD44 expression showed increased tumorigenicity over the cells that lacked CD44 expression. When implanted in NOD/SCID mice, $CD44^{high}$ cells were able to form tumors in 20 out of 31 injections whereas the $CD44^{low}$ population only formed 1 tumor out of 40 total injections. Tumors generated from $CD44^{high}$ cells were phenotypically diverse for CD44 expression indicating that $CD44^{high}$ cells are able to both differentiate in to $CD44^{low}$ cells but also self-renew into $CD44^{high}$ cells. Gene expression analysis of $CD44^{high}$ and CD44- populations showed that $CD44^{high}$ cells highly expressed Bmi-1 while $CD44^{low}$ cells showed no detectable expression of this protein suggesting that CD44 marker enriches for cells with stem cell-like properties. However, mice injected with fewer then 5×10^3 were unable to form tumors indicating that this marker alone may enrich for cancer stem cells but not necessarily be sufficient to isolate a pure population of these cells.

Later experiments by Clay et al suggest that aldehyde dehydrogenase (ALDH), a marker first used in breast cancer, expression may further enrich a cancer stem cell population in HNSCC cells (64, 131). ALDH expression was low accounting for about 1.0-7.8% of the total cell population. $ALDH^{high}$ populations were highly tumorigenic forming tumors in 7 out of 15 injections with as few as 50-100 cells, and are able to replicate the original tumor heterogeneity. Krishnamurthy and colleagues later showed

that the combined expression of ALDH and CD44 further enhanced the ability to identify the cancer stem cell population (93). Using 1,000 $ALDH^{high}CD44^{high}$ cells, tumors were formed in 13 out 15 injections while only 3 out of 15 tumors were generated when 10,000 $ALDH^{low}CD44^{low}$ cells were injected (93).

Further characterization of the microenvironment surrounding head and neck cancer stem cells suggests the existence of a perivascular niche that supports stem cell maintenance and resistance to anoikis (93). They observed that approximately 80% of $ALDH^{high}$ cells are located within 100-μm radius of neighboring blood vessels. This area was identified as the perivascular niche as it was calculated to be the area of diffusion of oxygen and nutrients from the blood vessels. Exposure to endothelial-cell secreted factors enhanced the expression of ALDH, CD44, and stemness marker Bmi-1, as well as a 3-fold increase in the number of orospheres in low attachment conditions suggesting that endothelial cells play an important role in stem cell self-renewal. Ablation of endothelial cells via an artificial caspase-based death switch drastically decreased the $ALDH^{high}CD44^{high}$ positive population. Later experiments indicated that endothelial cell regulation of cancer stem cells is in part mediated by IL-6 (93). Although not as potent as full endothelial cell-conditioned media, treatment with rhIL-6 increased *in vitro* orosphere formation and the tumorigenic potential of cancer stem cells (unpublished observations).

Studies by Campos and colleagues found that upon induction by anchorage and serum starvation, cancer stem cells exposed to endothelial cell-conditioned media were more resistant to anoikis (132). This occurred via the PI-3/Akt pathway that is known to regulate proliferation and cell survival. Endothelial cell-conditioned media induces

phosphorylation of Akt. Blocking VEGF decreased Akt phosphorylation. Together, these studies provide evidence of a microenvironment that is capable of supporting and maintaining the cancer stem cell population. Targeting the crosstalk between cancer stem cells and other cells of their supportive niche may provide an effective way to abrogate the tumorigenic function of these cells.

Salivary Gland Cancer Stem Cells

The cancer stem cell hypothesis has yet to be fully explored in salivary gland tumors. However, initial experiments by Sun and colleagues indicate that ALDH isolates cancer stem cells in adenoid cystic carcinomas (133). Using a patient derived xenograft model, serially diluted $ALDH^{high}$ and $ALDH^{low}$ cells were injected into NOD/SCID mice. Under these conditions, 24 out of 60 injections of 100-1,000 $ALDH^{high}$ cells were able to form tumors. Notably, injection of as few as 50 $ALDH^{high}$ cells was able to generate a tumor. No tumors were observed in $ALDH^{low}$ injected mice at similar dilutions of cells. In total, 56/122 injections of $ALDH^{high}$ cells formed tumors were only 5/126 injections of $ALDH^{low}$ cells were able to form tumors. $ALDH^{high}$ cells also showed an increased ability to form spheres when plated in low-attachment plates as well as increased invasion in a Matrigel-coated Boyden chamber. $ALDH^{high}$ cells infected with luciferase vectors showed increased ability to metastasize when compared to $ALDH^{low}$ cells. Collectively, these data suggest that ALDH may indeed isolate a more tumorigenic population of cells.

Zhou and colleagues further characterized the expression of ALDH in adenoid cystic carcinomas (134). Immunohistochemical analysis of ALDH expression in human tumors indicated three staining patterns. Approximately 63% of patient's samples

showed staining only in the stromal cells, 26% had neither stromal nor epithelial staining, and 11% had both epithelial and stromal staining. Normal salivary gland showed staining for ALDH only in epithelial cells. However, these different patterns had no correlation to tumor size, perineural invasion, or overall survival. Additional experiments are needed to further verify ALDH as a cancer stem cell marker in adenoid cystic carcinoma. Studies by Fujita and colleagues found overlapping populations of CD44 and CD133 markers in adenoid cystic carcinomas. However, whether or not these markers isolate and more tumorigenic population of cells has yet to be testing in sphere or *in vivo* models (135).

As previously discussed, EGFR is commonly upregulated in adenoid cystic carcinoma tumors (10). Research in other cancer types has demonstrated the role of EGF signaling in the self-renewal of CSC suggesting this pathway may also play a role in the self-renewal of CSC in adenoid cystic carcinoma. A clinical trial in breast cancer determined that treatment with lapatinib, an EGFR/HER2 inhibitor, substantially reduced the $CD44^{high}/CD24^{low}$ stem cell population (136). In the same study, the authors showed that lapatinib decreased mammosphere formation *in vitro* (136). Korkaya and colleagues further confirmed these results (137). They showed that HER2 signaling significantly increased the Aldefluor stem cell population of normal mammary epithelial cells (NMECs) and increased mammosphere formation. Interestingly, HER2 positive but Aldefluor negative cells were unable to form mammospheres. Notably, this concept was also confirmed in head and neck squamous cell carcinoma models (138). HNSCC cells lines transfected with EGFRvIII demonstrated increased proliferation, decreased sensitivity to cisplatin treatment, and increased the $CD44^{high}$ population. The role of

EGFR in adenoid cystic carcinoma CSC has yet to be investigated but may be important for understanding the self-renewal and tumorigenicity of these cells.

In addition to EGFR, c-kit (CD117) is also commonly upregulated in adenoid cystic carcinoma (50-55). Interestingly, c-kit tyrosine receptor kinase binds stem cell factor (SCF) to trigger pathways involved in the maintenance of progenitor cells (139). Interestingly, this cell surface receptor is commonly used to isolate progenitor cells in submandibular glands (140). Expression of c-kit in these sample overlaps with expression of other commonly knows stem cell markers, (*e.g.* Nanog, Oct3/4), suggesting it plays an important role in the maintenance of stem cell properties (143). As a marker of stem cells in normal salivary gland, c-kit could also be a potential marker for CSC in adenoid cystic carcinoma as well. Studying the role of this protein in the context of CSC could provide useful insight into the isolation and regulation of these cells.

Unpublished work for our group also suggests the presence of CSC in mucoepidermoid carcinoma. Using the mucoepidermoid carcinoma cells lines that our laboratory has generated, we are able to generate orospheres (Figure III.3). These structures, first characterized in head and neck squamous cell carcinoma CSC, exploit the fact that stem cells possess anchorage independent growth (141-143). By culturing these cells in low attachment and serum free conditions, we are able to generate orospheres in unsorted cells suggesting that these cell lines do indeed contain a unique stem cell population. Cells cultured in 10% FBS were unable to form spheres and demonstrated lower viability in low attachment compared to cells cultured under serum-free conditions, suggesting that we have indeed isolated a stem cell-like population.

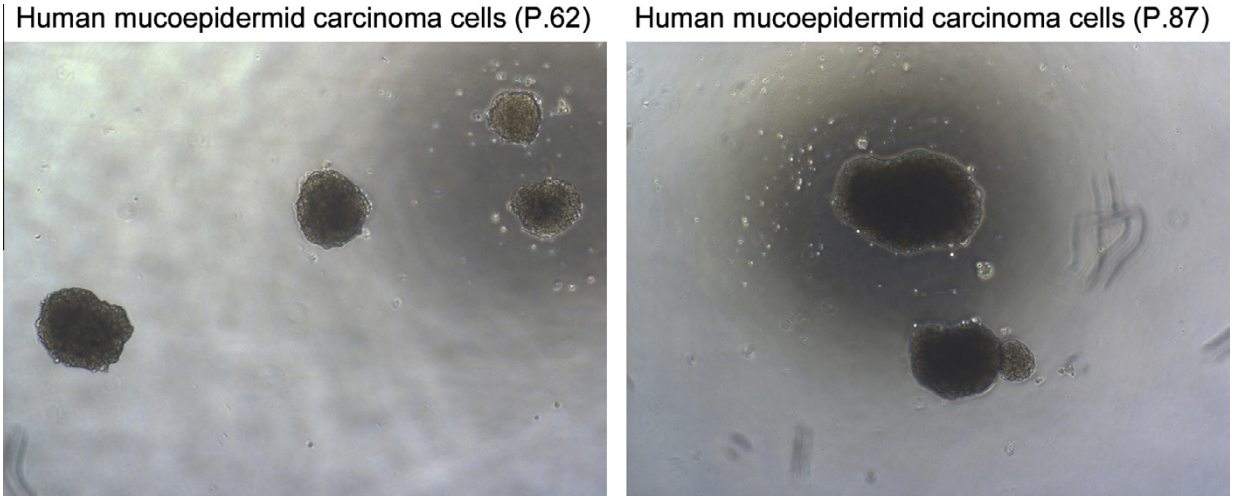

Figure III.3. Photomicrographs of spheres formed by mucoepidermoid carcinoma cells at passage 62 or 87 cultured in ultra-low attachment plates indicating the existence of cells exhibiting stem-like behavior in this cell line.

Conclusions

The most pressing clinical challenges in treatment of salivary gland cancers are tumor resistance to chemotherapy and the lack of targeted treatments that are safe and effective in these tumors. While surgery and radiation treatment successfully cure a subset of these patients, many present recurrent and/or metastatic disease several years later leading to significant morbidity. Cancer stem cells have been shown to be resistant to chemotherapy and radiation treatments leading to tumor relapse. These cells are also implicated in the progression and development of metastasis. It is possible that cancer stem cells are involved in the processes that result in the late recurrence or metastases that are frequently observed in patients with salivary malignancies. Therefore, selective targeting of this rare sub-population of tumorigenic cancer stem cells could inhibit tumor recurrence and metastasis, and improve patient survival and quality of life.

REFERENCES

1. Luukkaa H, Klemi P, Leivo I, Koivunen P, Laranne J, Mäkitie A, et al. Salivary gland cancer in Finland 1991--96: an evaluation of 237 cases. Acta Otolaryngol 2005;125:207-14.

2. Ailles LE, Weissman IL. Cancer stem cells in solid tumors. Curr Opin Biotechnol 2007;18:460-6.

3. Diehn M, Cho RW, Clarke MF. Therapeutic implications of the cancer stem cell hypothesis. Semin Radiat Oncol 2009;19:78-86.

4. Diehn M, Cho RW, Lobo NA, Kalisky T, Dorie MJ, Kulp AN, et al. Association of reactive oxygen species levels and radioresistance in cancer stem cells. Nature 2009;458:780-3.

5. Laurie SA, Licitra L. Systemic therapy in the palliative management of advanced salivary gland cancers. J Clin Oncol 2006;24:2673-8.

6. Miletich I. Introduction to salivary glands: structure, function and embryonic development. Front Oral Biol 2010;14:1-20.

7. Speight PM, Barrett AW. Salivary gland tumors. Oral Diseases 2002;8:229-40.

8. Spiro RH. Salivary neoplasms: overview of a 35-year experience with 2,807 patients. Head Neck Surg 1986;8:177-84.

9. Gillespie MB, Albergotti WG, Eisele DW. Recurrent salivary gland cancer. Curr Treat Options Oncol 2012;13:58-70.

10. Bell D, Hanna EY. Salivary gland cancers: biology and molecular targets for therapy. Curr Oncol Rep 2012;14:166-74.

11. Boukheris H, Curtis RE, Land CE, Dores GM. Incidence of carcinoma of the major salivary glands according to the WHO classification, 1992 to 2006: a population-based study in the United States. Cancer Epidemiol Biomarkers Prev 2009;18:2899-906.

12. O'Neill ID. t(11;19) translocation and CRTC1-MAML2 fusion oncogene in mucoepidermoid carcinoma. Oral Oncol 2009;45:2-9.

13. Land CE, Saku T, Hayashi Y, Takahara O, Matsuura H, Tokuoka S, et al. Incidence of salivary gland tumors among atomic bomb survivors, 1950–1987. Evaluation of radiation- related risk. Radiat Res 1996;146:28–36.

14. Mayne ST, Morse DE, Winn DM. Cancer Epidemiology and Prevention. New York: Oxford University Press, 2006. p. 674-696.

15. Eversole LR, Sabes WR, Rovin S. Aggressive growth and neoplastic potential of odontogenic cysts: with special reference to central epidermoid and mucoepidermoid carcinomas. Cancer 1975;35:270-82.

16. Ezsias A, Sugar AW, Milling MA, Ashley KF. Central mucoepidermoid carcinoma in a child. J Oral Maxillofac Surg 1994;52:512-5.

17. Ellis GL, Auclair PL. Tumors of the salivary glands—Atlas of tumor pathology. Fascicle 17 Washington: Armed Forces Institute of Pathology. 1996

18. Gingell JC, Beckerman T, Levy BA, Snider LA. Central mucoepidermoid carcinoma. Review of the literature and report of a case associated with an apical periodontal cyst. Oral Surg Oral Med Oral Pathol 1984;57:436-40.

19. Ito FA, Ito K, Vargas PA, de Almeida OP, Lopes MA. Salivary gland tumors in a brazilian population: a retrospective study of 496 cases. Int J Oral Maxillofac Surg 2005;34:533-6.

20. Luna MA. Salivary mucoepidermoid carcinoma: revisited. Adv Anat Pathol 2006;13:293–307.

21. Pires FR, de Almeida OP, de Araujo VC, Kolawski LP. Prognostic factors in head and neck mucoepidermoid carcinoma. Arch Otolaryngol Head Neck Surg 2004;130:174-80.

22. Akrish S, Peled M, Ben-Izhak O, Nagler RM. Malignant salivary gland tumors and cyclo-oxygenase-2: a histopathological and immunohistochemical analysis with implications on histogenesis. Oral Oncol 2009;45:1044-50.

23. Alos L, Lugan B, Castillo M, Nadal A, Carreras M, Caballero M, et al. Expression of membrane-bound mucins (MUC1 and MUC4) and secreted mucins (MUC2, MUC5AC, MUC5B, MUC6 and MUC7) in mucoepidermoid carcinomas of salivary glands. Am J Surg Pathol 2005;29:806-13.

24. Azevedo RS, de Almeida OP, Kowalski LP, Pires FR. Comparative cytokeratin expression in the different cell types of salivary gland mucoepidermoid carcinoma. Head Neck Pathol 2008;2:257-64.

25. Coxon A, Rozenblum E, Park YS, Joshi N, Tsurutani J, Dennis PA, et al. Mect1-Maml2 fusion oncogene linked to the aberrant activation of cyclic AMP/CREB regulated genes. Cancer Res 2005;65:7137-44.

26. Jaskoll T, Htet K, Abichaker G, Kaye FJ, Melnick M. CRTC1 expression during normal and abnormal salivary gland development supports a precursor cell origin for mucoepidermoid cancer. Gene Expr Patterns. 2011;11:57-63.

27. Bell D, Holsinger CF, El-Naggar AK. CRTC1/MAML2 fusion transcript in central mucoepidermoid carcinoma of mandible--diagnostic and histogenetic implications. Ann Diagn Pathol 2010;14:396-401.

28. Browand BC, Waldron CA. Central mucoepidermoid tumors of the jaws. Report of nine cases and review of the literature. Oral Surg Oral Med Oral Pathol 1975;40:631-43.

29. Chen AM, Granchi PJ, Garcia J, Bucci MK, Fu KK, Eisele DW. Local-regional recurrence after surgery without postoperative irradiation for carcinomas of the major salivary glands: impli- cations for adjuvant therapy. Int J Radiat Oncol Biol Phys 2007;67:982-7.

30. Cai BL, Xu XF, Fu SM, Shen LL, Zhang J, Guan SM, et al. Nuclear translocation of MRP1 contributes to multidrug resistance of mucoepidermoid carcinoma. Oral Oncol 2011;47:1134-40.

31. Bhaijee F, Pepper DJ, Pitman KT, Bell D. New developments in the molecular pathogenesis of head and neck tumors: a review of tumor-specific fusion oncogenes in mucoepidermoid carcinoma, adenoid cystic carcinoma, and NUT midline carcinoma. Ann Diagn Pathol 2011;15:69-77.

32. Wu L, Liu J, Gao P, Nakamura M, Cao Y, Shen H, et al. Transforming activity of MECT1- MAML2 fusion oncoprotein is mediated by constitutive CREB activation. EMBO J 2005;24:2391-402.

33. Tonon G, Modi S, Wu L, Kubo A, Coxon AB, Komiya T, et al. t(11;19)(q21;p13) translocation in mucoepidermoid carcinoma creates a novel fusion product that disrupts a Notch signaling pathway. Nat Genet 2003;33:208-430.

34. Behboudi A, Enlund F, Winnes M, Andren Y, Nordkvist A, Leivo I, et al. Molecular classification of mucoepidermoid carcinomas- prognostic significance of the MECT1-MAML2 fusion oncogene. Genes Chromosomes Cancer 2006;45:470-81.

35. Okabe M, Miyabe S, Nagatsuka H, Terada A, Hanai N, Yokoi M, et al. MECT1-MAML2 fusion transcript defines a favorable subset of mucoepidermoid carcinoma. Clin Cancer Res 2006;12:3902-07.

36. Anzick SL, Chen WD, Park Y, Meltzer P, Bell D, El-Naggar AK, et al. Unfavorable prognosis of CRTC1-MAML2 positive mucoepidermoid tumors with CDKN2A deletions. Genes Chromosomes Cancer 2010;49:59-69.

37. Bell D, Luna MA, Weber RS, Kaye FJ, El-Naggar AK. CRTC1/MAML2 fusion transcript in Warthin's tumor and mucoepidermoid carcinoma: evidence for a common genetic association. Genes Chromosomes Cancer 2008;47:309-14.

38. Cai Y, Wang R, Zhao YF, Jia J, Sun ZJ, Chen XM. Expression of Neuropilin-2 in salivary adenoid cystic carcinoma: its implication in tumor progression and angiogenesis. Pathol Res Pract 2010;206:793-9.

39. Jiang J, Tang Y, Zhu G, Zheng M, Yang J, Liang X. Correlation between transcription factor Snail1 expression and prognosis in adenoid cystic carcinoma of salivary gland. Oral Surg Oral Med Oral Pathol Oral Radiol Endod 2010;110:764-9.

40. Tang Y, Liang X, Zhu G, Zheng M, Yang J, Chen Y. Expression and importance of zinc-finger transcription factor Slug in adenoid cystic carcinoma of salivary gland. J Oral Pathol Med 2010;39:775-80.

41. Zhang J, Peng B, Chen X. Expressions of nuclear factor kappaB, inducible nitric oxide synthase, and vascular endothelial growth factor in adenoid cystic carcinoma of salivary glands: correlations with the angiogenesis and clinical outcome. Clin Cancer Res 2005;11:7334-43.

42. Hunt JL. An update on molecular diagnostics of squamous and salivary gland tumors of the head and neck. Arch Pathol Lab Med 2011;135:602-9.

43. Seethala RR. An update on grading of salivary gland carcinomas. Head Neck Pathol 2009;3:69-77.

44. Kim KH, Sung MW, Chung PS, Rhee CS, Park CI, Kim WH. Adenoid cystic carcinoma of the head and neck. Arch Otolaryngol Head Neck Surg 1994;120:721-6.

45. Matsuba HM, Spector GJ, Thawley SE, Simpson JR, Mauney M, Pikul FJ. Adenoid cystic salivary gland carcinoma. A histopathologic review of treatment failure patterns. Cancer 1986;57:519-24.

46. Rapidis AD, Givalos N, Gakiopoulou H, Faratzis G, Stavrianos SD, Vilos GA, et al. Adenoid cystic carcinoma of the head and neck. Clinicopathological analysis of 23 patients and review of the literature. Oral Oncol 2005;41:328-35.

47. Xue F, Zhang Y, Liu F, Jing J, Ma M. Expression of IgSF in salivary adenoid cystic carcinoma and its relationship with invasion and metastasis. J Oral Pathol Med 2005;34:295-7.

48. Persson M, Andrèn Y, Mark J, Horlings HM, Persson F, Stenman G. Recurrent fusion of MYB and NFIB transcription factor genes in carcinomas of the breast and head and neck. Proc Natl Acad Sci USA 2009;106: 18740-44.

49. Skálová A, Vanecek T, Sima R, Laco J, Weinreb I, Perez-Ordonez B, et al. Mammary analogue secretory carcinoma of salivary glands, containing the ETV6-NTRK3 fusion gene: a hitherto undescribed salivary gland tumor entity. Am J Surg Pathol 2010;34:599-608.

50. Edwards PC, Bhuiya T, Kelsch RD. C-kit expression in the salivary gland neoplasms adenoid cystic carcinoma, polymorphous low-grade adenocarcinoma, and monomorphic adenoma. Oral Surg Oral Med Oral Pathol Oral Radiol Endod 2003;95:586-93.

51. Fukuoka M, Yano S, Giaccone G, Tamura T, Nakagawa K, Douillard JY. Multi-institutional randomized phase II trial of gefitinib for previously treated patients with advanced non-small-cell lung cancer (The IDEAL 1 Trial) J Clin Oncol 2003;21:2237-46.

52. Holst VA, Marshall CE, Moskaluk CA, Frierson HF Jr. KIT protein expression and analysis of c-kit gene mutation in adenoid cystic carcinoma. Mod Pathol 1999;12:956-60.

53. Kris MG, Natale RB, Herbst RS, Lynch TJ Jr, Prager D, Belani CP, et al. Efficacy of gefitinib, an inhibitor of the epidermal growth factor receptor tyrosine kinase, in symptomatic patients with non-small cell lung cancer: a randomized trial. JAMA 2003;290:2149-58.

54. Mino M, Pilch BZ, Faquin WC. Expression of KIT (CD117) in neoplasms of the head and neck: an ancillary marker for adenoid cystic carcinoma. Mod Pathol 2003;16:1224-31.

55. Perez-Soler R. Phase II clinical trial data with the epidermal growth factor receptor tyrosine kinase inhibitor erlotinib (OSI-774) in non-small-cell lung cancer. Clin Lung Cancer 2004;6 Suppl 1:S20-3.

56. Heinrich MC, Blanke CD, Druker BJ, Corless CL. Inhibition of KIT tyrosine kinase activity: a novel molecular approach to the treatment of KIT-positive malignancies. J Clin Oncol 2002;20:1692-703.

57. O'Brien SG, Guilhot F, Larson RA, Gathmann I, Baccarani M, Cervantes F, et al. Imatinib compared with interferon and low-dose cytarabine for newly diagnosed chronic-phase chronic myeloid leukemia. N Engl J Med 2003;348:994-1004.

58. Verweij J, Casali PG, Zalcberg J, LeCesne A, Reichardt P, Blay JY, et al. Progression-free survival in gastrointestinal stromal tumours with high-dose imatinib: randomised trial. Lancet 2004;364:1127-34.

59. Hotte SJ, Winquist EW, Lamont E, MacKenzie M, Vokes E, Chen EX, et al. Imatinib mesylate in patients with adenoid cystic cancers of the salivary glands expressing c-kit: a Princess Margaret Hospital phase II consortium study. J Clin Oncol 2005;23:585-90.

60. Cohnheim J. Ueber entzundung und eiterung. Path Anat Physiol Kiln Med 1867;40:1–79.

61. Durante F. Nesso fisio-pathologico tra la struttura dei nei materni e la genesi di alcuni tumori maligni. Arch Memor Observ Chir Pract 1874;11:217-26.

62. Lapidot T, Sirard C, Vormoor J, Murdoch B, Hoanq T, Caceres-Cortes J, et al. A cell initiating human acute myeloid leukaemia after transplantation into SCIDmice. Nature 1994;367:645-48.

63. Al-Hajj M, Wicha MS, Benito-Hernandez A, Morrison SJ, Clarke MF. Prospective identification of tumorigenic breast cancer cells. Proc Natl Acad Sci USA 2003;100:3983-8.

64. Ginestier C, Hur MH, Charafe-Jauffret E, Monville F, Dutcher J, Brown M, et al. ALDH1 is a marker of normal and malignant human mammary stem cells and a predictor of poor clinical outcome. Cell Stem Cell 2007;1:555-67.

65. Hermann PC, Huber SL, Herrler T, Aicher A, Ellwart JW, Guba M, et al. Distinct populations of cancer stem cells determine tumor growth and metastatic activity in human pancreatic cancer. Cell Stem Cell 2007;1:313-23.

66. Li C, Heidt DG, Dalerba P, Burant CF, Zhang L, Adsay V, et al. Identification of pancreatic cancer stem cells. Cancer Res 2007;67:1030-7.

67. Li C, Wu JJ, Hynes M, Dosch J, Sarkar B, Welling TH, et al. c-Met is a marker of pancreatic cancer stem cells and therapeutic target. Gastroenterology 2011;141:2218–27e5.

68. Rasheed ZA, Yang J, Wang Q, Kowalski J, Freed I, Murter C, et al. Prognostic significance of tumorigenic cells with mesenchymal features in pancreatic adenocarcinoma. J Natl Cancer Inst 2010;102:340–51.

69. Beier D, Hau P, Proescholdt M, Lohmeier A, Wischhusen J, Oefner PJ, et al. CD133(1) and CD133(–) glioblastoma-derived cancer stem cells show differential growth characteristics and molecular profiles. Cancer Res 2007;67:4010-5.

70. He J, Liu Y, Zhu T, Zhu J, Dimeco F, Vescovi AL, et al. CD90 is identified as a marker for cancer stem cells in primary high-grade gliomas using tissue microarrays. Mol Cell Proteomics 2012;11:M111.010744.

71. Patrawala L, Calhoun T, Schneider-Broussard R, Zhou J, Claypool K, Tang DG. Side population is enriched in tumorigenic, stem-like cancer cells, whereas ABCG21 and ABCG22 cancer cells are similarly tumorigenic. Cancer Res 2005;65:6207-19.

72. Shu Q, Wong KK, Su JM, Adesina AM, Yu LT, Tsang YT, et al. Direct orthotopic transplantation of fresh surgical specimen pre- serves CD1331 tumor cells in clinically relevant mouse models of medulloblastoma and glioma. Stem Cells 2008;26:1414-24.

73. Singh SK, Clarke ID, Terasaki M, Boon VE, Hawkins C, Squire J, et al. Identification of a cancer stem cell in human brain tumors. Cancer Res 2003;63:5821-8.

74. Singh SK, Hawkins C, Clark ID, Squir JA, Bayani L, Hide T, et al. Identification of human brain tumour initiating cells. Nature 2004;432:396-401.

75. Son MJ, Woolard K, Nam DH, Lee J, Fine HA. SSEA-1 is an enrichment marker for tumor- initiating cells in human glioblastoma. Cell Stem Cell 2009;4(5):440-452.

76. Baba T, Convery PA, Matsumura N, Whitaker RS, Kondoh E, Perry T, et al.

Epigenetic regulation of CD133 and tumorigenicity of CD1331 ovarian cancer cells. Oncogene 2009;28:209-18.

77. Bapat SA, Mali AM, Koppikar CB, Kurrey NK. Stem and progenitor-like cells contribute to the aggressive behavior of human epithelial ovarian cancer. Cancer Res 2005;65:3025-9.

78. Fong MY, Kakar SS. The role of cancer stem cells and the side population in epithelial ovarian cancer. Histol Histopathol 2010;25:113-20.

79. Ferrandina G, Bonanno G, Pierelli L, Perillo A, Procoli A, Mariotti A, et al. Expression of CD133-1 and CD133-2 in ovarian cancer. Int J Gynecol Cancer 2008;18:506–14.

80. Szotek PP, Pieretti-Vanmarcke R, Masiakos PT, Dinulescu DM, Connolly D, Foster R, et al. Ovarian cancer side population defines cells with stem cell-like characteristics and Mullerian Inhibiting Substance responsiveness. Proc Natl Acad Sci USA 2006;103:11154-9.

81. Wang L, Mezencev R, Bowen NJ, Matyunina LV, McDonald JF. Isolation and characterization of stem-like cells from a human ovarian cancer cell line. Mol Cell Biochem 2012;363:257-68.

82. Zhang S, Balch C, Chan MW, Lai HC, Matei D, Schilder JM, et al. Identification and characterization of ovarian cancer-initiating cells from primary human tumors. Cancer Res 2008;68:4311-20.

83. Dalerba P, Dylla SJ, Part IK, Liu R, Wang X, Cho RW, et al. Phenotypic characterization of human colorectal cancer stem cells. Proc Natl Acad Sci USA 2007;104:10158-63.

84. Huang EH, Hynes MJ, Zhang T, Ginestier C, Dontu G, Appelman H, et al. Aldehyde dehydrogenase 1 is a marker for normal and malignant human colonic stem cells (SC) and tracks SC overpopulation during colon tumori- genesis. Cancer Res 2009;69:3382-9.

85. O'Brien CA, Pollett A, Gallinger S, Dick JE. A human colon cancer cell capable of initiating tumour growth in immunodeficient mice. Nature 2007;445:106-10.

86. Ricci-Vitiani L, Lombardi DG, Pilozzi E, Biffoni M, Todaro M, Peschle C, et al. Identification and expansion of human colon-cancer-initiating cells. Nature 2007;445:111-5.

87. Todaro M, Alea MP, Di Stefano AB, Cammareri P, Vermeulen L, Iovino F, et al. Colon cancer stem cells dictate tumor growth and resist cell death by production of interleukin-4. Cell Stem Cell 2007;1:389-402.

88. Prince ME, Sivanandan R, Kaczorowski A, Wolf GT, Kaplan MJ, Delerba P, et al. Identification of a subpopulation of cells with cancer stem cell properties in head and

neck squamous cell carcinoma. Proc Natl Acad Sci USA 2007;104:973–8.

89. Chen YC, Chen YW, Hsu HS, Tseng LM, Huang PI, Lu KH, et al. Aldehyde dehydrogenase 1 is a putative marker for cancer stem cells in head and neck squamous cancer. Biochem Biophys Res Commun 2009;385:307–13.

90. Krishnamurthy S, Dong Z, Vodopyanov D, Imai A, Helman JI, Prince ME, et al. Endothelial cell-initiated signaling promotes the survival and self-renewal of cancer stem cells. Cancer Res 2010;70:9969-78.

91. Cheung PF, Cheng CK, Wong NC, Ho JC, Yip CW, Lui VC, et al. Granulin-epithelin precursor is an oncofetal protein defining hepatic cancer stem cells. PLoS One 2011;6:e28246.

92. Ma S, Chan KW, Hu L, Lee TK, Wo JY, Ng IO, et al. Identification and characterization of tumorigenic liver cancer stem/progenitor cells. Gastroenterology 2007;132:2542–56.

93. Ma S, Chan KW, Lee TK, Tang KH, Wo JY, Zheng BJ, et al. Aldehyde dehydrogenase discriminates the CD133 liver cancer stem cell populations. Mol Cancer Res 2008;6:1146–53.

94. Yang ZF, Ho DW, Ng MN, Lau CK, Yu WC, Ngai P, et al. Significance of CD90+ cancer stem cells in human liver cancer. Cancer Cell 2008;13:153-66.

95. Yang ZF, Ngai P, Ho DW, Yu WC, Ng MN, Lau CK, et al. Identification of local and circulating cancer stem cells in human liver can- cer. Hepatology 2008;47:919–28.

96. Yin S, Li J, Hu C, Chen X, Yao M, Yan M, et al. CD133 positive hepatocellular carcinoma cells possess high capacity for tumorigenicity. Int J Cancer 2007;120:1444-50.

97. Cheng L, Ramesh AV, Flesken-Nikitin A, Choi J, Nikitin AY. Mouse models for cancer stem cell research. Toxicol Pathol 2010;38:62-71

98. Dontu G, Abdallah WM, Foley JM, Jackson KW, Clarke MF, Kawamura, et al. In vitro propagation and transcriptional profiling of human mam- mary stem/progenitor cells. Genes Dev 2003;17:1253-70.

99. Reynolds BA, Weiss S. Clonal and population analyses demonstrate that an EGF-responsive mammalian embryonic CNS precursor is a stem cell. Dev Biol 1996;175:1-13.

100. Weiss S, Reynolds BA, Vescovi AL, Morshead C, Craig CG, van der Kooy D. Is there a neural stem cell in the mammalian forebrain? Trends Neurosci 1996;19:387-93.

101. Mani SA, Guo W, Liao MJ, Eaton EN, Ayyanan A, Zhou AY, et al. The epithelial-mesenchymal transition generates cells with properties of stem cells. Cell 2008;133:704-15.

102. Chaffer CL, Brueckmann I, Scheel C, Kaestli AJ, Wiggins PA, Rodrigues LO, et al. Normal and neoplastic nonstem cells can spontaneously convert to a stem-like state. Proc Natl Acad Sci USA 2011;108:7950-5.

103. Hambardzumyan D, Squatrito M, Holland EC. Radiation resistance and stem-like cells in brain tumors. Cancer Cell 2006;10:454-6.

104. Korkaya H, Paulson A, Charafe-Jauffret E, et al. Regulation of mammary stem/progenitor cells by PTEN/Akt/beta-catenin signaling. PLoS Biol 2009;7:e1000121.

105. Reya T, Morrison SJ, Clarke MF, Weissman IL. Stem cells, cancer, and cancer stem cells. Nature 2001;414:105-11.

106. Shafee N, Smith CR, Wei S, Kim Y, Mills GB, Hortobagyi, et al. Cancer stem cells contribute to cisplatin resistance in Brca1/p53- mediated mouse mammary tumors. Cancer Res 2008;68:3243-50.

107. Simeone DM. Pancreatic cancer stem cells: implications for the treatment of pancreatic cancer. Clin Cancer Res 2008;14:5646-8.

108. Venezia TA, Merchant AA, Ramos CA, Whitehouse NL, Young AS, Shaw CA, et al. Molecular signatures of proliferation and quiescence in hematopoietic stem cells. PLoS Biol 2004;2:e301.

109. Cai J, Weiss ML, Rao MS. In search of ‘‘stemness.’’ Exp Hematol 2004;32:585-98.

110. Cairns J. The cancer problem. Sci Am 1975;233:64-72, 68-77.

111. Cairns J. Somatic stem cells and the kinetics of mutagenesis and carcinogenesis. Proc Natl Acad Sci U S A 2002;99:10567-70.

112. Park Y, Gerson SL. DNA repair defects in stem cell function and aging. Annu Rev Med 2005;56:495–508.

113. Potten CS, Owen G, Booth D. Intestinal stem cells protect their genome by selective segregation of template DNA strands. J Cell Sci 2002;115:2381-8.

114. Wang S, Yang D, Lippman ME. Targeting Bcl-2 and Bcl-XL with nonpeptidic small-molecule antagonists. Semin Oncol 2003;30:133-42.

115. Wicha MS, Liu S, Dontu G. Cancer stem cells: an old idea--a paradigm shift. Cancer Res 2006;66:1883-90.

116. Morrison SJ, Spradling AC. Stem cells and niches: mechanisms that promote stem cell maintenance throughout life. Cell 2008;132:598-611.

117. Tlsty TD, Coussens LM. Tumor stroma and regulation of cancer development. Annu Rev Pathol 2006;1:119-50.

118. Polverini PJ, Cotran PS, Gimbrone MA Jr, Unanue ER. Activated macrophages induce vascular proliferation. Nature 1977;269:804-6.

119. Cao JX, Cui YX, Long ZJ, Dai ZM, Lin JY, Liang Y, et al. Pluripotency-associated genes in human nasopharyngeal carcinoma CNE-2 cells are reactivated by a unique epigenetic sub-microenvironment. BMC Cancer 2010;10:68.

120. Kim SJ, Kim JS, Papadopoulos J, Wook Kim S, Maya M, Zhang F, et al. Circulating monocytes expressing CD31: implications for acute and chronic angiogenesis. Am J Pathol 2009;174:1972-80.

121. Oguma K, Oshima H, Aoki M, Uchio R, Naka K, Nakamura S, et al. Activated macrophages promote Wnt signalling through tumour necrosis factor-alpha in gastric tumour cells. EMBO J 2008;27:1671-81.

122. Galiè M, Konstantinidou G, Peroni D, Scambi I, Marchini C, Lisi V, et al. Mesenchymal stem cells share molecular signature with mesenchymal tumor cells and favor early tumor growth in syngeneic mice. Oncogene 2008;27:2542-51.

123. Ferlay J, Parkin DM, Steliarova-Foucher E. Estimates of cancer incidence and mortality in Europe in 2008. Eur J Cancer 2010;46:765–81.

124. Haddad RI, Shin DM. Recent advances in head and neck cancer. N Engl J Med 2008;359:1143-54.

125. Jemal A, Bray F, Center MM, Ferlay J, Ward E, Forman D. Global cancer statistics. CA Cancer J Clin 2011;61:69–90.

126. Allegra E, Baudi F, La Boria A, Fagiani F, Garozzo A, Costanzo FS. Multiple head and neck tumours and their genetic relationship. Acta Otorhinolaryngol Ital 2009;29:237–41.

127. Franchin G, Minatel E, Gobitti C, Talamini R, Vaccher E, Sartor G, et al. Radiotherapy for patients with early-stage glottic carcinoma: univariate and multivariate analyses in a group of consecutive, unselected patients. Cancer 2003;98:765-72.

128. Jones AS, Morar P, Phillips DE, Field JK, Husband D, Helliwell TR. Second primary tumors in patients with head and neck squamous cell carcinoma. Cancer 1995;75:1343-53.

129. Leemans CR, Tiwari R, Nauta JJ, van der Waal I, Snow GB. Recurrence at the primary site in head and neck cancer and the significance of neck lymph node metastases as a prognostic factor. Cancer 1994;73:187-90.

130. Sjögren EV, Wiggenraad RG, Le Cessie S, Snijder S, Pomp J, Baatenburg de Jong RJ. Outcome of radiotherapy in T1 glottic carcinoma: a population-based study. Eur Arch Otorhinolaryngol 2009;266:735-44.

131. Clay MR, Tabor M, Owen JH, Carey TE, Bradford CR, Wolf GT, et al. Single-marker identification of head and neck squamous cell carcinoma cancer stem cells with aldehyde dehydrogenase. Head Neck 2010;32:1195-201.

132. Campos MS, Neiva KG, Meyers KA, Krishnamurthy S, Nör JE. Endothelial derived factors inhibit anoikis of head and neck cancer stem cells. Oral Oncol 2012;48:26-32.

133. Sun S, Wang Z. ALDH high adenoid cystic carcinoma cells display cancer stem cell properties and are responsible for mediating metastasis. Biochem Biophys Res Commun 2010;396:843-8.

134. Zhou JH, Hanna EY, Roberts D, Weber RS, Bell D. ALDH1 immunohistochemical expression and its significance in salivary adenoid cystic carcinoma. Head Neck 2013;35:575-8.

135. Fujita S, Ikeda T. Cancer stem-like cells in adenoid cystic carcinoma of salivary glands: relationship with morphogenesis of histological variants. J Oral Pathol Med 2012;41(3):207-13.

136. Li X, Lewis MT, Huang J, Gutierrez C, Osborne CK, Wu MF, et al. Intrinsic resistance of tumorigenic breast cancer cells to chemotherapy. J Natl Cancer Inst 2008;100:672-9.

137. Korkaya H, Paulson A, Iovino F, Wicha MS. HER2 regulates the mammary stem/progenitor cell population driving tumorigenesis and invasion. Oncogene 2008;27:6120-30.

138. Abhold EL, Kiang A, Rahimy E, Kuo SZ, Wang-Rodriguez J, Lopez JP, et al. EGFR kinase promotes acquisition of stem cell-like properties: a potential therapeutic target in head and neck squamous cell carcinoma stem cells. PLoS One 2012;7:e32459.

139. Cheng M, Qin G. Progenitor cell mobilization and recruitment: SDF-1, CXCR4, α4-integrin, and c-kit. Prog Mol Biol Transl Sci 2012;111:243-64.

140. Lombaert IM, Hoffman MP. Epithelial stem/progenitor cells in the embryonic mouse submandibular gland. Front Oral Biol 2010;14:90-106.

141. Dontu G, Wicha MS. Survival of mammary stem cells in suspension culture: implications for stem cell biology and neoplasia. J Mammary Gland Biol Neoplasia 2005;10:75-86.

142. Reynolds BA, Weiss S. Generation of neurons and astrocytes from isolated cells of the adult mammalian central nervous system. Science 1992;255:1707-10.

143. Krishnamurthy S, Nör JE. Orosphere assay: A method for propagation of head and neck cancer stem cells. Head Neck 2012 Jul 13.

CHAPTER III

ALDH/CD44 identifies uniquely tumorigenic cancer stem cells in salivary gland mucoepidermoid carcinomas

Abstract

A small sub-population of cells characterized by increased tumorigenic potential, ability to self-renew and to differentiate into cells that make up the tumor bulk, has been characterized in some (but not all) tumor types. These unique cells, named cancer stem cells, are considered drivers of tumor progression in these tumors. The purpose of this work is to understand if cancer stem cells play a functional role in the tumorigenesis of salivary gland mucoepidermoid carcinomas. Here, we investigated the expression of putative cancer stem cell markers (ALDH, CD10, CD24, CD44) in primary human mucoepidermoid carcinomas by immunofluorescence, *in vitro* salisphere assays, and *in vivo* tumorigenicity assays in immunodeficient mice. Human mucoepidermoid carcinoma cells (UM-HMC-1, UM-HMC-3A, UM-HMC-3B) sorted for high levels of ALDH activity and CD44 expression ($ALDH^{high}CD44^{high}$) consistently formed primary and secondary salispheres *in vitro*, and showed enhanced tumorigenic potential *in vivo* (defined as time to tumor palpability, tumor growth after palpability), when compared to $ALDH^{low}CD44^{low}$ cells. Cells sorted for CD10/CD24, and CD10/CD44 showed varying trends of salisphere formation, but consistently low *in vivo* tumorigenic potential. Finally, cells sorted for CD44/CD24 showed inconsistent results in salisphere formation and

tumorigenic potential assays when different cell lines were evaluated. Collectively, these data demonstrate that salivary gland mucoepidermoid carcinomas contain a small population of cancer stem cells with enhanced tumorigenic potential that are characterized by high ALDH activity and CD44 expression. These results suggest that patients with mucoepidermoid carcinoma might benefit from therapies that ablate these highly tumorigenic cells.

Introduction

Advanced salivary gland mucoepidermoid carcinoma (MEC) is a relentless and typically fatal disease. Mucoepidermoid carcinoma is the most common malignant salivary gland cancer, accounting for 5-15% of all salivary tumors and 30-35% of malignant salivary tumors (1-7). These tumors arise in both the major and minor salivary gland and are characterized by the presence of mucous, epidermoid, and intermediate cells types. Low-grade tumors show noticeable cyst formation, a higher portion of mucous cells, and minimal cytological mutation while high-grade tumors are characterized by large concentrations of intermediate and squamous cells as well as increased mitotic activity. Current treatment consists of surgical resection with or without radiation, depending on tumor grade. Patients presenting with recurrent, locally invasive, or metastatic tumors do not have effective treatment options (8). Understanding the pathobiology of this cancer, particularly mechanisms involved in resistance to therapy, is critical to improve the survival and the quality of life of patients with mucoepidermoid carcinoma.

The cancer stem cell (CSC) hypothesis states that tumors contain a small sub-population of multipotent cells that are capable of self-renewal and differentiation, and are uniquely tumorigenic. These cells initiate and maintain tumor growth and

progression in several cancers including breast, head and neck, pancreatic, liver, ovarian, colorectal, and brain cancers (9-16). However, it is unclear if cancer stem cells play a functional role in the pathobiology of mucoepidermoid carcinoma. Importantly, cancer stem cells are thought to be resistant to chemotherapy and radiation due, at least in part, to slower proliferation rates and differential function of transporter proteins (17-19). It is believed that survival of these cells after treatment enables tumor relapse. Identification and understanding of how these cells function in mucoepidermoid carcinomas might lead to more effective therapies.

Isolation of cancer stem cells can be accomplished using protein markers that are differentially expressed in stem cells compared to the non-cancer stem cell population. One such marker is aldehyde dehydrogenase (ALDH)-1, a cytosolic enzyme that oxidizes aldehydes into carboxylic acids (20-22). ALDH1 is thought to play an important role in hematopoietic stem cell fate determination by regulating the conversion of retinol into retinoic acid (23). Importantly, ALDH1 identifies cancer stem cells in breast, lung, head and neck, colorectal, ovarian, pancreatic, bladder, prostate, and cervical cancers (10, 24-33). Another surface marker protein used extensively to identify cancer stem cells is CD44, a transmembrane glycoprotein. This protein functions in key cellular processes regulating survival, differentiation, growth, and cell motility (34). CD44 has been used as a stem cell marker in breast, head and neck, pancreatic, prostate, and colorectal cancers (34). The cell adhesion protein, CD24, is also an important stem cell marker used in breast, pancreatic, and colorectal cancers (9, 35, 36). Interestingly, cancer stem cells are identified within the $CD24^{low}$ population in breast tumors (9), while in pancreatic cancer they are identified within the $CD24^{high}$

population (35). And finally, the metallo-endoprotease CD10, a diagnostic marker in several tumors, has been implicated in invasion is breast, gastric, and colorectal cancer (37). This protein plays an important role in the maintenance of mammary gland stem cells, suggesting that it could also serve as a marker for stem cells in glandular malignancies (37).

While cancer stem cells have been identified and well characterized in several tumors, their presence and functional role has not been investigated in salivary gland mucoepidermoid carcinomas. Here, we used cell lines and xenograft models recently generated in our laboratory (38) to screen for cancer stem cells using several combinations of ALDH, CD44, CD24, and CD10 markers. Our findings indicate that cancer stem cells play a functional role in mucoepidermoid carcinoma, and that these cells can be isolated using the ALDH/CD44 marker combination. In contrast, combinations of CD44, CD24, and CD10 did not identify tumorigenic cells consistently. Together, these results unveil the function of a uniquely tumorigenic population of cancer stem cells in the pathogenesis of mucoepidermoid carcinomas.

Materials and Methods

Cell Culture

Human salivary gland mucoepidermoid carcinoma cell lines (UM-HMC-1, UM-HMC-3A, UM-HMC-3B) previously characterized in our laboratory (38) were cultured in high glucose Dulbecco's Modified Eagle's Medium (DMEM; Invitrogen, Carlsbad, CA, USA) supplemented with penicillin/streptomycin (Invitrogen), L-glutamine (Invitrogen), 10% FBS (Invitrogen), 20 ng/ml epidermal growth factor (EGF; Sigma-Aldrich, St. Louis, MO, USA), 400 ng/ml hydrocortisone (Sigma-Aldrich), and 5 μg/ml insulin (Sigma-Aldrich)

[38]. Cells were passaged using 0.05% trypsin/EDTA (Invitrogen). Primary human dermal microvascular endothelial cells (HDMEC; Lonza, Walkersville, MD, USA) were cultured using endothelial growth medium (EGM2-MV; Lonza).

Flow Cytometry

Trypsinized cells were filtered using 5 ml polystyrene round-bottom tumor with cell strainer caps (BD Pharmingen). Single cell suspensions of $2x10^6$ cells/ml were prepared and incubated with 5 µl Aldefluor® substrate (BAA), or 5 µl of the inhibitor diethylaminobenzaldehyde (DEAB) for 40 minutes at 37^0C, using the Aldefluor kit (StemCell; Vancouver, Canada). Cells were exposed to anti-CD44 (APC-Cat #559942, PE-Cat #550989), anti-CD24 (FITC-Cat #555427; BD Pharmingen), or anti-CD10 (APC-Cat #340923; BD Pharmingen) for 30 minutes at 4^0C. Positive anti-HLA-ABC (PE-Cat #560168; BD Pharmingen) was used to separate human cells from mouse cells, and 7-AAD (Cat #00-6993-50; eBiosciences) staining was used to verify cell viability.

Salisphere Assay

Non-adherent spheres of salivary mucoepidermoid carcinoma cells (salispheres), previously characterized in normal salivary cells [45], were cultured in DMEM/F-12 (Invitrogen) supplemented with 20 ng/ml EGF (Sigma-Aldrich), 20 ng/ml basic fibroblast growth factor (bFGF; Millipore), 1% penicillin/streptomycin (Invitrogen), 1% glutamax (Invitrogen), 1% N-2 supplement (Invitrogen), 1 µM dexamethasone (Sigma-Aldrich), and 10 µg/ml insulin (Sigma-Aldrich) (39). Cells were counted, diluted to 2,000 per 1.5 ml, and added to 6-well ultra-low attachment plates (Corning; Corning, NY, USA). For *in vitro* passaging, salispheres were collected and exposed to 0.25% trypsin for 5-10 minutes, and then mechanically dissociated. The trypsin was neutralized using a trypsin

neutralizing solution (TNS; Lonza). Colonies of 50 cells or more were considered salispheres.

***In vivo* studies**

Single cell suspensions of sorted mucoepidermoid carcinoma cells (UM-HMC-1, UM-HMC-3A, UM-HMC-3B) were seeded in biodegradable scaffolds with 9 x 10^5 human dermal microvascular endothelial cells (HDMEC; Lonza) and bilaterally implanted in the subcutaneous space on the dorsum of severe combined immunodeficient (SCID) mice (CB-17 SCID; Charles River, Wilmington, MA, USA), as we have shown (39, 40). Second generation tumors were generated by transplanting cells retrieved from the digestion of the first generation tumors in secondary mice. Tumors were minced into small fragments and digested using 1X collagenase-hyaluronidase (Stem Cell Technologies; Vancouver, BC, Canada) at 37^0C for 45 minutes, pipetting up and down every 15 minutes. Digested cells and tissues were passed through a 40-μm sieve (Fisher) and neutralized using 3-5 ml FBS. Cell suspensions were centrifuged and incubated with AKC lysis buffer (Invitrogen) for 1 minute, centrifuged, counted, and subjected to flow cytometry. For the studies designed to understand the effect of *in vitro* cell attachment conditions on the tumorigenic potential *in vivo*, cells were cultured with serum-free medium as salispheres (as described above), or in normal attachment conditions. After 7 days, attached cells were retrieved, 200,000 cells were seeded per biodegradable scaffold and transplanted into mice, as also described above. Alternatively, the salispheres were collected but not dissociated (to maintain the sphere structure), and 200,000 cells/scaffold were transplanted into mice. Tumor growth was

measured every seven days with calipers, and mice were euthanized when the tumors reached a maximum of 2,000 mm^3.

Western Blot

UM-HMC-3A and UM-HMC-3B were sorted for $ALDH^{high}CD44^{high}$. As controls, we combined the $ALDH^{high}CD44^{low}$, $ALDH^{low}CD44^{high}$, and $ALDH^{low}CD44^{low}$ as non-CSC cell population. NP-40 lysis buffer was used to prepare whole cell lysates that were resolved using PAGE. Membranes were probed using antibodies a 1:1000 dilution against human mTor, p-mTor, Akt, p-Akt, S6K, p-S6K (Cell Signaling; Beverly, MA, USA); 1:2000 dilution of EGFR, a 1:1000 dilution of p-EGFR, and beta-actin (Santa Cruz Biotechnology; Santa Cruz, CA, USA) overnight at 4^0C.

Immunofluorescence Staining

Cells were cultured in Lab-Tek® 4-well chamber slides (Thermo Scientific) overnight, fixed with 2% formaldehyde and 0.2% glutaraldehyde for 20 minutes, incubated in 0.1% Triton-X 100 for 10 minutes, and then in 0.3% hydrogen peroxide for 10 minutes. Paraffin-embedded sections were deparaffinized and treated with a 1X antigen retrieval solution in citrate buffer (Dako; Carpinteria, CA, USA) at 45-98^0C for 60 minutes followed by treatment with 3% hydrogen peroxidase for 10 minutes. Rabbit anti-human ALDH1A1 (Abcam; Cambridge, England) was incubated overnight and labeled with Alexafluor 488 (Anti-Rabbit, Invitrogen) the following day. Cells were incubated with mouse anti-human CD44 (Thermo Scientific), rabbit anti-human CD10 (Abcam), and mouse anti-CD24 (Abcam) for 1 hour then labeled with Alexafluor 594 (anti-mouse, Invitrogen), Alexafluor 488 (anti-rabbit, Invitrogen), and Alexafluor 488 (anti-mouse, Jackson ImmunoResearch) respectively. We analyzed tissues from diagnostic incisional

biopsies taken from 12 patients. A pathologist graded the samples according to WHO standards, but the tentative grades are subjective and observer-dependent.

Statistical analyses

Statistical analysis of *in vitro* data was performed using either a t-test or one-way ANOVA followed by post-hoc tests (SigmaStat 2.0 software; SPSS, Chicago, IL). Time to failure data was analyzed using the Kaplan-Meier method and the log-rank test. We employed linear mixed model regression to analyze the repeated measurements data on each tumor. Model fixed effects included time, marker, the interaction of time and marker, and model random effects included both mouse and tumor position. For all models a continuous autoregressive correlation structure was used, which assumes more correlated variances among temporally proximate observations. A log-transformation of the outcome variable (tumor volume) was to account for exponential increase of tumor volumes. Tumor growth rate since palpability (200 mm^3) was measured, and we controlled for size differences of the tumor at first palpability. Analysis was performed using the "nlme" package in the statistical software program R v 3.1.0. (41).

Results

Characterization of putative stem cell markers in human mucoepidermoid carcinomas

To investigate the expression patterns of cancer stem cell markers in human mucoepidermoid carcinomas, we obtained tissue sections from diagnostic incisional biopsies and performed immunofluorescence staining. We focused on stem cell markers that have been verified in other glandular malignancies, *i.e.* ALDH, CD44,

CD24, and CD10. We found that 7 of the 12 samples showed positive staining for all four markers. Ten of 12 samples stained positively for ALDH1, 12 of 12 samples stained for CD44, 9 of 12 samples stained for CD10, and 10 of the 12 samples stained for CD24 (Table III.1). Interestingly, we observed low staining levels for each one of these markers in normal salivary glands, when qualitatively compared with mucoepidermoid carcinomas (Figure III.1A).

Table III.1. Patient demographic and expression of CSC markers in human salivary gland mucoepidermoid carcinomas.

Case Number	Gender	Age (Years)	Localization	H&E Predominant Morphology	Tentative Grading	Tumor Size (mm)	Immunofluorescence Staining			
							ALDH	CD44	CD10	CD24
1	F	49	Hard palate	Mixed	Intermediate	10	Absent	Present	Absent	Present
2	M	46	Jugal mucosa	Solid	High	8	Present	Present	Absent	Present
3	F	24	Hard palate	Solid	Intermediate	30	Present	Present	Present	Present
4	F	14	Hard/soft palate	Solid	High	50	Present	Present	Present	Present
5	F	29	Palate	Mixed	High	20	Present	Present	Present	Present
6	F	26	Palate	Cystic	Low	15	Present	Present	Present	Present
7	F	NA	Hard palate	Cystic	Low	6	Absent	Present	Present	Absent
8	F	46	Retromolar region/ vestibule	Solid	High	40	Present	Present	Present	Present
9	M	62	Jugal mucosa	Cystic	High	12	Present	Present	Absent	Present
10	F	63	Hard palate	Solid	Intermediate	15	Present	Present	Present	Absent
11	F	67	Palate	Solid	Intermediate	15	Present	Present	Present	Present
12	F	55	Hard palate	Mixed	High	20	Present	Present	Present	Present

When less aggressive, cystic tumors were compared to more aggressive, solid tumors, we saw an increase in ALDH1 expression in the solid tumor (Figure III.1A). In contrast, CD44 stained highly in both tumor types (Figure III.1A). CD10 and CD24 showed differential expression between the cystic and solid tumor types. CD10 showed expression in both the cystic and solid tumors, however, more positive staining was

seen in the solid tumor (Figure III.1A). Interestingly, cells with high CD10 expression were localized mainly on the outside edge near the stroma suggesting that these cells may be important in intercellular signaling with the microenvironment. Tumor cells in these sections showed positive staining for CD24. However, the solid tumor areas showed more positive staining when compared to the cystic areas (Figure III.1A). Together, these results suggest that ALDH1, CD44, CD10, and CD24 are highly expressed in salivary gland mucoepidermoid carcinoma when compared to normal salivary gland and that expression of ALDH1, CD10, and CD24 may be differentially regulated in more aggressive cell types.

We also performed immunofluorescence staining on three human salivary mucoepidermoid carcinoma cell lines (UM-HMC-1, UM-HMC-3A, UM-HMC-3B) plated in Lab-Tek glass slides. We observed that ALDH1 staining is present but in only few cells (Figure III.2). In contrast, CD44 stained very highly in all cell lines evaluated (Figure III.2). CD10 stained positively but its expression was variable among the cell lines (Figure III.2). While UM-HMC-3B stained highly for CD10, UM-HMC-1 showed significantly less CD10 expression. UM-HMC-3A showed moderate staining when compared to UM-HMC-1 and UM-HMC-3B. Finally, all three cell lines showed similar levels of expression of CD24.

Characterization of putative stem cell markers in mucoepidermoid carcinoma cell lines

We used flow cytometry to screen three human salivary mucoepidermoid carcinoma cell lines (UM-HMC-1, UM-HMC-3A, UM-HMC-3B) for putative cancer stem

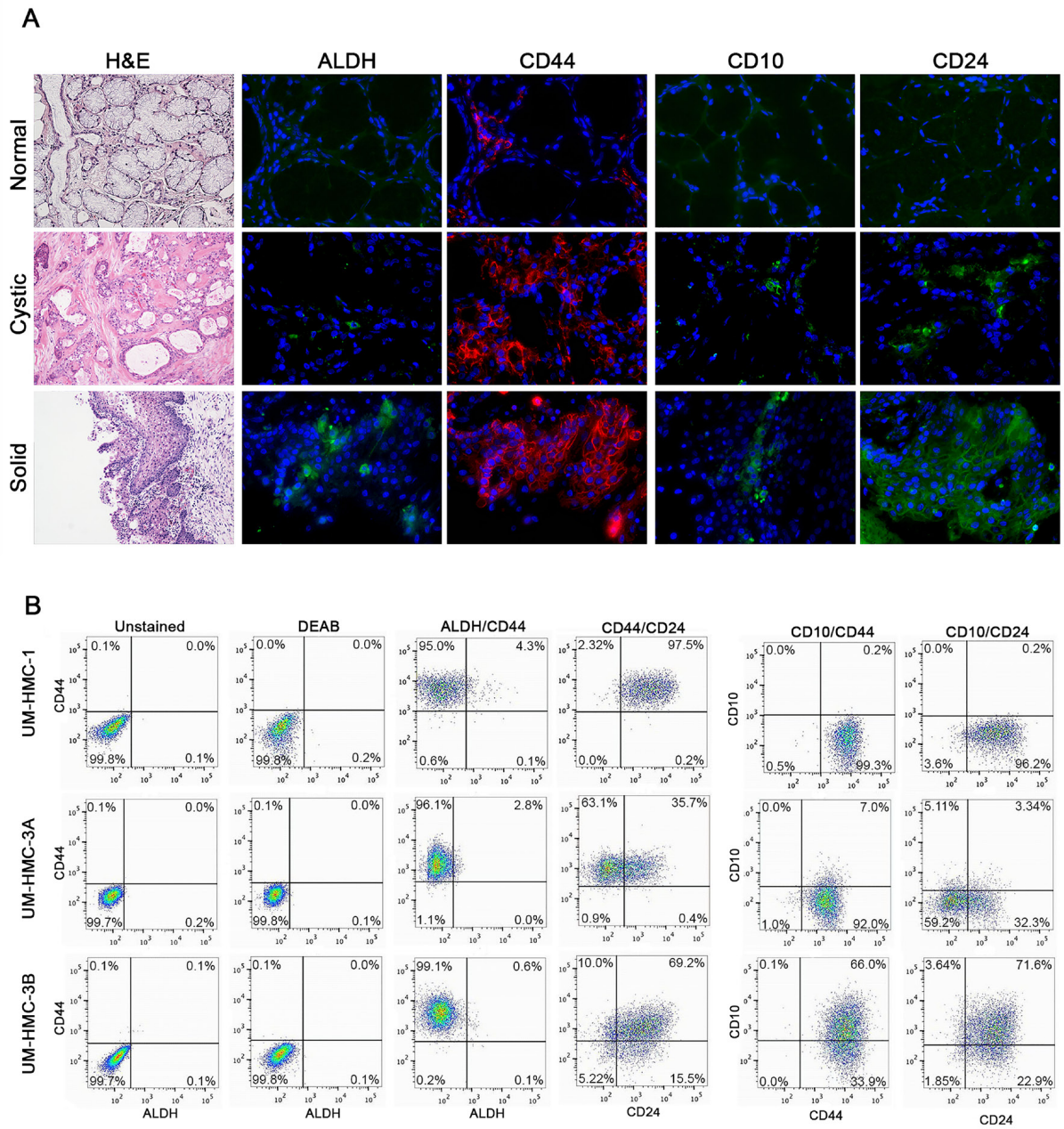
A
H&E
ALDH
CD44
CD10
CD24
Normal
Cystic
Solid
B
Unstained
DEAB
ALDH/CD44
CD44/CD24
CD10/CD44
CD10/CD24
UM-HMC-1
UM-HMC-3A
UM-HMC-3B
CD44
CD10
ALDH
CD24
C
High Staining Cells (%)
100%
90%
80%
70%
60%
50%
40%
30%
20%
10%
0%
ALDH
CD44
CD10
CD24
UM-HMC-1
UM-HMC-3A
UM-HMC-3B

Figure III.1: Characterization of putative stem cell markers in human mucoepidermoid carcinoma specimens. A. Representative photomicrographs of H&E and immuno uorescence images of tissue sections derived from patients with normal salivary gland; a low-grade, cystic tumor; or a high-grade, solid tumor. ALDH1, CD10, and CD24 are stained in green while CD44 is stained in red. H&E images were taken at 40X and immuno uorescence images were taken at 400X. **B.** Flow cytometry analysis of three cell lines (UM- HMC-1, UM-HMC-3A, UM-HMC-3B) stained for ALDH/CD44, CD44/CD24, CD10/CD44, and CD10/CD24. CD44-APC staining is shown on the horizontal axis while ALDH staining is shown on the vertical axis. CD44-PE is shown on the horizontal axis and CD10-APC is in the vertical axis. CD24-FITC is shown on the horizontal axis and CD10-APC or CD44-APC is shown on the vertical axis. **C.** Graph depicting the percentage of positive cells for ALDH, CD44, CD10, and CD24.

cell markers. UM-HMC cells consistently showed greater than 90% positive staining for CD44. In contrast, the percentage of ALDH high cells in UM-HMC-1 was only 4.4%, and in UM-HMC-3A and UM-HMC-3B was even lower (2.8%, 0.7% respectively) (Figure III.1B and 1C). When these two markers were combined, the most common population of cells was consistently $ALDH^{low}CD44^{high}$ (Figure III.1B).

UM-HMC cells showed variable staining for CD10 and CD24. UM-HMC-1 and UM-HMC-3B stained highly for CD24, while UM-HMC-3A showed less staining (Figure III.1B and 1C). CD10 staining was highest in UM-HMC-3B when compared to UM-HMC-3A and UM-HMC-1 cells (Figure III.1C). The combination of CD10/CD24 in UM-HMC-1 showed the majority of cells as $CD10^{low}CD24^{high}$. In UM-HMC3A cells, most cells stained $CD10^{low}CD24^{low}$ followed by $CD10^{low}CD24^{high}$, $CD10^{high}CD24^{low}$, and $CD10^{high}CD24^{high}$. UM-HMC-3B cells stained highly for $CD10^{high}CD24^{high}$ cells followed by $CD10^{low}CD24^{high}$, $CD10^{high}CD24^{low}$, and $CD10^{low}CD24^{low}$, showing an inverse expression profile when compared with UM-HMC-3A (Figure III.1B). When stained for combination CD44/CD24, UM-HMC-3B and UM-HMC-1 stained predominately $CD44^{high}CD24^{high}$, while UM-HMC-3A stained mainly $CD44^{high}CD24^{low}$. While all cell

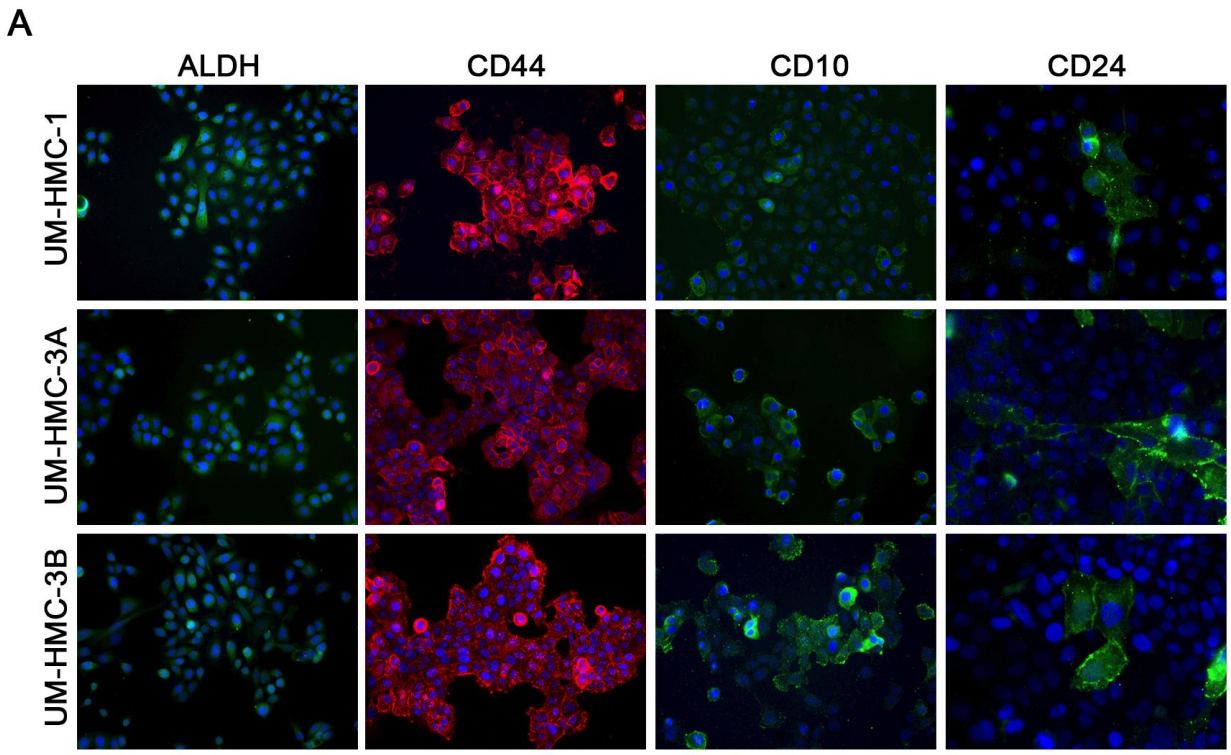

Figure III.2. Characterization of putative stem cell markers in human mucoepidermoid carcinoma cell lines. A. Representative photomicrographs of immunofluorescence staining for ALDH, CD44, CD10, or CD24 of a panel of mucoepidermoid carcinoma cells (UM-HMC-1, UM-HMC-3A, UM-HMC-3B) cultured in Lab-Tek chamber slides. Images were taken at 200X.

lines stained positively for CD44, CD24 expression was variable (Figure III.1B and 1C). CD10/CD44 combination also showed differential expression among cell lines. UM-HMC-1 and UM-HMC-3A showed low staining for CD10 and therefore, the most prevalent population in both lines was $CD10^{low}CD44^{high}$. UM-HMC-3B staining positively for $CD10^{high}CD44^{high}$ but also showed staining in the $CD10^{low}CD44^{high}$ population (Figure III.1B).

In summary, all UM-HMC cell lines showed positive staining for the four markers studied here. We observed that all cell lines consistently presented low ALDH activity and high CD44 expression. On the other hand, the expression of CD10 and CD24 was highly variable from cell line to cell line.

In vitro salisphere analysis of mucoepidermoid carcinoma cell lines

To begin the functional characterization of these putative marker combinations, we screened the UM-HMC cell lines for salisphere formation under ultra-low attachment, serum-free conditions. The three cell lines studied here formed salispheres. However, UM-HMC-1 cells generated less salispheres than UM-HMC-3A and UM-HMC-3B under these culture conditions (Figure III.3A and 3B). To evaluate the effectiveness of each specific marker combination to select cells with enhanced self-renewal capacity, primary salispheres were dissociated and passaged into secondary salispheres (Figure III.3C). Interestingly, we observed a trend for increasing number of salispheres with passaging when unsorted cells were evaluated (Figure III.3A).

To begin to understand the ability of marker combinations to select for cancer stem cells, we FACS-sorted the UM-HMC-3A and UM-HMC-3B cell lines according to ALDH activity, CD10, CD24, and/or CD44 protein expression. Sorted cells were plated in ultra-low attachment conditions and grown for seven days before the number of salispheres was determined. Salispheres were then dissociated and allowed to grow for additional seven days under the same culture conditions. The $ALDH^{low}CD44^{low}$ cells showed little to no salisphere growth. In contrast, both the $ALDH^{high}CD44^{high}$ and $ALDH^{low}CD44^{high}$ populations showed significant salisphere formation in primary and secondary cultures (Figure III.4A, Table III.2). Because the $ALDH^{high}CD44^{low}$ population is so rare, we were unable to obtain sufficient cell numbers to be analyzed.

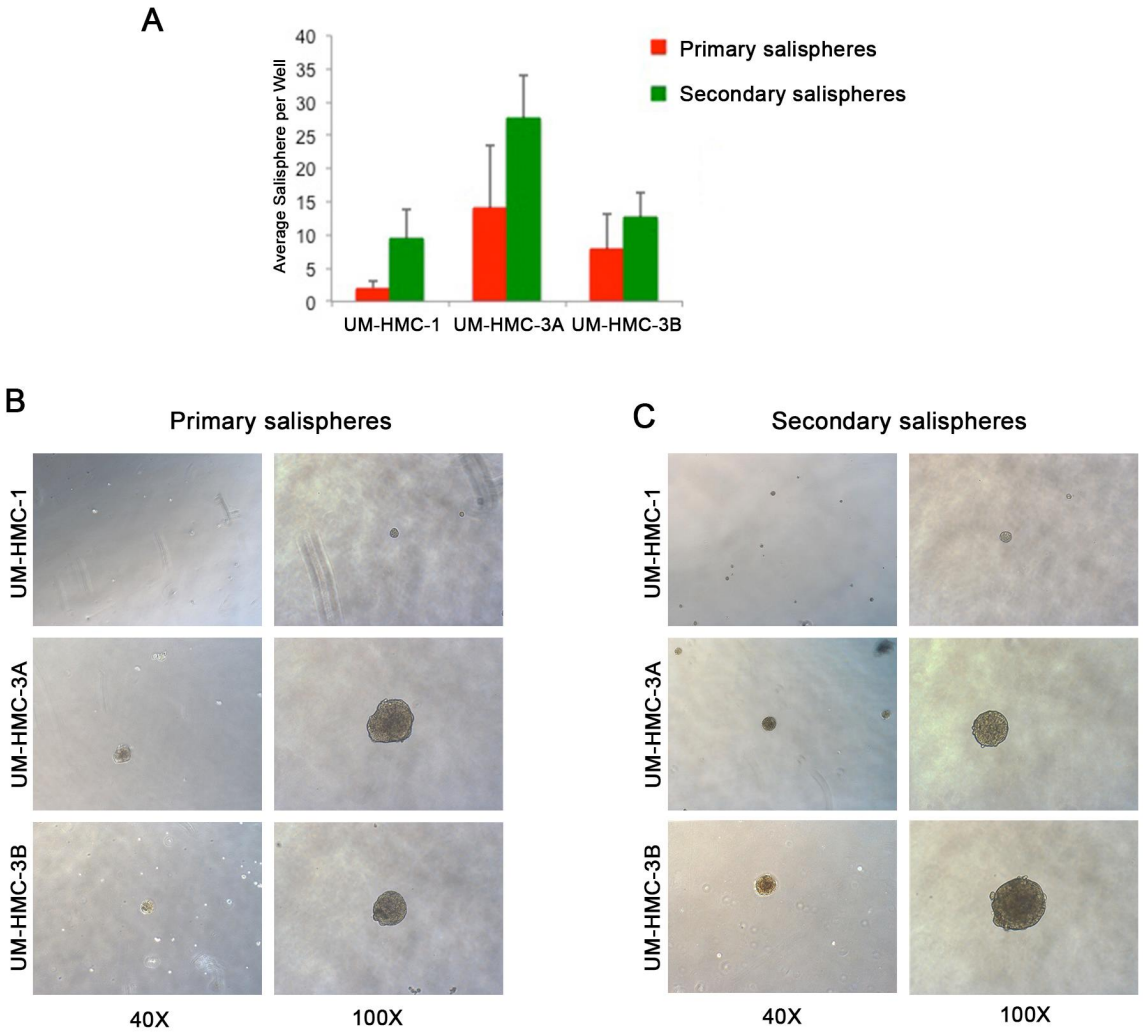

Figure III.3. Sphere analysis of unsorted HMC cells. A. Graph depicting the average number of sphere formed per well in a 6-well low attachment plate in UM-HMC-1, UM-HMC-3A, and UM-HMC-3B cells. **B.** Images of UM-HMC-1, UM-HMC-3A, and UM-HMC-3B primary spheres in low attachment culture. Images were taken at 40X and 100X. **C.** Images of UM-HMC-1, UM-HMC-3A, and UM-HMC-3B secondary spheres in low attachment culture. Images were taken at 40X and 100X.

Table III.2: *In-Vitro* salisphere formation and *in-vivo* tumorigenic potential of cells selected by the following putative CSC marker combinations.

ALDH/CD44	Salisphere Formation		*In Vivo* Tumorigenicity	
	UM-HMC-3A	UM-HMC-3B	Low-Passage	High-Passage
High/High	High	High	High	High
High/Low	NA	NA	NA	NA
Low/High	High	High	NA	NA
Low/Low	Low	Low	Low	Low
CD10/CD44				
High/High	Low	High	NA	Low
High/Low	Low	Intermediate	NA	Low
Low/High	Intermediate	Intermediate	NA	None
Low/Low	High	Low	NA	None
CD44/CD24				
High/High	Low	Low	Low	High
High/Low	Intermediate	Low	Low	Low
Low/High	Intermediate	High	High	Low
Low/Low	High	Low	Low	Intermediate
CD10/CD44				
High/High	Intermediate	High	None	NA
High/Low	Low	NA	NA	NA
Low/High	High	Intermediate	NA	NA
Low/Low	Low	NA	Low	NA

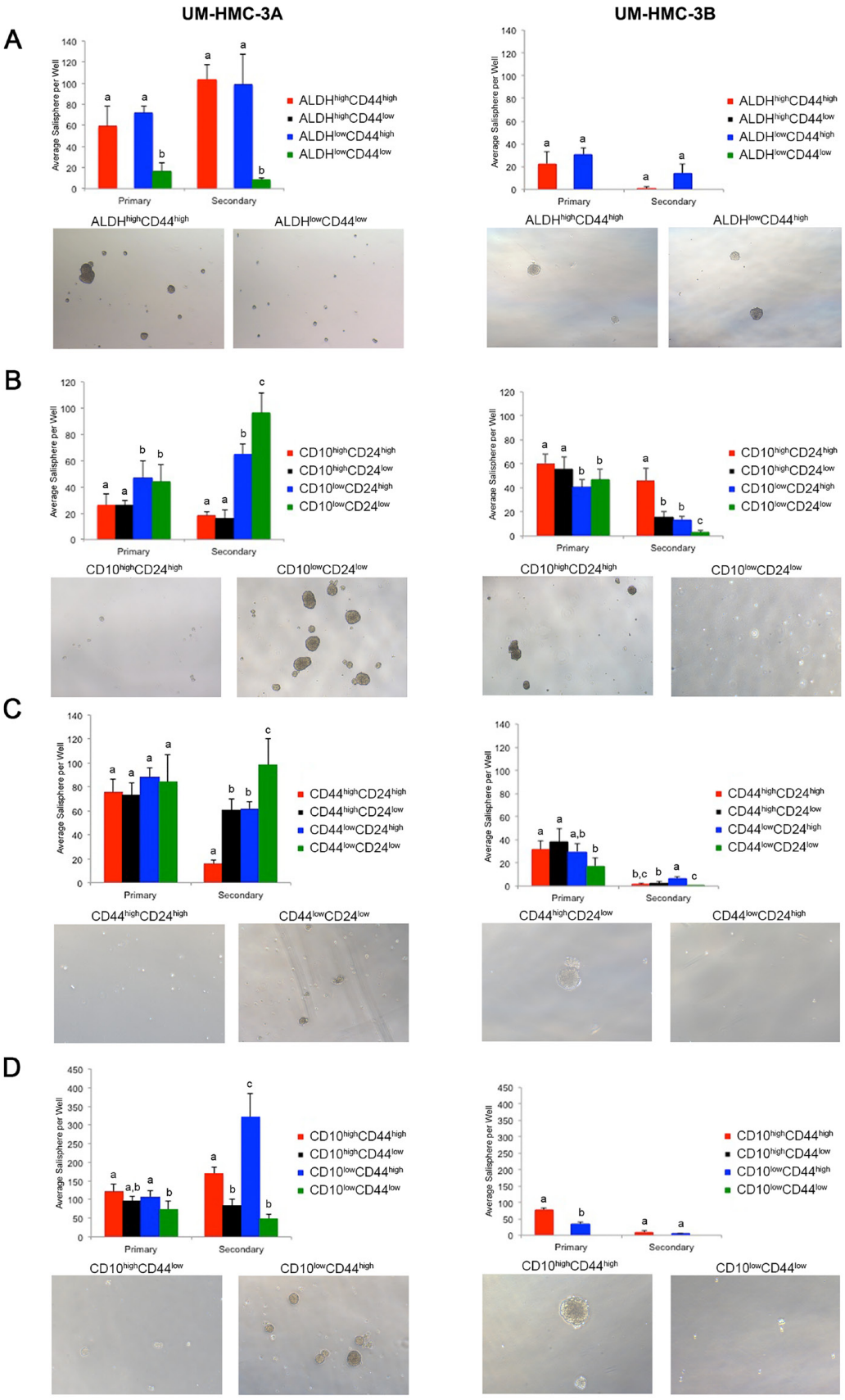
UM-HMC-3A
UM-HMC-3B
A
Average Salisphere per Well
Primary
Secondary
ALDHhighCD44high
ALDHhighCD44low
ALDHlowCD44high
ALDHlowCD44low
B
CD10highCD24high
CD10highCD24low
CD10lowCD24high
CD10lowCD24low
C
CD44highCD24high
CD44highCD24low
CD44lowCD24high
CD44lowCD24low
D
CD10highCD44high
CD10highCD44low
CD10lowCD44high
CD10lowCD44low

Figure III.4: *In vitro* salisphere analysis of FACS-sorted mucoepidermoid carcinoma cell lines (UM-HMC-3A, UM-HMC- 3B). A.-D. Ultra-low attachment plates were seeded with 2,000 cells/well (6-well plates), and cells were cultured for seven days to generate primary salispheres. Then, salispheres were dissociated into single cell suspensions, seeded in new ultra-low attachment plates, and secondary salispheres were counted after additional seven days. **A.** Graph depicting the average number of salispheres per well of cell lines FACS-sorted for ALDH/CD44 (*n* = 4-6). **B.** Graph depicting the average number of salispheres per well of cell lines FACS-sorted for CD10/CD24 expression (*n* = 5-6). **C.** Graph depicting the average number of salispheres per well of cell lines FACS-sorted for CD44/ CD24 cells (*n* = 6). D, Graph depicting the average number of salispheres per well of cell lines FACS-sorted for CD10/CD44 sorted cells (*n* = 5-6). All images were taken at 40X. Statistical analysis was performed using one-way ANOVA. Different low case letters indicate statistical difference at $p < 0.05$.

Cells sorted for CD10/CD24 showed significant differences in the number of salispheres. In the UM-HMC-3A cells, the $CD10^{low}CD24^{low}$ population significantly outgrew the other populations. The $CD10^{low}CD24^{high}$ population also showed considerable salisphere formation in this cell line. Interestingly, the UM-HMC-3B cells showed an outgrowth of the $CD10^{high}CD24^{high}$ population in secondary salispheres (Figure III.4B, Table III.2). UM-HMC-3A cells sorted according to CD44/CD24 marker combination also showed significant differences in salisphere formation, specifically in the $CD44^{low}CD24^{low}$ population. In contrast, UM-HMC-3B cells showed growth in the $CD44^{low}CD24^{high}$ population in secondary salispheres (Figure III.4C, Table III.2). Finally, UM-HMC-3A and UM-HMC-3B cells were sorted by CD10/CD44. In the UM-HMC-3A cells, the $CD10^{low}CD44^{high}$ population formed the most secondary salispheres. In the UM-HMC-3B cells, the only populations that had sufficient numbers to enable us to perform this assay were the $CD10^{high}CD44^{high}$ and $CD10^{low}CD44^{high}$ cells. We observed that $CD10^{high}CD44^{high}$ formed significantly more primary salispheres than the $CD10^{low}CD44^{high}$ cells (Figure III.4D, Table III.2).

We observed that the marker combinations tested here showed different patterns of salisphere growth. $ALDH^{high}CD44^{high}$ and $ALDH^{low}CD44^{high}$ populations showed consistent salisphere formation, and therefore this combination was selected for the first *in vivo* studies (see below). The CD10/CD24, CD44/CD24, and CD10/CD44 marker combinations showed significant variability in salisphere growth. Nevertheless, these marker combinations were also tested *in vivo* for tumorigenic potential.

Combination of ALDH activity and CD44 expression selects highly tumorigenic cells

As a critical follow-up to the *in vitro* studies, putative cancer stem cell markers were verified *in vivo* to ascertain self-renewal and tumorigenic potential. We first decided to FACS-sort for ALDH/CD44 and implant these cells *in vivo* to observe possible differences in tumorigenic potential. Because of the extended length of time needed to grow low passage cell line-derived tumors, we digested UM-HMC-3A (passage 14) and UM-HMC-3B (passage 27) xenograft tumors and then sorted these cells for ALDH/CD44. The sorted cells were seeded with primary human endothelial cells into biodegradable scaffolds, and transplanted into the SCID mice, as described earlier (38-40). Either 400 of the $ALDH^{high}CD44^{high}$ cells, or 4,000 of the $ALDH^{low}CD44^{low}$ cells (*i.e.* 10x more cells), were transplanted into mice and serially passaged *in vivo*. In the first generation xenografts, we observed that only $ALDH^{high}CD44^{high}$ cells generated tumors (Figure III.5A and 5B). Interestingly, $ALDH^{high}CD44^{high}$-sorted cells were able to generate tumors with similar histology as compared to the tumors generated from the unsorted cells (Figure III.5D). We next took the tumors generated with $ALDH^{high}CD44^{high}$ cells, digested, stained, re-sorted, and transplanted 400 $ALDH^{high}CD44^{high}$ or 4,000

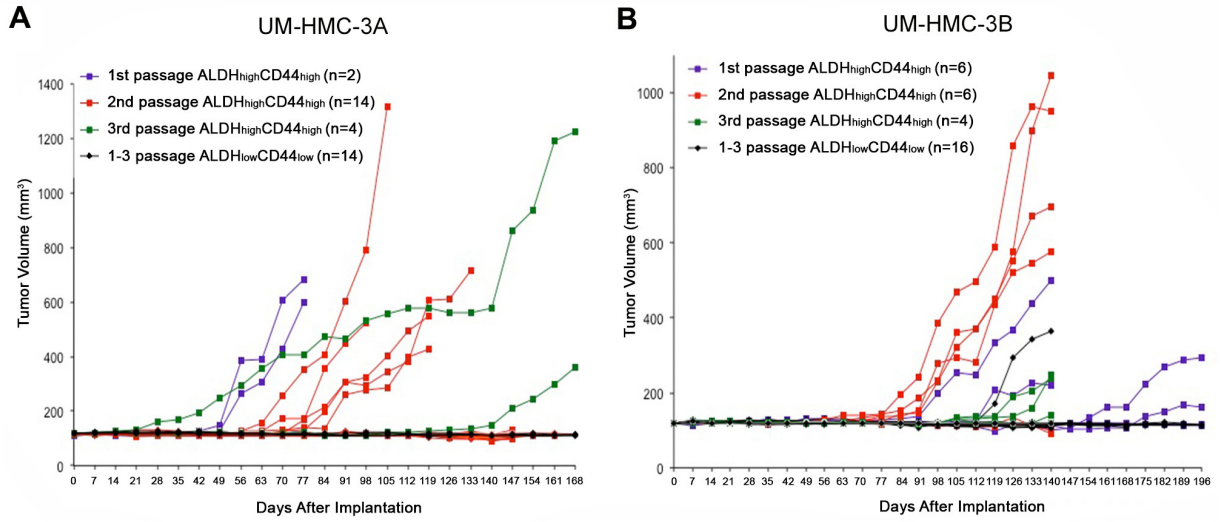

C

Implanted Cells	Tumors formed/mice			
	1st passage xenografts	2nd passage xenografts	3rd passage xenografts	Total
UM-HMC-3A ALDH^{high}CD44^{high} 400 Cells/Scaffold	2 of 2 (100%)	5 of 14 (36%)	2 of 4 (50%)	9 of 20 (45%)
UM-HMC-3A ALDH^{low}CD44^{low} 4,000 Cells/Scaffold	0 of 2 (0%)	0 of 14 (0%)	0 of 4 (0%)	0 of 20 (0%)
UM-HMC-3B ALDH^{high}CD44^{high} 400 Cells/Scaffold	3 of 6 (50%)	4 of 6 (67%)	2 of 4 (50%)	9 of 16 (56%)
UM-HMC-3B ALDH^{low}CD44^{low} 4,000 Cells/Scaffold	0 of 6 (0%)	1 of 6 (17%)	0 of 4 (0%)	1 of 16 (6%)

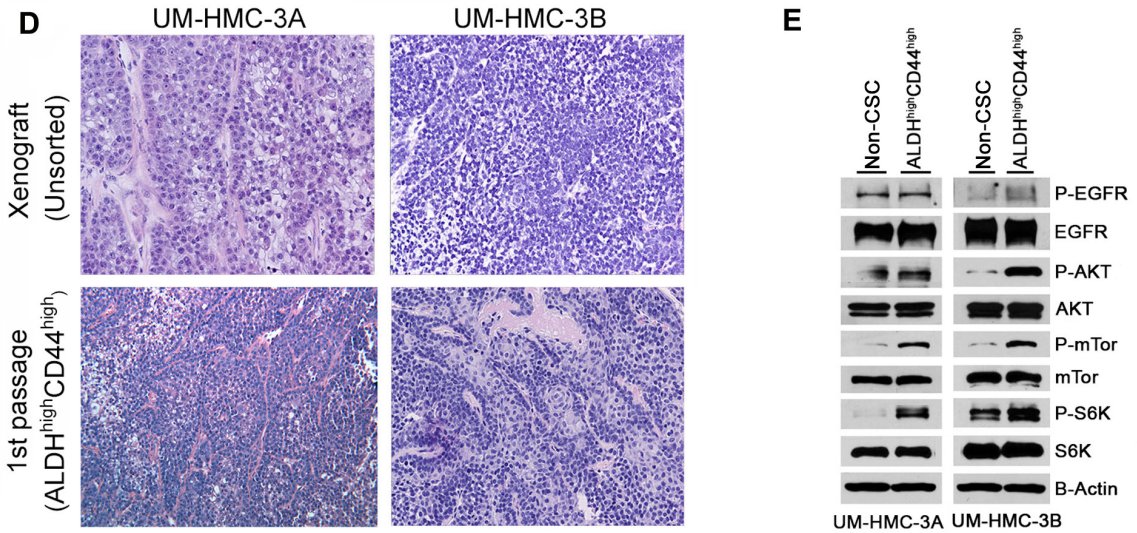

Figure III.5: Tumorigenic potential of low passage mucoepidermoid carcinoma cells sorted for ALDH/CD44. A., B. Graphs depicting tumor volume of **A.** UM-HMC-3A or **B.** UM-HMC-3B xenograft cells FACS-sorted for ALDH/CD44. Scaffolds were seeded with either 400 $ALDH^{high}CD44^{high}$ or 4,000 $ALDH^{low}CD44^{low}$ cells and transplanted into the subcutaneous space of SCID mice. Existing tumors were retrieved, re-sorted and 400 $ALDH^{high}CD44^{high}$ or 4,000 $ALDH^{low}CD44^{low}$ cells seeded into new scaffolds, and serially passaged *in vivo*. **C.** Table depicting the number of tumors grown in the $ALDH^{high}CD44^{high}$ *versus* $ALDH^{low}CD44^{low}$ populations for each passage performed. **D.** H&E staining of tumors generated with FACS-sorted $ALDH^{high}CD44^{high}$ and $ALDH^{low}CD44^{low}$ cells. Images were taken at 100X. **E.** UM-HMC-3A and UM-HMC-3B cells were sorted for $ALDH^{high}CD44^{high}$ or combined $ALDH^{high}CD44^{low}$, $ALDH^{low}CD44^{high}$, and $ALDH^{low}CD44^{low}$ (non-CSC population). NP-40 lysis buffer was used to prepare whole cell lysates that were resolved using PAGE. Membranes were probed using antibodies a 1:1000 dilution against human mTor, p-mTor, Akt, p-Akt, S6K, p-S6K, p-EGFR; 1:2000 dilution of EGFR, and beta-actin.

$ALDH^{low}CD44^{low}$ cells into new mice. While the $ALDH^{high}CD44^{high}$ cells generated tumors in 9/20 transplants, $ALDH^{low}CD44^{low}$ cells generated tumors in only 1/20 transplants (Figure III.5A and 5B). Finally, we did a third cycle of *in vivo* passaging of the $ALDH^{high}CD44^{high}$ tumors. Here, only mice transplanted with $ALDH^{high}CD44^{high}$ cells generated tumors (Figure III.5A and 5B). Notably, no secondary tumors were generated from the only $ALDH^{low}CD44^{low}$ tumor that grew in this experiment. Overall, we observed 18 tumors generated with 400 $ALDH^{high}CD44^{high}$ cells, while only one tumor was generated when 4,000 $ALDH^{low}CD44^{low}$ cells were transplanted (Figure III.5C). Collectively, these data showed that $ALDH^{high}CD44^{high}$ cells exhibit enhanced tumorigenic potential, when compared with $ALDH^{low}CD44^{low}$ cells. Notably, the unique tumorigenic potential of $ALDH^{high}CD44^{high}$ cells persisted over multiple *in vivo* tumor passages, suggesting enhanced self-renewal of this sub-population of cells.

As the $ALDH^{high}CD44^{high}$ showed elevated tumorigenic potential, we performed western blot analysis to determine if UM-HMC-3A and UM-HMC-3B $ALDH^{high}CD44^{high}$

cells showed activation of the PI3K-Akt pathway important in cancer stem cells function. While the levels of EGFR and phosphor-EGFR remained stable between the combined $ALDH^{high}CD44^{low}$, $ALDH^{low}CD44^{high}$, and $ALDH^{low}CD44^{low}$ populations (non-stem cell) and $ALDH^{high}CD44^{high}$ cells, there was an upregulation of phosphor-mTor and phospho-S6K in the UM-HMC-3A cells (Figure III.5E). In the UM-HMC-3B cells, we also observed an upregulation of p-mTor and p-S6K as well as an upregulation of p-Akt (Figure III.5E). Together these results suggest that the PI3K-Akt pathway is upregulated in the $ALDH^{high}CD44^{high}$ compared to the non-stem cell population.

We next wanted to understand whether these differences in tumorigenic potential where reproducible using higher passage cells in independent *in vivo* experiments. We sorted UM-HMC-3B cells (passage 103) for $ALDH^{high}CD44^{high}$ and $ALDH^{low}CD44^{low}$, seeded the sorted cells with primary human endothelial cells into biodegradable scaffolds, and transplanted them into the SCID mice. Tumors were measured weekly and considered palpable once they reached 200 mm^3 (Figure III.6A, Table III.2). Kaplan-Meyer analysis demonstrated that the tumorigenic potential of $ALDH^{high}CD44^{high}$ cells was higher than the $ALDH^{low}CD44^{low}$ cells (log-rank test, p=0.025) (Figure III.6B). We performed regression analysis to determine the impact of ALDH/CD44 marker combination on tumor growth rate. Once tumors had grown to 200 mm^3 we performed a linear mixed effect model on the tumor size, including the following variables in our model of log tumor volume: size of tumor at first palpability; $ALDH^{high}CD44^{high}$ state; time; time by $ALDH^{high}CD44^{high}$ cell state interaction (Figure III.6C). As expected, the volume of the tumor increased proportionally to the size of the initially palpable tumor (p=0.0094), as well as with time (p=0.0037). There was also a significant increase in

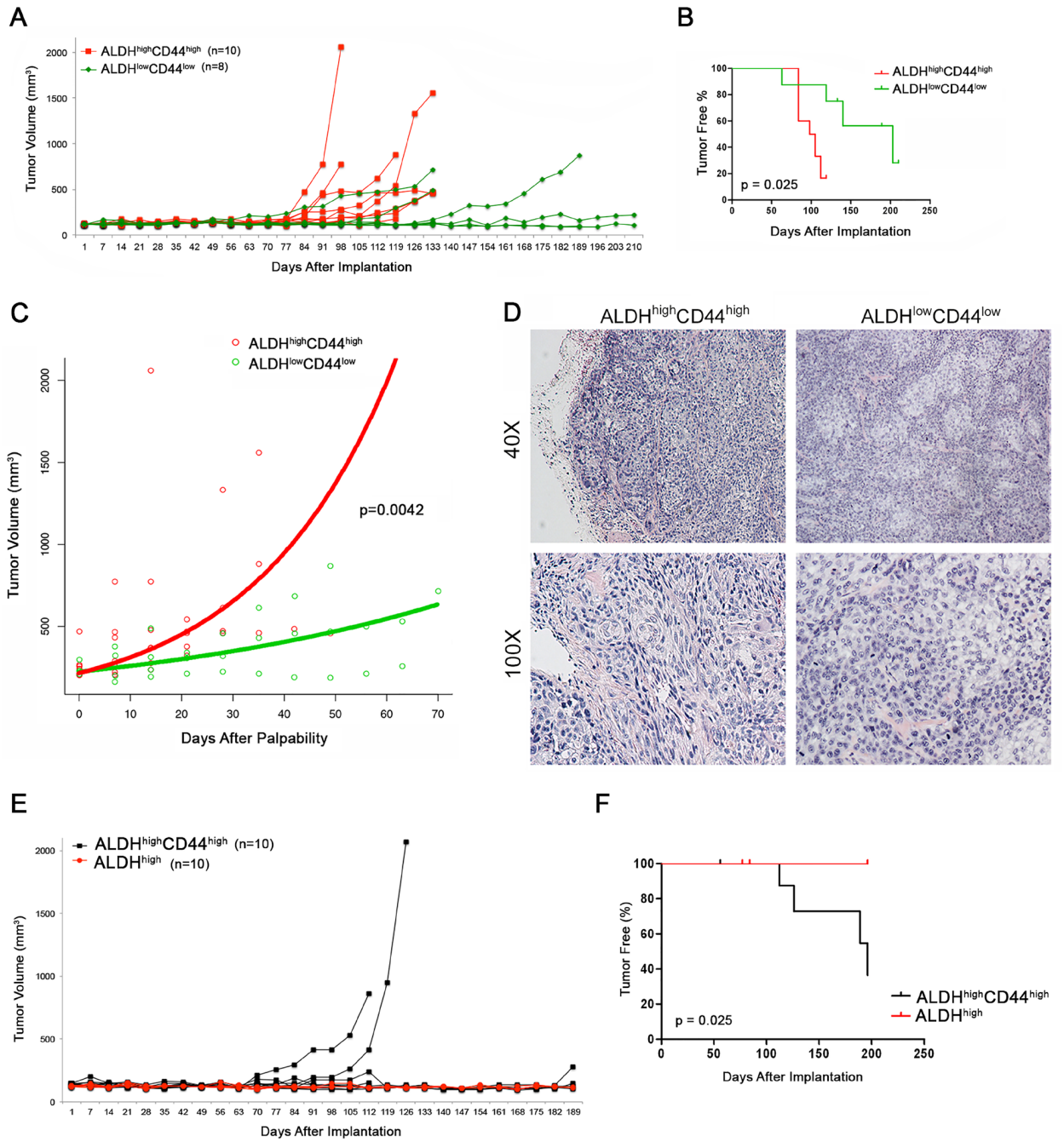

Figure III.6: Tumorigenic potential of high passage mucoepidermoid carcinoma cells sorted for ALDH/CD44. A. Graph depicting the volume of tumors generated by the transplantation of FACS-sorted UM-HMC-3B cells ($ALDH^{high}C44^{high}$ or $ALDH^{low}CD44^{low}$) in immunode cient mice. 5,000 sorted UM-HMC-3B cells (passage 103) and 900,000 endothelial (HDMEC) cells were seeded on biodegradable scaffolds and transplanted into the subcutaneous space of SCID mice. Tumors were measured weekly and mice were euthanized once the tumors reached 700-1,500 mm^3. **B.** Kaplan-Meyer analysis of time to palpability of tumors generated with $ALDH^{high}CD44^{high}$ or $ALDH^{low}CD44^{low}$ cells. Tumors were

considered palpable once they reached 200 mm^3. **C.** Regression analysis of growth after palpability (200 mm^3) of tumors generated with FACS-sorted $ALDH^{high}CD44^{high}$ or $ALDH^{low}CD44^{low}$ cells. **D.** H&E staining of tumors generated with FACS-sorted $ALDH^{high}CD44^{high}$ and $ALDH^{low}CD44^{low}$ cells. Images were taken at 40X and 100X. **E.** Graph depicting the volume of tumors generated by the transplantation of FACS-sorted UM-HMC-3B cells ($ALDH^{high}C44^{high}$ or $ALDH^{high}$) in immunode cient mice. 5,000 sorted UM-HMC-3B cells (passage 104) and 900,000 endothelial (HDMEC) cells were seeded on biodegradable scaffolds and transplanted into the subcutaneous space of SCID mice. Tumors were measured weekly and mice were euthanized once the tumors reached 700-1,500 mm^3. **F.** Kaplan-Meyer analysis of time to palpability of tumors generated with $ALDH^{high}C44^{high}$ or $ALDH^{high}$ cells.

tumor growth rate for $ALDH^{high}CD44^{high}$ tumors compared to $ALDH^{low}CD44^{low}$ tumors ($p=0.0042$). We plotted the time since first-palpability *versus* tumor volume. Overlaid on this graph are the model-derived growth predictions. To generate the curves for each group, we used the mean size at time of first palpability for each group, and the appropriate estimated coefficients and interactions from the model. Tumors generated with $ALDH^{high}CD44^{high}$ cells showed a distinctly different morphology from the tumors generated with $ALDH^{low}CD44^{low}$ cells (Figure III.6D). Both are characterized by large solid areas, but tumors generated with $ALDH^{high}CD44^{high}$ cells showed more intermediate-like cells, with spindle shape, oval nuclei and highly anaplastic areas. In contrast, the tumors generated with $ALDH^{low}CD44^{low}$ cells showed a more monotonous morphology with round cells exhibiting round nuclei and clusters of epidermoid-like cells with eosinophilic cytoplasm. Interestingly, anaplastic cells were more rare in the tumors generated with $ALDH^{low}CD44^{low}$ cells.

As the majority of high passage UM-HMC-3B cells stain highly for CD44, we next questioned whether ALDH could be used as a single marker for this aggressive cancer stem cell phenotype. To investigate this, we took high passage (passage 104) UM-

HMC-3B cells and sorted for ALDH^{high}CD44^{high} and ALDH^{high} then transplanted these cells with human endothelial cells on biodegradable scaffolds into the SCID mice. In these studies, we were able to generate tumors in 4 (out of 10) scaffolds seeded with ALDH^{high}CD44^{high} cells while no tumors were generated in the ALDH^{high} cells (Figure III.6E). Our Kaplan-Meyer analysis shows that the tumorigenic potential of ALDH^{high}CD44^{high} cells is greater than the ALDH^{high} cells (log-rank test, p-0.025) (Figure III.6F). These data suggest that ALDH by itself does not enrich for an aggressive cancer stem cell phenotype in salivary gland mucoepidermoid carcinoma.

We next performed FACS analysis of the ALDH/CD44 sorted xenograft tumors over multiple passages to verify if ALDH^{high}CD44^{high} cells were able to differentiate. We observed that tumors generated with pure populations of ALDH^{high}CD44^{high} cells were able to continuously repopulate the other ALDH/CD44 sub-populations and that the fraction of the different sub-populations was consistent with the original unsorted xenograft tumors (Figure III.7A and 7B). We also performed immunofluorescence staining of the original unsorted tumors and compared with the 1st passage ALDH^{high}CD44^{high}-sorted tumors. We found once again that the ALDH^{high}CD44^{high} generated tumors were able to repopulate the remaining three sub-populations (Figure III.7C). We also performed immunofluorescence staining in tumors generated from our second independent experiment with FACS-sorted ALDH^{high}CD44^{high} cells or ALDH^{low}CD44^{low} cells to determine the ability of these relatively pure sub-populations of cells to regenerate complex tumors once transplanted in mice. We found that CD44 stained ubiquitously the vast majority of the cells in all tumors, including those

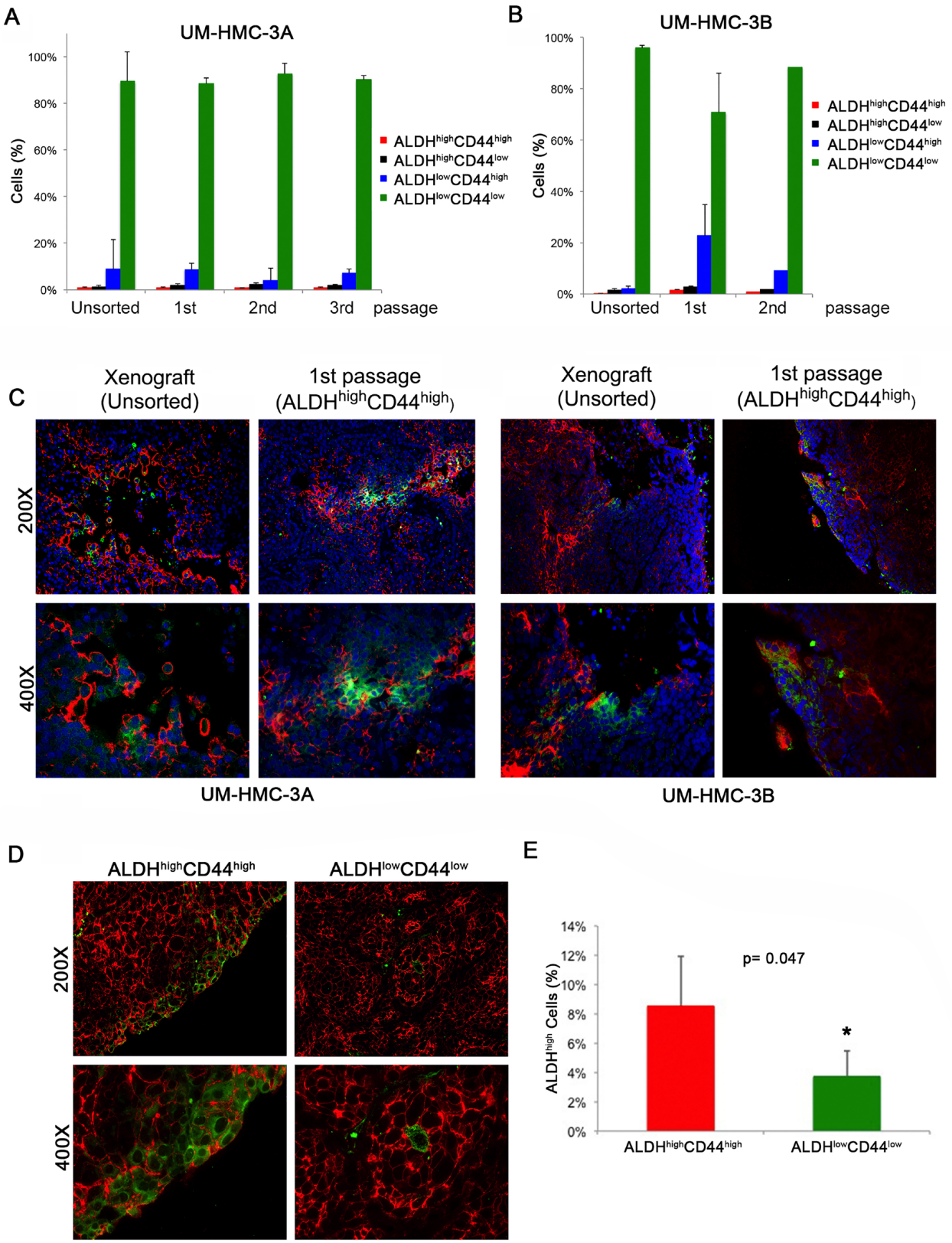
A
UM-HMC-3A
100%
80%
60%
40%
20%
0%
Cells (%)
Unsorted
1st
2nd
3rd
passage
ALDHhighCD44high
ALDHhighCD44low
ALDHlowCD44high
ALDHlowCD44low
B
UM-HMC-3B
100%
80%
60%
40%
20%
0%
Cells (%)
Unsorted
1st
2nd
passage
ALDHhighCD44high
ALDHhighCD44low
ALDHlowCD44high
ALDHlowCD44low
C
Xenograft (Unsorted)
1st passage (ALDHhighCD44high)
Xenograft (Unsorted)
1st passage (ALDHhighCD44high)
200X
400X
UM-HMC-3A
UM-HMC-3B
D
ALDHhighCD44high
ALDHlowCD44low
200X
400X
E
14%
12%
10%
8%
6%
4%
2%
0%
ALDHhigh Cells (%)
p= 0.047
*
ALDHhighCD44high
ALDHlowCD44low

Figure III.7. Characterization of xenograft tumors generated with cells sorted for ALDH/CD44. A. Graph depicting the percentage of ALDH/CD44 cells in tumors generated with FACS-sorted UM-HMC-3A (passage 14) over three *in vivo* passages. **B.** Graph depicting the percentage of ALDH/CD44 staining cells in tumors generated with FACS-sorted UM-HMC-3B (passage 27) over two *in vivo* passages. **C.** Immuno uorescence staining of tumors generated from the original unsorted UM-HMC-3A (passage 14) and UM-HMC-3B (passage 27) xenograft cells compared to tumors generated from 400 $ALDH^{high}CD44^{high}$ cells sorted from the original xenografts. CD44 is stained in red while ALDH-1 is stained in green. **D.** Immuno uorescence staining of tumors generated with FACS-sorted $ALDH^{high}CD44^{high}$ or $ALDH^{low}CD44^{low}$ cells. CD44 is stained in red while ALDH-1 is stained in green. **E.** Graph depicting the percentage of $ALDH^{high}$ cells in tumors generated with cells FACS-sorted for $ALDH^{high}CD44^{high}$ or $ALDH^{low}CD44^{low}$ as determined by flow cytometry with Aldefluor.

generated with $ALDH^{low}CD44^{low}$ cells. The pattern of ALDH expression was different. Tumors generated with FACS-sorted $ALDH^{high}CD44^{high}$ showed more ALDH1 staining than tumors generated with $ALDH^{low}CD44^{low}$ cells (Figure III.7D and 7E). Interestingly, the presence of cells that are positive for the stem cell marker ALDH1 in tumors generated with FACS-sorted $ALDH^{low}CD44^{low}$ cells suggests that perhaps some of these cells are capable of dedifferentiation. Nevertheless, the percentage of $ALDH^{high}$ cells was lower in the tumors generated with $ALDH^{low}CD44^{low}$ cells when compared to tumors generated with $ALDH^{high}CD44^{high}$ cells (Figure III.7E).

Tumorigenic potential of mucoepidermoid carcinoma cells FACS-sorted for CD10/CD24, CD44/CD24, CD10/CD44

In addition to the work performed with ALDH/CD44, we have also performed extensive testing of three additional putative stem cell marker combinations (CD10/CD24, CD44/CD24, CD10/CD44) to determine if these markers could enrich for cancer stem cells *in vivo*. We transplanted UM-HMC-3B FACS-sorted cells (CD10/CD24 or

CD10/CD44) into mice, as described above. We observed only two tumors generated upon transplantation of the CD10/CD24-sorted cells, 1 (out of 6) in the $CD10^{high}CD24^{high}$

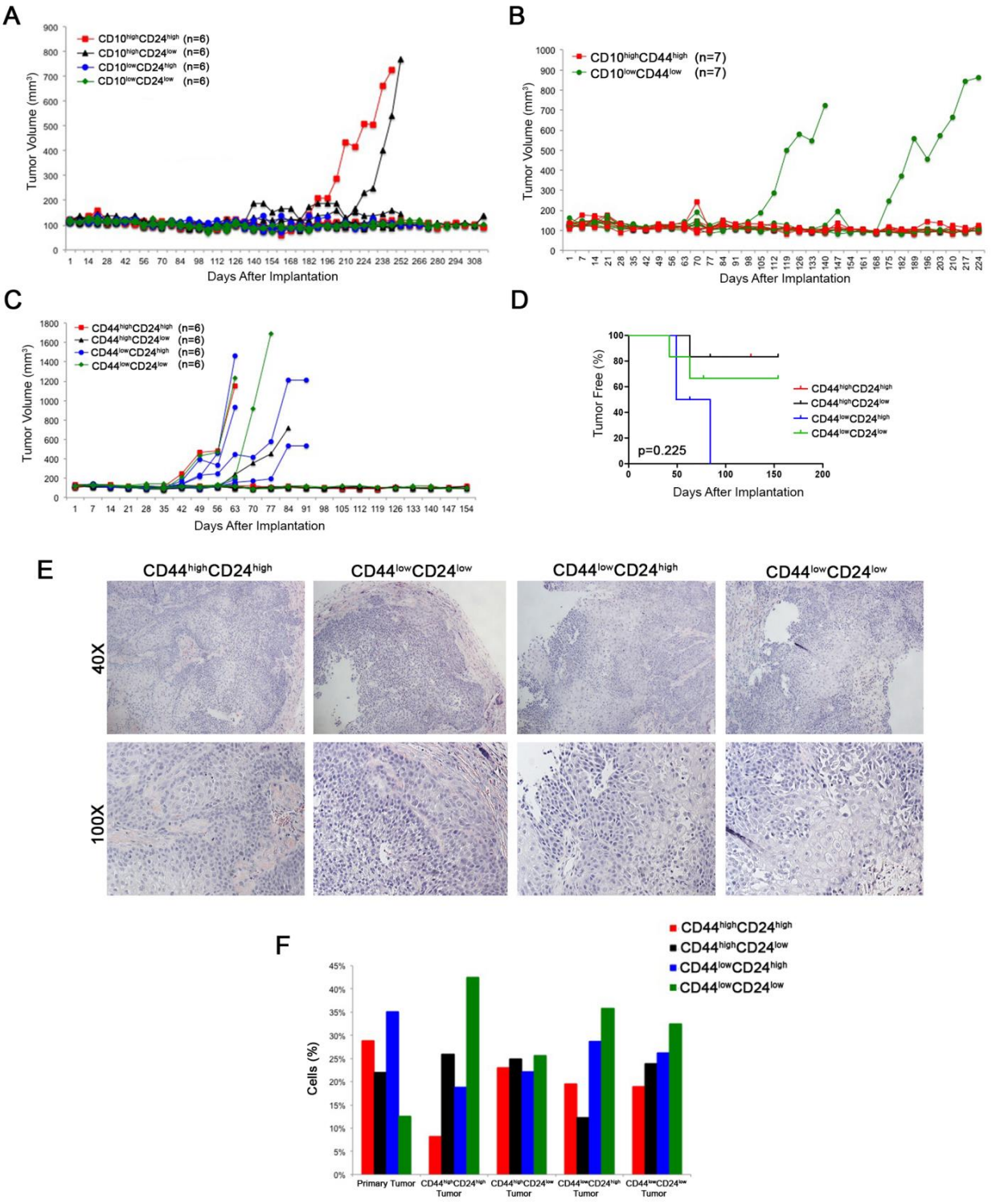

Figure III.8. *In-Vivo* tumorigenicity of low passage CD44/CD24 sorted cells. A. Tumor growth chart of CD10/CD24 sorted cells. Scaffolds were seated with 2,000 CD10/CD24 sorted cells and 900,000 HDMEC cells. **B.** Tumor growth chart of CD10/CD44 sorted cells. Scaffolds were seated with either 500 $CD10^{high}CD44^{high}$ cells or 5,000 $CD10^{low}CD44^{low}$ cells along with 900,000 HDMEC cells. **C.** Tumor growth chart of tumors generated from UM-HMC-3B (passage 27) 9^{th} generation xenograft cells that were sorted according to the expression of CD44/CD24. **D.** Graph depicting the time to palpability of CD44/CD24 sorted tumors. Tumors were considered palpable once they reached 200 mm^3. **E.** H&E staining of sections taken from UM-HMC-3B (passage 27) 9^{th} generation xenograft CD44/CD24 sorted cells. **F.** Flow cytometry analysis of UM-HMC-3B (passage 27) 9^{th} generation xenograft CD44/CD24 sorted tumors. Primary tumors were digested and stained for CD44 and CD24.

group and 1 (out of 6) in the $CD10^{high}CD24^{low}$ group (Figure III.8A, Table III.2). Further, only two $CD10^{low}CD44^{low}$ tumors were formed when CD10/CD44-sorted cells were transplanted (Figure III.8B, Table III.2). These data demonstrated that these two marker combinations involving CD10 do not select for uniquely tumorigenic cancer stem cells.

We next performed experiments with the CD44/CD24 marker combination using cells that were sorted from ongoing UM-HMC-3B xenograft tumors. Because different sub-populations of CD44/CD24 are used to isolate cancer stem cells in different cancer types, we FACS-sorted all four sub-populations and implanted them as described above. Four (out of 6) $CD44^{low}CD24^{high}$ transplants grew tumors, whereas only 1 (out of 6) mouse transplanted with $CD44^{high}CD24^{high}$ or $CD44^{high}CD24^{low}$, and 2 (out of 6) mice developed tumors when transplanted with $CD44^{low}CD24^{low}$ cells (Figure III.8C; Figure III.9F, Table III.2). While these initial results suggested that $CD44^{low}CD24^{high}$ sub-populations were more tumorigenic, we did not observe significant differences in the time to palpability upon Kaplan-Meyer analyses (Figure III.8D), nor did we observe that a certain sub-population of cells generated tumors with a particularly aggressive histology (Figure III.8E). We then digested the tumors and re-stained for CD44/CD24 to analyze how the sub-populations of cells redistributed during growth in mouse. In the

original xenograft tumors used to collect the cells for this experiment, the $CD44^{low}CD24^{low}$ sub-population was the lowest (Figure III.8F). In contrast, in the tumors generated from FACS-sorted cells, we observed an overall trend for high fractions of $CD44^{low}CD24^{low}$ cells irrespective of what was the sub-population used to generate the tumors.

These surprising results led us to repeat this experiment using cells sorted directly from the UM-HMC-3B cell line. In this experiment, the four sub-populations of cells sorted for CD44/CD24 were able to grow tumors (Figure III.9A, 9F, Table III.2), but no difference was seen in the time to palpability ($p=0.403$) among these four experimental conditions (Figure III.9B). Nevertheless, we did observe significant differences in tissue morphology. The $CD44^{low}CD24^{low}$ and $CD44^{high}CD24^{high}$ tumors grew more aggressively and showed a solid morphology with large areas of anaplasia. In contrast, $CD44^{high}CD24^{low}$ and $CD44^{low}CD24^{high}$ cells generated tumors exhibiting a less aggressive, mucous cell phenotype (Figure III.9C). We again performed regression analyses to determine if differences in tumor growth rates existed based on the different sub-populations of cells that were used to generate these tumors. Based on the significant histologic differences that we observed between four combinations of CD24 and CD44 cells, we included the following variables in our model of log tumor volume: size of tumor at first palpability; CD24 state; CD44 state; CD24 by time interaction; CD44 by time interaction; and CD24 by CD44 by time interaction. The rate of tumor growth was significantly less in CD24-positive ($p=0.0003$), and CD44-positive ($p=0.0003$) tumors compared to the negative populations. There was a significant

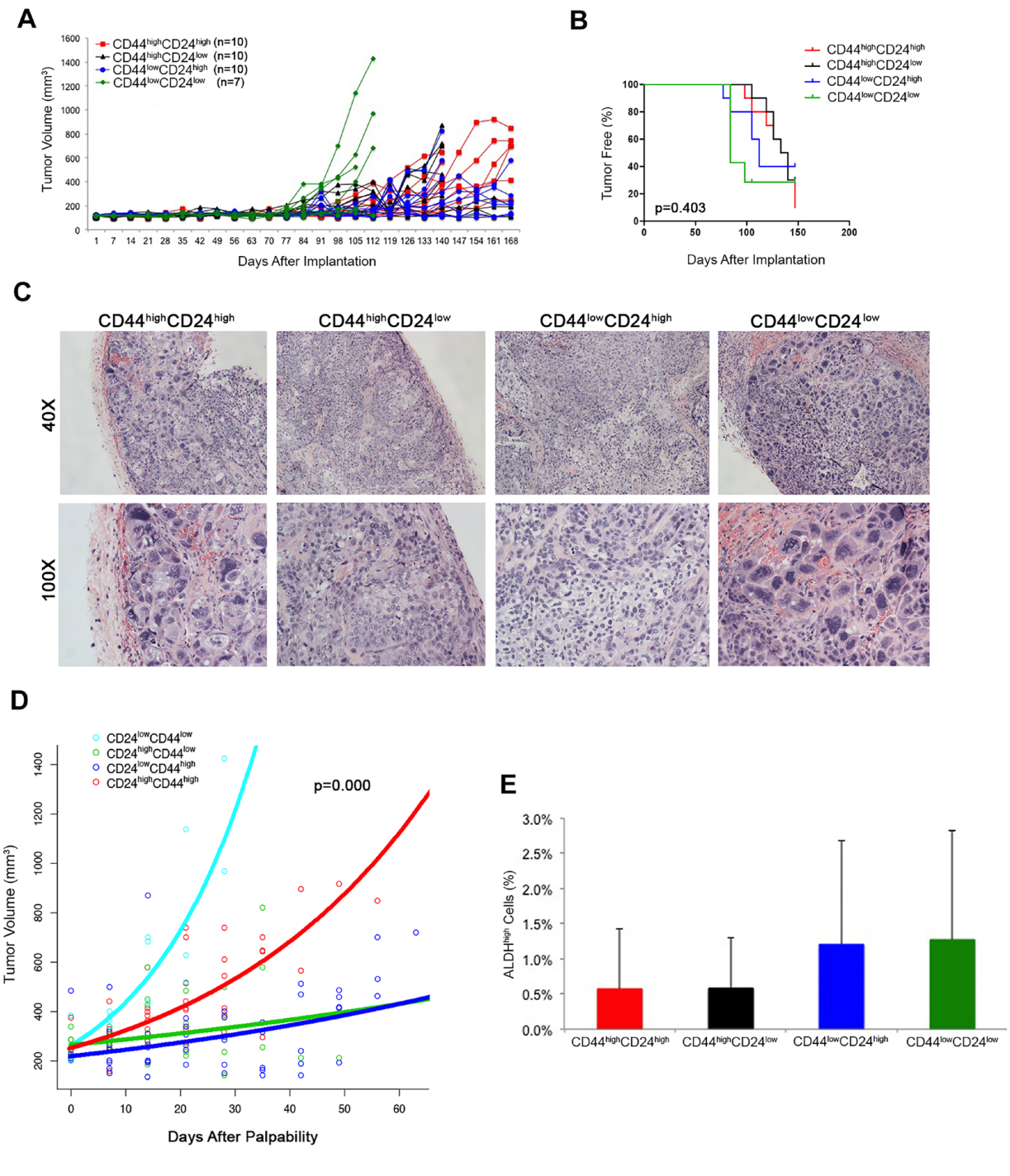

F

	Tumors formed/mice			
Implanted Cells	CD44^{high}CD24^{high}	CD44^{high}CD24^{low}	CD44^{low}CD24^{high}	CD44^{low}CD24^{low}
UM-HMC-3B Cell Line	9 of 10 (90%)	7 of 10 (70%)	8 of 10 (80%)	5 of 9 (56%)
UM-HMC-3B High Passage Cell Line Xenograft	1 of 6 (17%)	1 of 6 (17%)	4 of 6 (67%)	**2 of 6 (34%)**

Figure III.9. Tumorigenic potential of mucoepidermoid carcinoma cells sorted for CD44/CD24. A. *In vivo* transplantation of 5,000 UM-HMC-3B (passage 103) FACS-sorted cells ($CD44^{high}CD24^{high}$, $CD44^{high}CD24^{low}$, $CD44^{low}CD24^{high}$, or $CD44^{low}CD24^{low}$) with 900,000 endothelial (HDMEC) cells seeded on biodegradable scaffolds and transplanted into the subcutaneous space of SCID mice. **B.** Kaplan-Meyer analysis of time to palpability of tumors generated with cell sorted for CD44/CD24. Tumors were considered palpable once they reached 200 mm^3. **C.** H&E staining of tumors generated by the transplantation of UM-HMC-3B cells sorted for CD44/CD24. Images were taken at 40X and 100X. **D.** Regression analysis of growth after palpability (200 mm^3) of tumors generated with cells FACS-sorted for CD44 and CD24. **E.** Graph depicting the percentage of $ALDH^{high}$ cells in tumors generated with cells FACS-sorted for CD44/CD24. **F.** Table depicting the number of tumors formed in each CD44/CD24 sorted sup-population in both the UM-HMC-3B cell line and the UM- HMC-3B low passage cell line xenograft model.

interaction effect, which yielded a higher rate of growth for $CD44^{high}CD24^{high}$ tumors ($p<0.0001$). We again plotted the time since first-palpability *versus* tumor volume (Figure III.9D). To further investigate the absence of differences in tumor initiating potential (as determined by time to palpability) among the cells sorted for CD44/CD24, we analyzed whether any sub-population was enriched for ALDH. Interestingly, no significant difference in the fraction of $ALDH^{high}$ cells was observed when we compared tumors generated with FACS-sorted $CD44^{high}CD24^{high}$, $CD44^{high}CD24^{low}$, $CD44^{low}CD24^{high}$, or $CD44^{low}CD24^{low}$ cells (Figure III.9E). Collectively, these data indicate that the CD44/CD24 marker combination does not enable consistent identification of a unique population of highly tumorigenic cells in salivary gland mucoepidermoid carcinomas.

Discussion

Poor survival of patients with advanced stage salivary gland mucoepidermoid carcinomas demand better understanding of the pathobiology of these tumors and the development of new, mechanism-based therapies. Research in other cancer types

suggests that cancer stem cells play an important role in resistance to therapy and tumor relapse (18, 41-44). Much has been done therapeutically to target the self-renewal pathways important in cancer stem cell function. Several groups have therapies to inhibit the Notch, Wnt, and Hedgehog pathways (46). In addition, Her2-specific antibodies have been used to target breast cancer stem cells while IL-6 antibodies have been used in head and neck squamous cell carcinomas (47, 27). The relentless growth of mucoepidermoid carcinomas, compounded with resistance to every therapy that was attempted this far, is a major clinical challenge that might be correlated with the function of cancer stem cells. However, whether or not cancer stem cells play a role in the pathobiology of salivary mucoepidermoid carcinomas has not been investigated due a lack of adequate research models *(i.e*. cell lines, xenograft models) and unavailability of markers that enable the identification of sub-populations of cells with unique tumorigenic potential. Previously, we generated and characterized a number of cells lines and xenograft models of salivary gland mucoepidermoid carcinoma (38).

By co-transplanting sorted human mucoepidermoid carcinoma cells with primary human microvascular endothelial cells in biodegradable scaffolds, we were able to generate xenograft tumors vascularized with human blood vessels, as previously described (38-40). We have showed that this experimental approach enables the crosstalk between tumor cells and endothelial cells of the same species, which has a demonstrable impact to both tumor growth as well as response to therapy (48). Here, we demonstrated that the combination of ALDH activity and CD44 expression enables the identification of highly tumorigenic cells in salivary gland mucoepidermoid carcinoma. While primary cells are a preferred model to study, we are limited by the

rarity by these tumors, as well as the difficulty and length of time needed to grow primary cells *in vitro* and *in vivo*. However, the results presented here, together with the recent characterization of cell lines and xenograft models of mucoepidermoid carcinoma [38], will enable studies focused on the understanding of the mechanisms underlying the role of cancer stem cells in resistance to therapy, and the development of strategies to overcome this resistance.

While the salisphere assay is a useful method to screen for cancer stem cells markers *in-vitro*, the ability of these markers to enrich for cells that are able to self-renew and are multipotent must be verified *in-vivo*. Most of these *in vivo* experiments lasted around 200 days, and some of them lasted more than one year (*e.g.* sequential *in vivo* passaging of sorted cells). The extended time necessary to achieve tumor palpability, and the relatively slow tumor growth after palpability consumed significant resources and delayed the progression of this work. However, we believe that the results observed in these preclinical experiments reflect the normal behavior of human mucoepidermoid carcinomas, which are slow growing, albeit relentless, tumors.

A series of complementary independent *in vivo* studies demonstrated that the ALDH/CD44 marker combination enriches for cancer stem cells in mucoepidermoid carcinomas. While ALDH can be used as an independent marker for cancer stem cells in other cancer types, we have demonstrated that a two-marker combination of ALDH and CD44 is necessary to enrich for this aggressive cancer stem cell phenotype (10). In contrast, cells sorted for CD10/CD24 or CD10/CD44 showed differences in salisphere formation, but poor ability to generate tumors *in vivo*. We concluded that these marker combinations do not enrich for cancer stem cells, at least in the models studied here.

We also concluded that the CD44/CD24 combination does not enrich for cancer stem cells. In this case, we observed differences in salisphere formation and tumor growth. However, the sub-populations of interest were not consistent from experiment to experiment. Interestingly, several tumors generated in these experiments were very aggressive, showing solid morphology with large areas of anaplasia. Paradoxically, these aggressive tumors were observed primarily when cells sorted for $CD44^{high}CD24^{high}$ or $CD44^{low}CD24^{low}$ were transplanted. A mechanistic understanding of these puzzling findings is beyond the scope of this manuscript. However, these data reinforced the concept that the CD44/CD24 combination is likely not a viable marker combination for mucoepidermoid carcinoma cancer stem cells.

The PI3K-Akt signaling pathway has been found to be important in the maintenance of cancer stem cells (49, 50). Interestingly, the EGFR and HER2-Akt-mTOR pathways are activated in salivary gland cancer (51). We observed that $ALDH^{high}CD44^{high}$ cells potently express P-mTor and p-S6K, when compared to control cells. Considering the promising results of clinical and preclinical studies with rapamycin and rapalogs, the observation that mucoepidermoid carcinoma stem cells present high constitutive activity of the mTor pathway potentially has considerable translational impact. Indeed, these results might lead to a new therapeutic target for this malignancy that will be explored in future studies by our laboratory.

While we have concluded from our studies that $ALDH^{high}CD44^{high}$ cells demonstrate CSC properties, further research must be done to verify if both ALDH and CD44 play an active role in the maintenance of this stem cell phenotype. ALDH1 has been widely used as a cancer stem cells marker due to its role in normal stem cells

function. However, whether or not it plays an active role in cancer stem cell maintenance in mucoepidermoid carcinoma is unclear (23). Further, little is known about the role of CD44 in the progression of mucoepidermoid carcinomas. CD44 has been shown to play an important role in resistance to radiation and chemotherapy and may play a role in tumor recurrence of head and neck squamous cell carcinomas (52). The protein is encoded by one gene, but due to post-transcriptional modifications and alternative splicing, many variants of CD44 exist (52). Studies have implicated CD44v6 to be more effective in isolating CSC, however, work in HNSCC showed similar levels of expression between CD44s and CD44v6 suggesting that this effect may be specific to various cancer types (53-57). The antibody that was used in our studies was not specific to the CD44v6 splice variant. It is possible to using antibodies specific to this variant may lead to a further enrichment of the cancer stem cells in mucoepidermoid carcinomas, but this hypothesis was not tested here.

Collectively, this work demonstrates that salivary gland mucoepidermoid carcinomas exhibit a small sub-population of cells with uniquely high tumorigenic potential. These cells can be identified by high ALDH activity and CD44 expression. Considering the role of cancer stem cells in tumor recurrence and resistance to therapy in other glandular cancers (*e.g.* breast, pancreatic), it is tempting to predict that these cells may also play a functional role in the relentless growth and resistance to therapy typically exhibited by human mucoepidermoid carcinomas. These results suggest that patients with mucoepidermoid carcinoma might benefit from the targeted ablation of this sub-population of uniquely tumorigenic cancer stem cells.

References

1. Spiro RH. Salivary neoplasms: overview of a 35-year experience with 2807 patients. Head Neck Surg 1986;8:177–84.

2. Eversole LR, Sabes WR, Rovin S. Aggressive growth and neoplastic potential of odontogenic cysts: with special reference to central epidermoid and mucoepidermoid carcinomas. Cancer 1975;35:270–82.

3. Ezsiás A, Sugar AW, Milling MA, Ashley KF. Central mucoepidermoid carcinoma in a child. J Oral Maxillofac Surg 1994;52:512–5.

4. Gingell JC, Beckerman T, Levy BA, Snider LA. Central mucoepidermoid carcinoma. Review of the literature and report of a case associated with an apical periodontal cyst. Oral Surg Oral Med Oral Pathol 1984;57:436–40.

5. Ito FA, Ito K, Vargas PA, Almeida OP, Lopes MA. Salivary gland tumors in a Brazilian population: a retrospective study of 496 cases. Int J Oral Maxillofac Surg 2005;34:533–6.

6. Luna MA. Salivary mucoepidermoid carcinoma: revisited. Adv Anat Pathol 2006;13:293–307.

7. Pires FR, Almeida OP, de Araújo VC, Kowalski LP. Prognostic factors in head and neck mucoepidermoid carcinoma. Arch Otolaryngol Head Neck Surg 2004;130:174–80.

8. Bell D, Hanna EY. Salivary gland cancers: biology and molecular targets for therapy. Curr Oncol Rep 2012;14:166–74.

9. Al-Hajj M, Wicha MS, Benito-Hernandez A, Morrison SJ, Clarke MF. Prospective identification of tumorigenic breast cancer cells. Proc Natl Acad Sci USA 2003;100:3983–8.

10. Ginestier C, Hur MH, Charafe-Jauffret E, Monville F, Dutcher J, Brown M, et al. ALDH1 is a marker of normal and malignant human mammary stem cells and a predictor of poor clinical outcome. Cell Stem Cell 2007;1:555–67.

11. Prince ME, Sivanandan R, Kaczorowski A, Wolf GT, Kaplan MJ, Delerba P, et al. Identification of a subpopulation of cells with cancer stem cell properties in head and neck squamous cell carcinoma. Proc Natl Acad Sci USA 2007;104:973–8.

12. Hermann PC, Huber SL, Herrler T, Aicher A, Ellwart JW, Guba M, et al. Distinct populations of cancer stem cells determine tumor growth and metastatic activity in human pancreatic cancer. Cell Stem Cell 2007;1:313–23.

13. Ma S, Chan KW, Hu L, Lee TK, Wo JY, Ng IO, et al. Identification and characterization of tumorigenic liver cancer stem/progenitor cells. Gastroenterology 2007;132:2542–56.

14. Singh SK, Clarke ID, Terasaki M, Boon VE, Hawkins C, Squire J, et al. Identification of a cancer stem cell in human brain tumors. Cancer Res 2003;63:5821–8.

15. O'Brien CA, Pollett A, Gallinger S, Dick JE. A human colon cancer cell capable of initiating tumour growth in immunodefficient mice. Nature 2007;445:106–10.

16. Bapat SA, Mali AM, Koppikar CB, Kurrey NK. Stem and progenitor-like cells contribute to the aggressive behavior of human epithelial ovarian cancer. Cancer Res 2005;65:3025–9.

17. Hambardzumyan D, Squatrito M, Holland EC. Radiation resistance and stem-like cells in brain tumors. Cancer Cell 2006;10:454–6.

18. Korkaya H, Paulson A, Charafe-Jauffret E, Ginestier C, Brown M, Dutcher J, et al. Regulation of mammary stem/progenitor cells by PTEN/Akt/beta-catenin signaling. PLoS Biol 2009; 7:e1000121.

19. Diehn M, Cho RW, Lobo NA, Kalisky T, Dorie MJ, Kulp AN, et al. Association of reactive oxygen species levels and radioresistance in cancer stem cells. Nature 2009;458:780–3.

20. Russo JE, Hilton J. Characterization of cytosolic aldehyde dehydrogenase from cyclophosphamide resistant L1210 cells. Cancer Res 1988;48:2963-8.

21. Labrecque J, Bhat PV, Lacroix A. Purification and partial characterization of a rat kidney aldehyde dehydrogenase that oxidizes retinal to retinoic acid. Biochem Cell Biol 1993;71:85-9.

22. Riveros-Rosas H, Julian-Sanchez A, Pinã E. Enzymology of ethanol and acetaldehyde metabolism in mammals. Arch Med Res 1997;28:453-71.

23. Chute JP, Muramoto GG, Whitesides J, Colvin M, Safi R, Chao NJ, et al. Inhibition of aldehyde dehydrogenase and retinoid signaling induces the expansion of human hematopoietic stem cells. Proc Natl Acad Sci USA 2006;103:11707-12.

24. Ucar D, Cogle CR, Zucali JR, Ostmark B, Scott EW, Zori R, et al. Aldehyde dehydrogenase activity as a functional marker for lung cancer. Chem Biol Interact 2009;178:48-55.

25. Jiang F, Qiu Q, Khanna A, Todd NW, Deepak J, Xing L, et al. Aldehyde dehydrogenase 1 is a tumor stem cell-associated marker in lung cancer. Mol Cancer Res 2009;7:330-8.

26. Clay MR, Tabor M, Owen JH, Carey TE, Bradford CR, Wolf GT, et al. Single-marker identification of head and neck squamous cell carcinoma cancer stem cells with aldehyde dehydrogenase. Head Neck 2010;32:1195-1201.

27. Krishnamurthy S, Warner KA, Dong Z, Imai A, Nör C, Ward BB, et al. Endothelial interleukin-6 defines the tumorigenic potential of primary human cancer stem cells. Stem Cells 2014;32:2845-57.

28. Huang EH, Hynes MJ, Zhang T, Ginestier C, Dontu G, Appelman H, et al. Aldehyde dehydrogenase 1 is a marker for normal and malignant human colonic stem cells (SC) and tracks SC overpopulation during colon tumorigenesis. Cancer Res 2009;69:3382-9.

29. Silva IA, Bai S, McLean K, Yang K, Griffith K, Thomas D, et al. Aldehyde dehydrogenase in combination with CD133 defines angiogenic ovarian cancer stem cells that portend poor patient survival. Cancer Res 2011;71:3991-4001.

30. Rasheed Z, Wang Q, Matsui W. Isolation of stem cells from human pancreatic cancer xenografts. J Vis Exp 2010; 2169.

31. Su Y, Qiu Q, Zhang X, Jiang Z, Leng Q, Liu Z, et al. Aldehyde dehydrogenase 1 A1-positive cell population is enriched in tumor-initiating cells and associated with progression of bladder cancer. Cancer Epidemiol Biomarkers Prev 2010;19:327-37.

32. van den Hoogen C, van der Horst G, Cheung H, Buijs JT, Lippitt JM, Guzmán-Ramírez N, et al. High aldehyde dehydrogenase activity identifies tumor-initiating and metastasis-initiating cells in human prostate cancer. Cancer Res 2010; 70: 5163-73.

33. Bortolomai I, Canevari S, Facetti I, De Cecco L, Castellano G, Zacchetti A, et al. Tumor initiating cells: development and critical characterization of a model derived from the A431 carcinoma cell line forming spheres in suspension. Cell Cycle 2010;9:1194-206.

34. Cao L, Hu X, Zhang J, Liang P, Zhang Y. CD44(+) CD324(-) expression and prognosis in gastric cancer patients. J Surg Oncol 2014;110:727-33.

35. Li C, Heidt DG, Dalerba P, Burant CF, Zhang L, Adsay V, et al. Identification of Pancreatic Cancer Stem Cells. Cancer Res 2007;67:1030-7.

36. Choi D, Lee HW, Hur KY, Kim JJ, Park GS, Jang SH, et al. Cancer stem cell markers CD133 and CD24 correlate with invasiveness and differentiation in colorectal adenocarcinoma. World J Gastroenterol 2009;15:2258-64.

37. Bachelard-Cascales E, Chapellier M, Delay E, Pochon G, Voeltzel T, Puisieux A, et al. The CD10 enzyme is a key player to identify and regulate human mammary stem cells. Stem Cells 2010; 28:1081-8.

38. Warner KA, Adams A, Bernardi L, Nor C, Finkel KA, Zhang Z, et al. Characterization of tumorigenic cell lines from the recurrence and lymph node metastasis of a human salivary mucoepidermoid carcinoma. Oral Oncol 2013;49:1059-66.

39. Nör JE, Peters MC, Christensen JB, Sutorik MM, Linn S, Khan MK, et al. Engineering and characterization of functional human microvessels in immunodefficient mice. Lab Invest 2001;81:453-63.

40. Nör JE, Christensen J, Liu J, Peters M, Mooney DJ, Strieter RM, et al. Up-Regulation of Bcl-2 in microvascular endothelial cells enhances intratumoral angiogenesis and accelerates tumor growth. Cancer Res 2001;61:2183–8.

41. Hambardzumyan D, Squatrito M, Holland EC. Radiation resistance and stem- like cells in brain tumors. Cancer Cell 2006;10:454–6.

42. Reya T, Morrison SJ, Clarke MF, Weissman IL. Stem cells, cancer, and cancer stem cells. Nature 2001;414:105–11.

43. Shafee N, Smith CR, Wei S, Kim Y, Mills GB, Hortobagyi, et al. Cancer stem cells contribute to cisplatin resistance in Brca1/p53-mediated mouse mammary tumors. Cancer Res 2008;68:3243–50.

44. Adams A, Warner K, Nör JE. Salivary gland cancer stem cells. Oral Oncol 2013;49:845-53.

45. Lombaert IM, Brunsting JF, Wierenga PK, Faber H, Stokman MA, Kok T, et al. Rescue of salivary gland function after stem cell transplantation in irradiated glands. PLoS One 2008;3.e2063.

46. Takabe N, Harris PJ, Warren RQ, Ivy SP. Targeting cancer stem cells by inhibiting Wnt, Notch, and Hedgehog pathways. Nat Rev Clin Oncol 2011;8:97-106

47. Li X, Lewis MT, Huang J, Gutierrez C, Osborne CK, Wu MF, et al. Intrinsic resistance of tumorigenic breast cancer cells to chemotherapy. J Natl Cancer Inst. 2008;100:672-9.

48. Korkaya H, Paulson A, Charafe-Jauffret E, Ginestier C, Brown M, Dutcher J, et al. Regulation of mammary stem/progenitor cells by PTEN/Akt/beta-catenin signaling. S Biol. 2009;7:e1000121.

49. Dubrovska A, Kim S, Salamone RJ, Walker JR, Maira SM, García-Echeverría C, et al. The role of PTEN/Akt/PI3K signaling in the maintenance and viability of prostate cancer stem-like cell populations. Natl Acad Sci U S A. 2009;106:268-73.

50. Suzuki S, Dobashi Y, Minato H, Tajiri R, Yoshizaki T, Ooi A. EGFR and HER2-Akt-mTOR signaling pathways are activated in subgroups of salivary gland carcinomas. Virchows Arch. 2012;461:271-82.

51. Kokko LL, Hurme S, Maula SM, Alanen K, Grénman R, Kinnunen I, et al. Significance of site-specific prognosis of cancer stem cell marker CD44 in head and neck squamous-cell carcinoma. Oral Oncol 2011;47:510-16.

52. Mack B, Gires O. CD44s and CD44v6 expression in head and neck epithelia. PLoS One 2008;3:e3360.

53. Todaro M, Gaggianesi M, Catalano V, Benfante A, Iovino F, Biffoni M, et al. CD44v6 is a marker of constitutive and reprogrammed cancer stem cells driving colon cancer metastasis. Cell Stem Cell 2014;14:342-56.

54. Jijiwa M, Demir H, Gupta S, Leung C, Joshi K, Orozco N, et al. CD44v6 regulates growth of brain tumor stem cells partially through the AKT-mediated pathway. PLoS One 2011;6:e24217.

55. Yang YM, Chang JW. Bladder cancer initiating cells (BCICs) are among EMA-CD44v6+ subset: novel methods for isolating undetermined cancer stem (initiating) cells. Cancer Invest 2008;26:725-33.

56. Spiegelberg D, Kuku G, Selvaraju R, Nestor M. Characterization of CD44 variant expression in head and neck squamous cell carcinomas. Tumour Biol 2014;35:2053-62.

CHAPTER IV

Ablation of cancer stem cells via MDM2 inhibition in salivary gland mucoepidermoid carcinoma

Abstract

A rare population of cancer stem cells, characterized by increased tumorigenic potential and multipotency, has been described in several cancer types. This tumorigenic population of cells is defined by $ALDH^{high}CD44^{high}$ in salivary gland mucoepidermoid carcinoma. While frequently mutated in many cancer types, wild type p53 plays in important role in the induction of apoptosis under mutagenic stress as well as stem cell quiescence and differentiation. MI-773, a small molecule inhibitor, functions to prevent MDM2 inhibition of p53 thereby allowing p53 to induce apoptosis and differentiation within the cell. The purpose of our research is to therapeutically target cancer stem cells thereby sensitizing the tumors to chemotherapy treatments. In-vitro treatment of mucoepidermoid carcinoma cells UM-HMC-1, UM-HMC-3A, and UM-HMC-3B with MI-773 was shown to drastically increase expression of p53, MDM2, and p21. We also observed an induction of G1 cell cycle arrest as well as apoptosis. Interestingly, a marked decrease in expression of the marker of self-renewal, Bmi-1, was seen in stem cells treated with MI-773. In correlation, treatment with low doses (1 μm) of MI-773 significantly reduced the proportion of $ALDH^{high}CD44^{high}$ cells. Short-term in-vivo treatment of MI-773 in cell line-derived xenografts also induced cell cycle arrest and apoptosis. Importantly, a significant reduction in $ALDH^{high}CD44^{high}$ cell population and

Bmi-1 expression was also seen in the xenografts. Collectively, our data suggests that p53 is an important regulator of stem cell differentiation in mucoepidermoid carcinomas and that targeting of MDM2 effectively reduces the cancer stem cell population in these tumors.

Introduction

Salivary gland mucoepidermoid carcinomas (MEC) are the most common salivary malignancy, accounting for 30-35% of all malignant salivary gland tumors (1-8). Patients diagnosed with mucoepidermoid carcinomas are treated using surgical resection and radiation therapies (9). While this treatment is often sufficient for patients with low to intermediate-grade tumors, patients with high-grade tumors often display recurrent disease years after initial treatment which is, in most cases, fatal (10). Importantly, mucoepidermoid carcinomas are chemotherapy-resistant leaving no other treatment options available for these patients with advanced, recurrent disease (11). Improved understanding of pathobiology driving MEC growth is essential for the identification of effective therapies.

A subpopulation of cells, termed cancer stem cells (CSC), is uniquely tumorigenic and capable of multipotency and self-renewal. Cancer stem cells are essential for both initiating and maintaining the growth of many cancer types (12). Importantly, cancer stem cells are resistance to conventional chemotherapies and radiation treatments due to the suppressed rate of growth and the presence of transporter proteins as well as micro-environmental influences (13-15). Survival of these cells after treatment allows for tumor regrowth and recurrence. Previous work done in our laboratory identified cancer stem cells in salivary gland mucoepidermoid carcinomas

(16). MEC cells sorted for $ALDH^{high}CD44^{high}$ are highly tumorigenic in *in-vivo* models compared to the non-CSC population of cells. Importantly, $ALDH^{high}CD44^{high}$ cells are capable of self-renewal and multipotency. Selective targeting and ablation of $ALDH^{high}CD44^{high}$ cells is critical towards achieving total disease remission in patients with mucoepidermoid carcinoma.

p53 is a transcription factor that plays an essential role in many cellular functions. Among the most critical are regulating the cell cycle and senescence as well as the induction of apoptosis upon the damage to the genome (17-19). Importantly, p53 plays a key role in adult and embryonic stem cell differentiation. In normal differentiated cells, deletion or repression of p53 function lead to greater efficiency in dedifferentiating into induced pluripotent stem cells (20-24). In the context of cancer, research has shown that loss of p53 also led to the expansion of malignant reprogrammed progenitor cells in cancer (25). Mouse double minute 2, MDM2, is a key regulator of p53. MDM2 binds the transactivation domain and ubiquitinates p53, signaling it for degradation in the proteasome (26). MDM2 serves as an oncogene and is overexpressed in many cancers as it prohibits p53 from inducing apoptosis upon malignant expansion.

Many MDM2/p53 small molecule inhibitors have been generated that interrupt MDM2 binding to p53. One molecule in particular, MI-773, has been shown to have significantly greater specificity and affinity to MDM2 when compared to p53 binding, a previously developed MDM2 inhibitor, Nutlin-3a, binding, and previous analog MI-219 binding (27). Importantly, MI-773 was able to activate p53 activity and induce apoptosis in cancer cells at a much greater efficiency when compared to Nutlin-3a (27). Notably, this therapeutic effect was seen in cell lines with both wild-type and mutated p53 (28).

While much work has been done to determine the therapeutic effect of MI-773 in inducing apoptosis and diminishing tumor volume, no studies have been performed to characterize MI-773 efficacy in salivary gland mucoepidermoid carcinoma or it's impact on stem cell function. Hence, the focus of our study is to investigate the therapeutic effect of MI-773 on cancer stem cells in salivary gland mucoepidermoid carcinomas. Our findings suggest that MDM2/p53 binding inhibition is not only effective in inducing apoptosis and cell cycle arrest in mucoepidermoid carcinoma cells, but is also a powerful agent in reducing the $ALDH^{high}CD44^{high}$ cancer stem cell population. Together, these findings unveil a unique therapy for the treatment of mucoepidermoid carcinoma cancer stem cells.

Materials and Methods

Cell Culture

HMC cells, previously characterized in our laboratory, (UM-HMC-1, UM-HMC-3A, and UM-HMC3B) cells were cultured using DMEM (Gibco) enriched with 10% FBS (Gibco), 1% 200nM L-Glutamine (Gibco), 1% Penicillin and Streptomycin (Gibco), 20 ng/mL epidermal growth factor (Sigma), 400 ng/mL hydrocortisone (Sigma), 5 ug/mL insulin (Sigma #I-1882). Cells were trypsinized using 0.05% trypsin (Gibco). Human endothelial cells were grown using EBM media (Lonza) (29).

Immunohistochemistry and Immunofluorescence Staining

Tissue section slides for immunohistochemistry and immunofluorescence staining were de-paraffinized using xylene and ethanol washes. Following de-paraffinization, sections were incubated with 0.1% Triton-x100 for 10 minutes, 3% hydrogen peroxide for 10 minutes, and Background Sniper (Biocare Medical) for 10-30 minutes.

Immunohistochemistry slides were incubated with anti-p53 (Santa Cruz) and anti-MDM2 (Santa Cruz) overnight at 4C. Following incubation with primary antibody, sections were washed two times for 10 minutes and incubated with MACHI 3 Probe (Biocare Medical) for 20 minutes. After two 10 minute washes, sections were incubated with MACHI 3 HRP Polymer for 20 minutes and again washed two times for 10 minutes. Sections were then incubated with DAB for 3 minutes and quenched in water. Sections were finally incubated with hematoxycin for 45 seconds, dehydrated in ethanol and mounted. Immunofluorescence sections were incubated with anti-ALDH (Abcam) overnight at room temperature. The following day, sections were washed for three 5-minute washes and incubated with Alexafluor 488 (Anti-Rabbit, Invitrogen). After three 5 minute washes, sections were incubated with 3% hydrogen peroxide for 30 minutes followed by 1 hour incubation with anti-CD44 (Thermo Scientific) and a 20 minute incubation with Aliexafluor 594 (Anti-Mouse, Invitrogen). Slides were imaged with DAPI. TUNEL staining was performed using TUNEL staining kit (Roche) and a DAPI stain. Seven 200X image fields were taken per section and the pixel density was quantitated using ImageJ software.

Western Blot

HMC cell and tissue section lysates were digested using NP-40. Lysates were run using PAGE gels and probed using anti-p53 (SantaCruz), anti-MDM2 (SantaCruz), anti-p21 (Cell Signaling), Bmi-1 (Cell Signaling), anti Cyclin-A (Santa Cruz), anti-Cyclin-D (Santa Cruz), anti-Cyclin-E (Cell Signalling), anti-CDK2 (Santa Cruz), anti-CDK4 (Santa Cruz), anti-CDK6 (Santa Cruz), and anti-Bcl-xL (BD Transduction).

PCR and Sequencing

RNA was isolated from sorted and unsorted HMC cells and reverse transcribed. cDNA was PCR amplified using sense and anti-sense primers targeting full length p53 and residues 54-716, 460-1179, and 876-1412. PCR products were run on a 1.5% agarose gel. Fragments were excised and purified for Sanger sequencing.

WST-1

HMC cells were plated at 500 cells per well in a 96-well plate and allowed to attached overnight. MI-773 was solubilized in DMSO and added at varying concentrations to the cells using DMSO only treatments as a control. Cells were incubated with the drug for 24, 48, or 72 hours. 10uL of WST-1 reagent (Roche) was added to the cells and incubated at 37C for 4 hours. Plates were then analyzed using a plate reader.

Flow Cytometry

For ALDH/CD44 staining, cells were trypsinized and alloquoted 2 million cells per tube. 10uL of Aldefluor (Caymen Chemicals) was added to each tube and 10 uL of DEAB was added to the DEAB control tube. Cells were incubated for 40 minutes at 37C then stained with 5uL of CD44 (BD) for 30 minutes at 4C. For propidium iodine staining, cells were fixed in 70% ethanol overnight at -20C and stained in 1mg/mL propidium iodide (BD), 1% sodium citrate, 1mg/mL RNaseA, 10% Triton X-100 for 20 minutes. For Annexin V staining, cells were washed in PBS then suspendeded in 1X Binding Buffer (BD). 5uL of Annexin V (APC, BD) was added to 100,000 cells and incubated for 20 minutes at room temperature. In all flow cytometry experiments, 7AAD was used as a live/dead control (BD).

In-Vivo Implantation

UM-HMC-3A, UM-HMC-3B, and HDMEC cells were trypsinized and counted. 600,000 UM-HMC-3A or UM-HMC-3B cells were seeded with 400,000 HDMEC cells in Matrigel on biodegradable scaffolds as previously described (30). Scaffolds were implanted subcutaneously on the dorsal section of CB17 SCID mice (Charles River). Scaffolds were measured weekly until the tumors reached an average volume of 500mm^3. MI-773 was diluted in poly-ethylene glycol and vitamin E. Mice were treated with 200mg/kg, 100mg/kg, or 50mg/kg for 6 days by gavage. Following the 6 days of treatment, mice were euthanized and the tumors removed. Once the tumors were removed, the tissue was digested using Tumor Dissociation Kit (Miltenyi Biotec #130-095-929) and the gentleMACS Dissociator (#130-093-235). Single cell tumor tissue suspensions stained for FACS analysis as previously described.

Results

MDM2 and p53 expression in MEC patient specimens and HMC cell lines

To investigate the expression of MDM2 and p53 in MEC patient samples, we stained two MEC patient tissue sections and observed robust MDM2 expression while little p53 expression was seen (Figure IV.1A). We next performed western blot analysis to determine MDM2 and p53 expression in HMC cell lines generated in our lab (29). Both UM-HMC-1 and UM-HMC-3A cell lines showed strong MDM2 expression and lower p53 expression (Figure IV.1B). Interestingly, we noticed an opposite trend in UM-HMC-3B cells, which showed minimal MDM2 expression and elevated p53 expression (Figure IV.1B). We next compared MDM2 and p53 expression in ALDH^{high}CD44^{high} cancer stem cells (CSCs) and non-cancer stem cells. Little difference in expression was

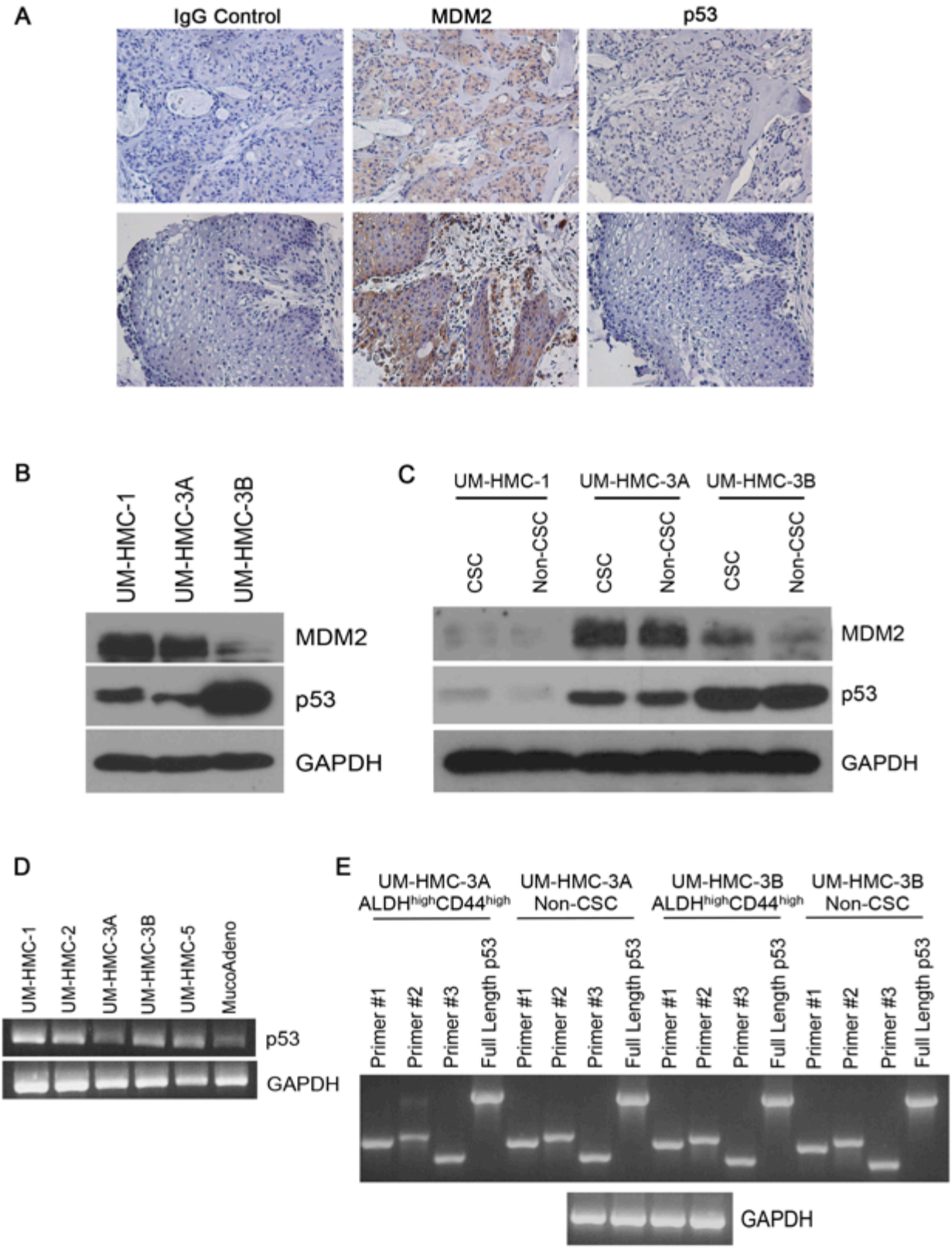
A
IgG Control
MDM2
p53
B
UM-HMC-1
UM-HMC-3A
UM-HMC-3B
MDM2
p53
GAPDH
C
UM-HMC-1
UM-HMC-3A
UM-HMC-3B
CSC
Non-CSC
CSC
Non-CSC
CSC
Non-CSC
MDM2
p53
GAPDH
D
UM-HMC-1
UM-HMC-2
UM-HMC-3A
UM-HMC-3B
UM-HMC-5
MucoAdeno
p53
GAPDH
E
UM-HMC-3A ALDHhighCD44high
UM-HMC-3A Non-CSC
UM-HMC-3B ALDHhighCD44high
UM-HMC-3B Non-CSC
Primer #1
Primer #2
Primer #3
Full Length p53
GAPDH

Figure IV.1. MDM2 and p53 expression in MEC patient specimens and HMC cell lines. A, Representative images of immunohistochemistry staining for MDM2 and p53 in two MEC patient tissue samples. Images were taken at 200X. **B,** Western blot analysis of p53 and MDM2 expression in UM-HMC-1, UM-HMC-3A, and UM-HMC-3B cells. **C,** Western blot analysis of p53 and MDM2 expression in UM-HMC-1, UM-HMC-3A, and UM-HMC-3B cells FACS sorted for both the $ALDH^{high}CD44^{high}$ cancer stem cell population and the remaining cells that were not $ALDH^{high}CD44^{high}$ (i.e. non-cancer stem cells). **D,** PCR analysis of p53 RNA levels in UM-HMC-1, UM-HMC-2, UM-HMC-3A, UM-HMC-3B, UM-HMC-5, and a control mucoadeno carcinoma sample. **E,** PCR analysis of p53 RNA expression for both full length p53 as well as primers targeting nucleotides 52-716 (Primer #1), nucleotides 460-1179 (Primer #2), and 876-1412 (Primer #3) of the p53 coding region. RNA was extracted from UM-HMC-3A and UM-HMC-3B cells FACS sorted for both the $ALDH^{high}CD44^{high}$ cancer stem cells population and the non-$ALDH^{high}CD44^{high}$ (i.e. non-cancer stem cell) cell population.

observed in UM-HMC-1 and UM-HMC-3A CSC versus non-CSC cells (Figure IV.1C). Interestingly, a higher expression of MDM2 was seen in UM-HMC-3B CSC cells compared to the non-CSC population suggesting that MDM2 may be differentially regulated in the cancer stem cells (Figure IV.1C). Expression of p53 remained consistent between CSC and non-CSC in UM-HMC-3B cells (Figure IV.1C).

To investigate the mRNA expression of p53 in HMC cells, we used PCR primers targeting the full-length p53 gene as well as three primers targeting different areas of the p53 gene. As PCR amplification of longer genes can generated false mutations, we used three primers that targeted three smaller areas of the p53 genes. Primer #1 targeted residues 54-716 while primers #2 and #3 targeted residues 460-1179, and 876-1412 respectively. PCR analysis was performed on UM-HMC-1, UM-HMC-2, UM-HMC-3A, UM-HMC-3B, UM-HMC-5, and mucoadenocarcinoma cell line cDNA (Figure IV.1D). Similar mRNA expression of p53 was seen between the HMC cell lines. We next sorted UM-HMC-1 (data not shown), UM-HMC-3A, and UM-HMC-3B cells for the $ALDH^{high}CD44^{high}$ cells and non-CSC population and ran PCR analysis on cDNA generated from the cells. In our analysis, we used both full-length primers as well as the

A.

	p53 Mutation
UM-HMC-1	A278P
UM-HMC-3A	A278P, V157F
UM-HMC-3B	A278P, V157F

B. UM-HMC-1

Met E E P Q S D P S V E P P L S Q E T F S D L W K L L P E N N V L S P L P S Q
A Met D D L Met L S P D D I E Q W F T E D P G P D E A P R Met P E A A P R V A P A
P A A P T P A A P A P A P S W P L S S S V P S Q K T Y Q G S Y G F R L G F L H S G
T A K S V T C T Y S P A L N K Met F C Q L A K T C P V Q L W V D S T P P P G T R F
R A Met A I Y K Q S Q H Met T E V V R R C P H H E R C S D S D G L A P P Q H L I R
V E G N L R V E Y L D D R N T F R H S V V V P Y E P P E V G S D C T T I H Y N Y
Met C N S S C Met G G Met N R R P I L T I I T L E D S S G N L L G R N S F E V R V C
A C **P** G R D R R T E E E N L R K K G E P H H E L P P G S T K R A L P N N T S S S P
Q P K K K P L D G E Y F T L Q I R G R E R F E Met F R E L N E A L E L K D A Q A G
K E P G G S R A H S S H L K S K K G Q S T S R H K K L Met F K T E G P D S D

C. UM-HMC-3A

Met E E P Q S D P S V E P P L S Q E T F S D L W K L L P E N N V L S P L P S Q
A Met D D L Met L S P D D I E Q W F T E D P G P D E A P R Met P E A A P R V A P A
P A A P T P A A P A P A P S W P L S S S V P S Q K T Y Q G S Y G F R L G F L H S G
T A K S V T C T Y S P A L N K Met F C Q L A K T C P V Q L W V D S T P P P G T R **F**
R A Met A I Y K Q S Q H Met T E V V R R C P H H E R C S D S D G L A P P Q H L I R
V E G N L R V E Y L D D R N T F R H S V V V P Y E P P E V G S D C T T I H Y N Y
Met C N S S C Met G G Met N R R P I L T I I T L E D S S G N L L G R N S F E V R V C
A C **P** G R D R R T E E E N L R K K G E P H H E L P P G S T K R A L P N N T S S S P
Q P K K K P L D G E Y F T L Q I R G R E R F E Met F R E L N E A L E L K D A Q A G
K E P G G S R A H S S H L K S K K G Q S T S R H K K L Met F K T E G P D S D

D. UM-HMC-3B

Met E E P Q S D P S V E P P L S Q E T F S D L W K L L P E N N V L S P L P S Q
A Met D D L Met L S P D D I E Q W F T E D P G P D E A P R Met P E A A P R V A P A
P A A P T P A A P A P A P S W P L S S S V P S Q K T Y Q G S Y G F R L G F L H S G
T A K S V T C T Y S P A L N K Met F C Q L A K T C P V Q L W V D S T P P P G T R **F**
R A Met A I Y K Q S Q H Met T E V V R R C P H H E R C S D S D G L A P P Q H L I R
V E G N L R V E Y L D D R N T F R H S V V V P Y E P P E V G S D C T T I H Y N Y
Met C N S S C Met G G Met N R R P I L T I I T L E D S S G N L L G R N S F E V R V C
A C **P** G R D R R T E E E N L R K K G E P H H E L P P G S T K R A L P N N T S S S P
Q P K K K P L D G E Y F T L Q I R G R E R F E Met F R E L N E A L E L K D A Q A G
K E P G G S R A H S S H L K S K K G Q S T S R H K K L Met F K T E G P D S D

Figure IV.2. p53 sequence in HMC cells. A, Table depicting the p53 mutations in UM-HMC-1, UM-HMC-3A, and UM-HMC-3B cells. **B,** p53 sequence in UM-HMC-1 cells. Three PCR products from nucleotides 54-716, 460-1179, 876-1412 were purified and sent for Sanger sequencing. Mutations are highlighted in red. **C,** p53 sequence in UM-HMC-3A cells. Three PCR products from nucleotides 54-716, 460-1179, 876-1412 were purified and sent for Sanger sequencing. Mutations are highlighted in red. **D,** p53 sequence in UM-HMC-3B cells. Three PCR products from nucleotides 54-716, 460-1179, 876-1412 were purified and submitted for Sanger sequencing. Mutations are highlighted in red.

three primers. Similar levels of p53 mRNA was observed between the CSC and non-CSC populations. We next Sanger sequenced the PCR products from the three primer set in UM-HMC-1, UM-HMC-3A, and UM-HMC-3B cell lines and found a A278P mutation in UM-HMC-1, UM-HMC-3A, and UM-HMC-3B cells as well as a V157F mutation in UM-HMC-3A and UM-HMC-3B cells (Figure IV.2A-D).

Together these results indicate that our HMC cells express both p53 and MDM2 in both the cancer stem cell and the non-cancer stem cell populations suggesting that MI-773 could be a potential therapeutic agent for targeting the MEC cancer cells and a possible agent for targeting CSC in mucoepidermoid carcinoma.

Effect of MDM2/p53 binding inhibition by MI-773 on the ALDH^{high}CD44^{high} population in HMC cells

To directly test the effectiveness of MI-773 treatment on the cancer stem cells in MEC, we treated UM-HMC-1 cells with 1uM MI-773 for 48, 72, and 96 hours and performed FACS analysis for the cells for ALDH^{high}CD44^{high} cells. At 48, 72, and 96 hours time points, we observed a dramatic decrease in the ALDH^{high}CD44^{high} cancer stem cell population (Figure IV.3A). To determine whether this decrease was due to selective apoptosis of the CSC population or differentiation into a non-CSC cell type, we performed a water-soluble tetrazolium-1 (WST-1 analysis. After 72 hour treatment of ALDH^{high}CD44^{high} sorted cells and non-CSC cells with varying concentration of MI-773,

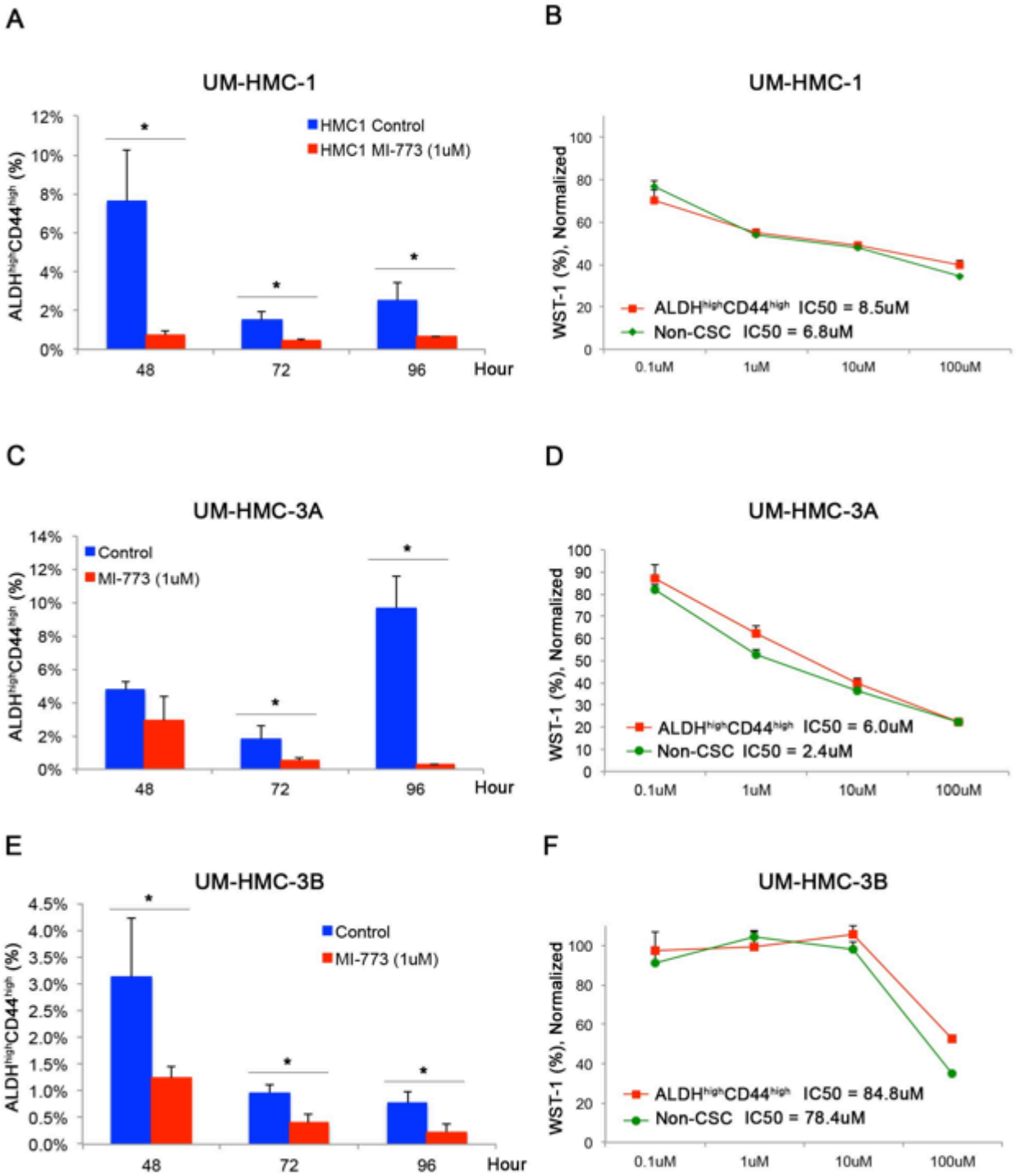

Figure IV.3. Effect of MDM2/p53 binding inhibition by MI-773 on the ALDH^{high}CD44^{high} population in HMC cells. A, FACS analysis of UM-HMC-1 cells after 48, 72, and 96-hour treatments with 1uM MI-773. Cells were plated at 500,000 cells per flask and treated with 1uM MI-773. After the 48, 72, and 96-hour time points, the cells were detached and analyzed for the ALDH^{high}CD44^{high} cancer stem cells population. **B,** WST-1 analysis of UM-HMC-1 cells FACS sorted for the ALDH^{high}CD44^{high} cancer stem cells and the non-ALDH^{high}CD44^{high} cells population. After sorting, cells were plated at 500 cells per well in a 96 well tissue culture plate. Once seated, a concentration gradient (0.1uM-100uM) of MI-773 was added and cells were

exposed for 72 hours. Following the 72 hours treatment, 10uL of WST-1 reagent was added for 4 hours after which the plates were analyzed. **C,** FACS analysis of UM-HMC-3A cells after 48, 72, and 96-hour treatments with 1uM MI-773. Cells were plated at 500,000 cells per flask and treated with 1uM MI-773. After the 48, 72, and 96-hour time points, the cells were detached and analyzed for the $ALDH^{high}CD44^{high}$ marker combination. **D,** WST-1 analysis of UM-HMC-3A cells FACS sorted for the $ALDH^{high}CD44^{high}$ cancer stem cells and the non-$ALDH^{high}CD44^{high}$ cells population. After sorting, cells were plated at 500 cells per well in a 96 well tissue culture plate. Once seated, a concentration gradient (0.1uM-100uM) of MI-773 was added and cells were exposed for 72 hours. Following the 72 hours treatment, 10uL of WST-1 reagent was added for 4 hours and after which the plates were analyzed. **E,** FACS analysis of UM-HMC-3B cells after 48, 72, and 96-hour treatments with 1uM MI-773. Cells were plated at 500,000 cells per flask and treated with 1uM MI-773. After the 48, 72, and 96-hour time points, the cells were detached and analyzed for the $ALDH^{high}CD44^{high}$ marker combination. **F,** WST-1 analysis of UM-HMC-3B cells FACS sorted for the $ALDH^{high}CD44^{high}$ cancer stem cells and the non-$ALDH^{high}CD44^{high}$ cells population. After sorting, cells were plated at 500 cells per well in a 96 well tissue culture plate. Once seated, a concentration gradient (0.1uM-100uM) of MI-773 was added and cells were exposed for 72 hours. Following the 72 hours treatment, 10uL of WST-1 reagent was added for 4 hours and after which the plates were analyzed.

we saw little difference in IC50 values for the CSC versus non-CSC population (CSC: 8.5uM, Non-CSC: 6.8uM) suggesting that MI-773 induces differentiation of the CSC population rather then preferentially affecting the CSC cell number (Figure IV.3B). We next performed this analysis in UM-HMC-3A cells and again saw a dramatic decrease in $ALDH^{high}CD44^{high}$ cells, particularly after 72 and 96 hours of treatment (Figure IV.3C).Again, we saw little difference in the IC50 values of the CSC versus non-CSC population (CSC: 6.0uM, Non-CSC: 2.4uM) suggesting again that MI-773 induces differentiation of the $ALDH^{high}CD44^{high}$ cells (Figure IV.3D). Finally, we again repeated this analysis in UM-HMC-3B cells and again saw a dramatic decrease in the CSC population after 48, 72, and 96 hours of treatment and little difference in IC50 values (CSC: 84.5uM, Non-CSC: 78.4uM) (Figure IV.3E and 3F). Interestingly, both the CSC and non-CSC UM-HMC-3B cells showed resistance to MI-773 treatments as indicated by the high IC50 values, however, the lack of difference between the IC50 values again suggests that the reduction in $ALDH^{high}CD44^{high}$ cells is due to differentiation rather then apoptosis.

Together our results suggest that MI-773 is a potent and effective agent in reducing the $ALDH^{high}CD44^{high}$ cancer stem cell population in HMC cells. Our data also suggests that this reduction in CSC is due by differentiation of the cancer stem cells into non-CSC rather then selectively inducing apoptosis in the cancer stem cells.

The effect of MDM2/p53 binding inhibition by MI-773 on HMC cell number

To determine any the presence of off target effects of MI-773 in targeting the MDM2/p53 interaction, we used shRNA vectors to silence p53 expression in UM-HMC-3A cells. shp53 #1 and shp53 #2 vectors showed reduction in p53 expression while shp53 #2 showed little decrease in p53 expression compared to the shControl vector (Figure IV.4B). Interestingly, we also saw a significant reduction in MDM2 and p21 (Figure IV.4B). Using these cells, we performed a WST-1 analysis treating the p53 silenced and control cells with varying concentration of MI-773. The shControl cells showed an IC50 value of 4.6uM while shp53 #1, shp53 #2, and shp53 #3 cells showed IC50 values of 67.9uM, 18.4uM, and 59.7uM respectively (Figure IV.4A). These results demonstrate that silencing of p53 confers resistance of UM-HMC-3A cells to MI-773 treatment and suggests that the therapeutic effect of MI-773 is primarily through p53 activation.

To determine the overall effect of MI-773 on HMC cell number and expression of proteins downstream of p53, we performed WST-1 and western blot analysis on UM-HMC-1, UM-HMC-3A, and UM-HMC-3B unsorted cells. When UM-HMC-1 cells were subjected to varying concentrations of MI-773 for 24, 48, and 72 hours, we saw a significant decrease in the total cell number. While 24-hour treatment had little effect on the number of cells, the IC50 at 48 and 72 hours was 37.9uM and 0.9uM respectively

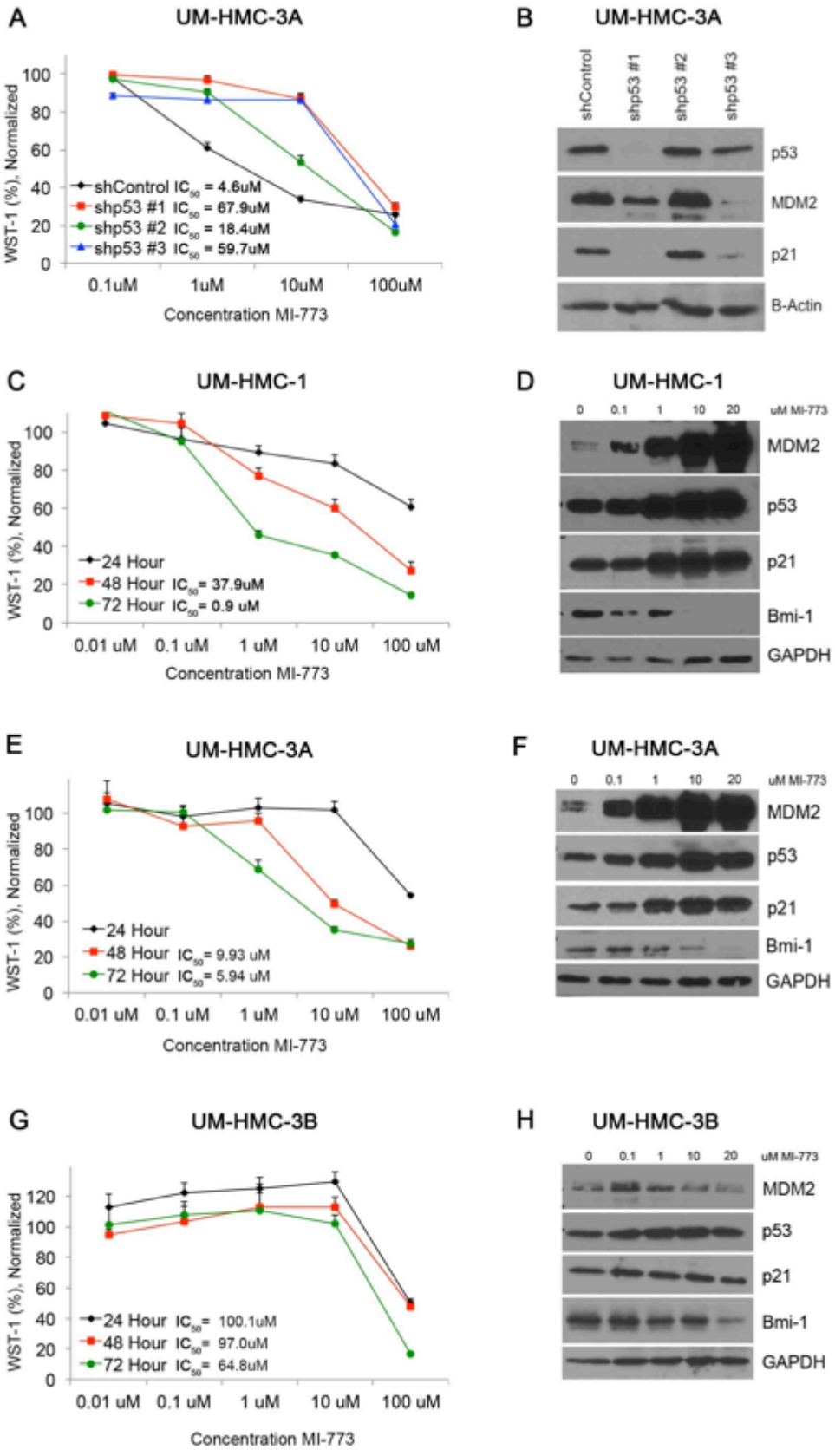
A
UM-HMC-3A
WST-1 (%), Normalized
shControl IC50 = 4.6uM
shp53 #1 IC50 = 67.9uM
shp53 #2 IC50 = 18.4uM
shp53 #3 IC50 = 59.7uM
0.1uM
1uM
10uM
100uM
Concentration MI-773
B
UM-HMC-3A
shControl
shp53 #1
shp53 #2
shp53 #3
p53
MDM2
p21
B-Actin
C
UM-HMC-1
WST-1 (%), Normalized
24 Hour
48 Hour IC50= 37.9uM
72 Hour IC50= 0.9 uM
0.01 uM
0.1 uM
1 uM
10 uM
100 uM
Concentration MI-773
D
UM-HMC-1
0
0.1
1
10
20
uM MI-773
MDM2
p53
p21
Bmi-1
GAPDH
E
UM-HMC-3A
WST-1 (%), Normalized
24 Hour
48 Hour IC50= 9.93 uM
72 Hour IC50= 5.94 uM
0.01 uM
0.1 uM
1 uM
10 uM
100 uM
Concentration MI-773
F
UM-HMC-3A
0
0.1
1
10
20
uM MI-773
MDM2
p53
p21
Bmi-1
GAPDH
G
UM-HMC-3B
WST-1 (%), Normalized
24 Hour IC50= 100.1uM
48 Hour IC50= 97.0uM
72 Hour IC50= 64.8uM
0.01 uM
0.1 uM
1 uM
10 uM
100 uM
Concentration MI-773
H
UM-HMC-3B
0
0.1
1
10
20
uM MI-773
MDM2
p53
p21
Bmi-1
GAPDH

Figure IV.4. The effect of MDM2/p53 binding inhibition by MI-773 on HMC cell number. A, WST-1 analysis of UM-HMC-3A shcontrol and shp53 cells. p53 was knocked down using three different lentiviral shp53 vectors. Transfected cells were plated at 500 cells per well and exposed to varying concentrations of MI-773 for 72 hours. After 4 hours of incubation with WST-1, the plates were analyzed and normalized to a DMSO control. **B,** Western blot analysis of lysates created from shp53 knockdown cells. **C,** WST-1 analysis of UM-HMC-1 cells treated with varying concentrations of MI-773 for 24, 28, and 72 hours. UM-HMC-1 cells were seated at 500 cells per well. After each time point, 10uL of WST-1 reagent was added to the cells for 4 hours and then analyzed. All cells were normalized to a DMSO control. **D,** Western blot analysis of UM-HMC-1 cells treated with 0.1, 1, 10, or 20 uM MI-773 for 24 hours. **E,** WST-1 analysis of UM-HMC-3A cells treated with varying concentrations of MI-773 for 24, 28, and 72 hours. UM-HMC-3A cells were seated at 500 cells per well. After each time point, 10uL of WST-1 reagent was added to the cells for 4 hours and then analyzed. All cells were normalized to a DMSO control. **F,** Western blot analysis of UM-HMC-3A cells treated with 0.1, 1, 10, or 20 uM MI-773 for 24 hours. **G,** WST-1 analysis of UM-HMC-3B cells treated with varying concentrations of MI-773 for 24, 28, and 72 hours. UM-HMC-3B cells were seated at 500 cells per well. After each time point, 10uL of WST-1 reagent was added to the cells for 4 hours and then analyzed. All cells were normalized to a DMSO control. **H,** Western blot analysis of UM-HMC-3B cells treated with 0.1, 1, 10, or 20 uM MI-773 for 24 hours.

(Figure IV.4C). We next treated UM-HMC-1 cells with 0uM, 0.1uM, 1uM, 10uM, and 20uM MI-773 and made lysates for western blot analysis. With increasing concentrations of MI-773, we saw a robust accumulation of p53 and and increase in MDM2 and p21 expression suggesting that p53 is indeed activated (Figure IV.4D). Interestingly, we also saw a dramatic reduction of self-renewal marker, Bmi-1, suggesting that we are indeed reducing the cancer stem cell population upon treatment with MI-773 (Figure IV.4C). We next performed WST-1 analysis using UM-HMC-3A cells and again saw a significant reduction in the number of cells, particularly after 48 and 72 hours of treatment, with IC50 values measured at 9.93uM and 5.94uM respectively (Figure IV.4E). Once again, we saw a dramatic increase in expression of MDM2, p53, and p21 and a reduction in Bmi-1 expression again suggesting that p53 is indeed activated upon treatment with MI-773 and that the MI-773 reduces the CSC population (Figure IV.4F). Finally, we performed WST-1 and western blot analysis on treated UM-HMC-3B cells a found a drastically different trend. Upon treatment with MI-

773, UM-HMC-3B cells showed significantly higher IC50 values when compared to UM-HMC-1 and UM-HMC-3A at 24, 48, and 72 hours treatments (IC50 values were 100.1uM, 97.0uM, and 64.8uM respectively) (Figure IV.4G). When western blot analysis was performed, we saw little to no increase in MDM2, p53, or p21 expression (Figure IV.4H). Interestingly, we again observe a reduction in Bmi-1 expression, suggesting that while the overall cell number is not affected by MI-773, the CSC population is still susceptible to MI-773 treatment.

Overall, our data suggests that MI-773 is able to effectively reduce cell number in UM-HMC-1 and UM-HMC-3A cells. While the proliferative activity of UM-HMC-3B cells showed little sensitivity to MI-773, we conclude that the agent is capable of reducing the number of cancer stem-like cells in all cell lines.

Induction of cell cycle arrest and apoptosis in HMC cells by MI-773

To investigate the mechanism by which MI-773 is able to reduce HMC cell populations, we treated HMC cells with 1uM MI-773 and stained with propidium iodide to assess cell cycle status. We treated the UM-HMC-3A cells with 1uM MI-773 to determine the cell cycle profile of the treated versus untreated cells. After both 24 and 48 hours, we observed and increase of cells in G1 and a decrease in cells in both S and G2, suggesting that MI-773 induces G1 cell cycle arrest in UM-HMC-3A cells (Figure IV.5A). We next treated our UM-HMC-3A cells with 5uM, 10uM, and 15uM MI-773 for 24 hours to see if MI-773 treatment induced apoptosis. After treatment, the cells were stained with both 7AAD and Annexin-V. We observed an increase of cells positive for Annexin-V alone (early apoptosis) as well as cells positive for both Annexin-V and 7AAD (late apoptosis) (Figure IV.5B).

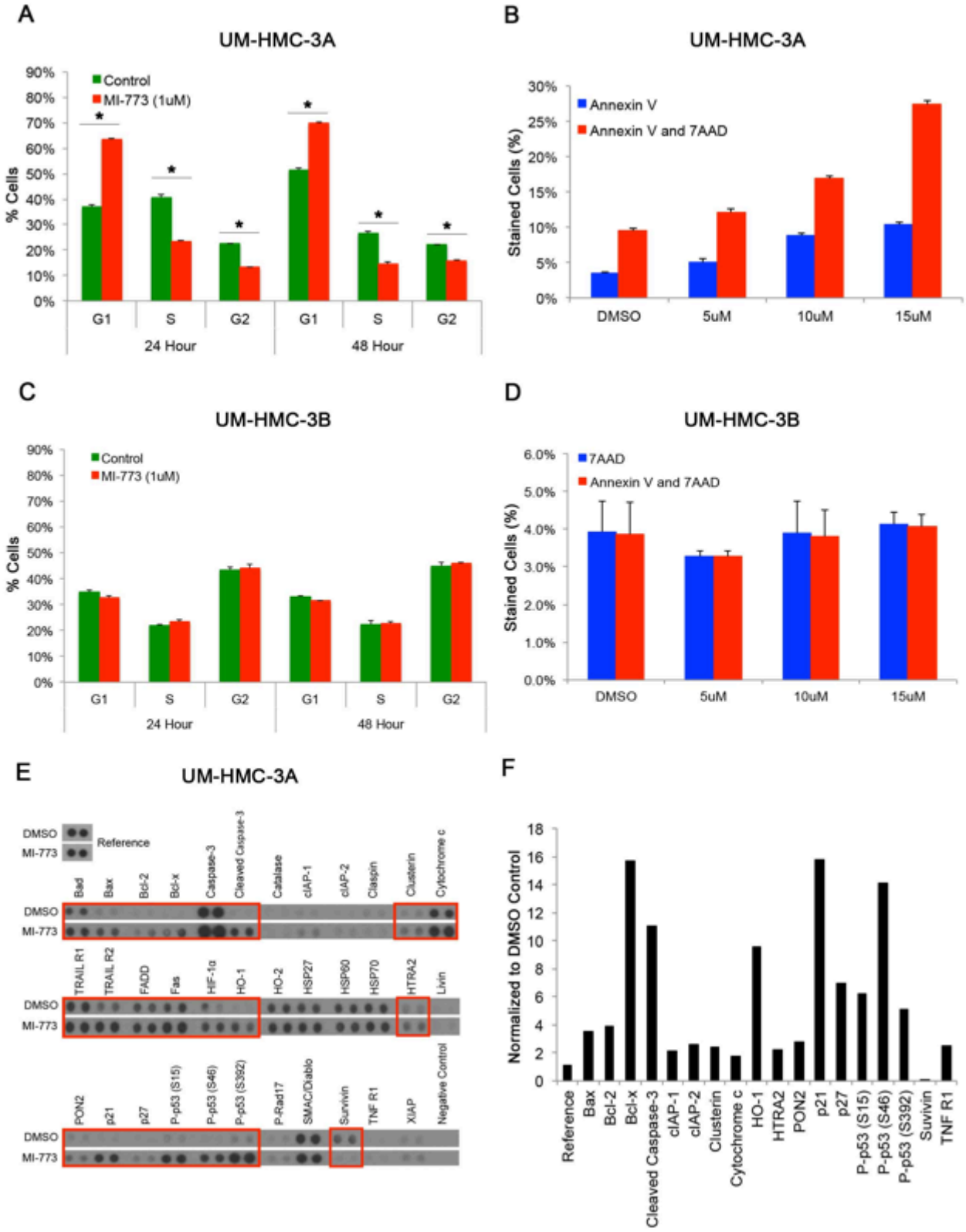
A
UM-HMC-3A
Control
MI-773 (1uM)
% Cells
G1
S
G2
24 Hour
48 Hour
B
UM-HMC-3A
Annexin V
Annexin V and 7AAD
Stained Cells (%)
DMSO
5uM
10uM
15uM
C
UM-HMC-3B
D
UM-HMC-3B
7AAD
E
UM-HMC-3A
Reference
F
Normalized to DMSO Control

Figure IV.5. Induction of cell cycle arrest and apoptosis in HMC cells by MI-773. A, Cell cycle analysis of UM-HMC-3A cells treated with 1uM MI-773 for 24 and 48 hours. Cells were plated at 500,000 cells per flask. Control cells were treated with DMSO. **B,** Annexin V and 7AAD FACS analysis following treatment of UM-HMC-3A cells with 5, 10, or 15 uM MI-773 for 24 hours. Control cells were treated with DMSO. **C,** Cell cycle analysis of UM-HMC-3B cells treated with 1uM MI-773 for 24 and 48 hours. Cells were plated at 500,000 cells per flask. Control cells were treated with DMSO. **D,** Annexin V and 7AAD FACS analysis following treatment of UM-HMC-3B cells with 5, 10, or 15 uM MI-773 for 24 hours. Control cells were treated with DMSO. **E,** Apoptosis Antibody Array (R&D) analysis in UM-HMC-3A cells treated with 5uM MI-773 for 24 hours. **F,** Blot from Apoptosis Array was quantitated using ImageJ software. Blot quantitation for MI-773 treated lysates were normalized to the values of the DMSO treated blots.

Since UM-HMC-3B cells are uniquely resistant to MI-773 treatment, we sought to verify that MI-773 is incapable of inducing cell cycle arrest in this population. Upon treatment with 1uM of MI-773 for 24 or 48 hours, we observed no difference in the cell cycle profile in treated cells versus control cells consistent with our previous results (Figure IV.5C). To determine whether MI-773 was able to induce apoptosis in UM-HMC-3B cells, we treated the cells with 5uM, 10uM, and 15uM MI-773 for 24 hours. Following treatment we stained the cells for both Annexin-V and 7AAD and saw no difference in percentage of 7AAD positive cells or Annexin-V and 7AAD positive cells in the control treated versus the MI-773 treated (Figure IV.5D). Again, these results further confirm that UM-HMC-3B cells are resistant to MI-773 induced cell cycle arrest and apoptosis.

To identify the apoptotic pathways upregulated upon treatment with MI-773, we treated UM-HMC-3A cells with 5uM MI-773 for 24 hours and ran the Apoptosis Antibody Array (R&D). We observed a significant up regulation of pro-apoptotic proteins such as Bcl-x, cleaved caspase-3, cytochrome c, p21, p27, and phosphorylated p53 (Figure IV.5E and 5F). Together these results suggest that treatment with MI-773 is capable of inducing p53 induced G1 cells cycle arrest and apoptosis in UM-HMC-3A. In contrast, MI-773 was unable to induce cell cycle arrest or apoptosis in UM-HMC-3B cells.

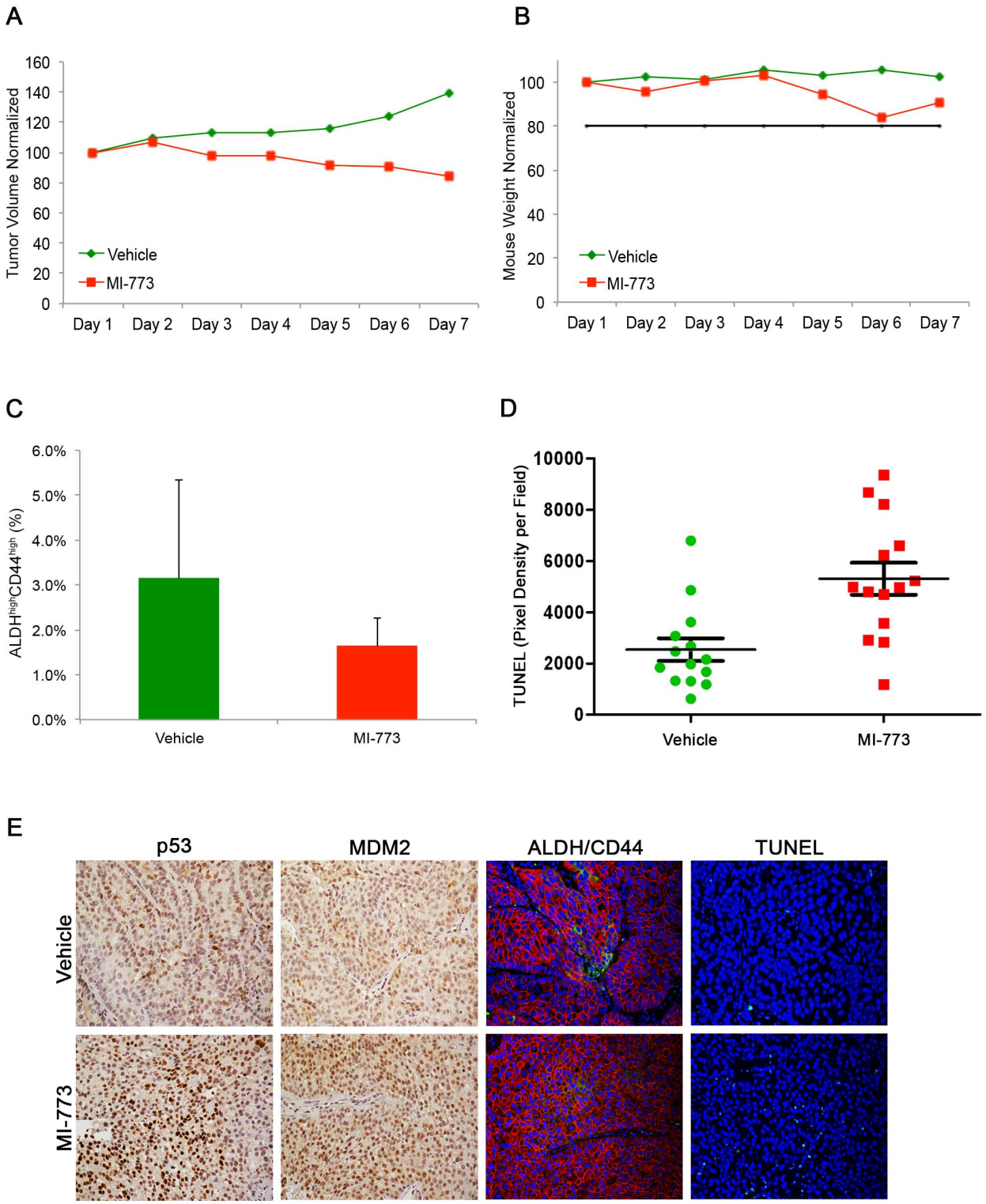

Figure IV.6. Effect of MDM2/p53 binding inhibition by MI-773 on cancer stem cells in UM-HMC-3A cells *in-vivo*. A, Graph depicting the tumor volume during 6 days of 50mg/kg treatment with MI-773. 600,000 UM-HMC-3A cells were co-implanted with 400,000 human endothelial cells (HDMEC) on biodegradable scaffolds in the subcutaneous space of SCID mice. Once tumor reached an average volume of 500mm^3, the mice were treated by daily oral gavage with 50mg/kg MI-773 or a vehicle control. **B,** Graph depicting the average mouse weight

during the 6-day treatment sequence. **C,** Graph depicting the percentage of $ALDH^{high}CD44^{high}$ cells in MI-773 treated tumors. After 6 days of treatment, the tumors were resected and digested into a single cells suspension. The cells were then stained and FACS analyzed. **D,** Graph depicting the pixel density per field of sections stained for TUNEL in MI-773 or vehicle treated tumors. Seven fields at 200X were taken per tumor section and quantified using the ImageJ software. Error bars indicated the standard error of the mean. **E,** Immunohistochemistry and immunofluorescence analysis of MI-773 or vehicle treated tumors. Immunohistochemistry images were taken at 100x and the immunofluorescence images were taken at 200X.

Consistent with our previous results, UM-HMC-3B cells are resistant to MI-773 treatment.

Effect of MDM2/p53 binding inhibition by MI-773 on cancer stem cells in UM-HMC-3A cells *in-vivo*

To determine the therapeutic efficacy of MI-773 in reducing tumor volume and ablating cancer stem cells *in-vivo*, we co-implanted UM-HMC-3A cells with human endothelial cells (HDMEC) on a biodegradable scaffold in mice as previously described (30). Once the tumors reached an average volume of $500mm^3$, the mice were treated daily for six days with 50mg/kg MI-773 by oral gavage. After the six-day treatment cycle, we began to see a regression in tumor volume compared to the vehicle treated tumors (Figure IV.6A).To measure the presence of any toxic effects in the mice, we monitored the weight of the mouse with each treatment (Figure IV.6B). While the mouse weight in the treated group was slightly reduced during treatment, much of the weight loss was recovered by the end of treatment.

At day seven, the tumors were removed and digested into single cells suspensions for FACS analysis. After staining the cells for ALDH/CD44, we observed a reduction in the $ALDH^{high}CD44^{high}$ cancer stem cells population, consistent with our previous observation *in-vitro* (Figure IV.6C). To further validate this finding, tumor tissue sections were stained for ALDH/CD44. We also observed a reduction in the presence of

ALDH/CD44 positive cells (Figure IV.6E). Tissue sections were also stained for TUNEL to determine the number of cells undergoing apoptosis (Figure IV.6D and 6E). The pixel density of the images was quantitated using ImageJ and we observed a significant increase in the pixel density of the images in the MI-773 treated tumors when compared to the vehicle treated tumors (Figure IV.6D). Tumor tissue sections were also stained with p53 and MDM2 to determine if both proteins were upregulated upon activation of p53. In the MI-773 treated tumors compared to the vehicle treated tumors, we saw an increase in both p53 and MDM2 expression (Figure IV.6E).

To test whether a higher treatment dose of MI-773 would be more effective in reducing tumor volume and ablating cancer stem cells, we performed a second six-day *in-vivo* study administering 100mg/kg MI-773. Once again, 600,000 UM-HMC-3A cells were co-implanted with 400,000 HDMEC cells on biodegradable scaffolds and implanted subcutaneously in SCID mice. When the tumors reached an average volume of $500mm^3$, the mice were treated with 100mg/kg MI-773 by daily oral gavage for six days and tumor volume measurements were taken daily. Overall we observed a decrease in tumor volume in mice treated with MI-773 compared to vehicle treated tumors (Figure IV.7A). To assess any toxic effects, we measured the mouse weight daily and observed a slight decrease in MI-773 treated mouse weight (Figure IV.7B). After six days of treatment, the tumors were resected and tissue sections were stained for MDM2 and p53 to ensure that p53 was indeed activated upon treatment with MI-773.

Immunohistochemistry staining revealed an increase in expression of both MDM2 and p53 in MI-773 treated tumors compared to vehicle treated tumors

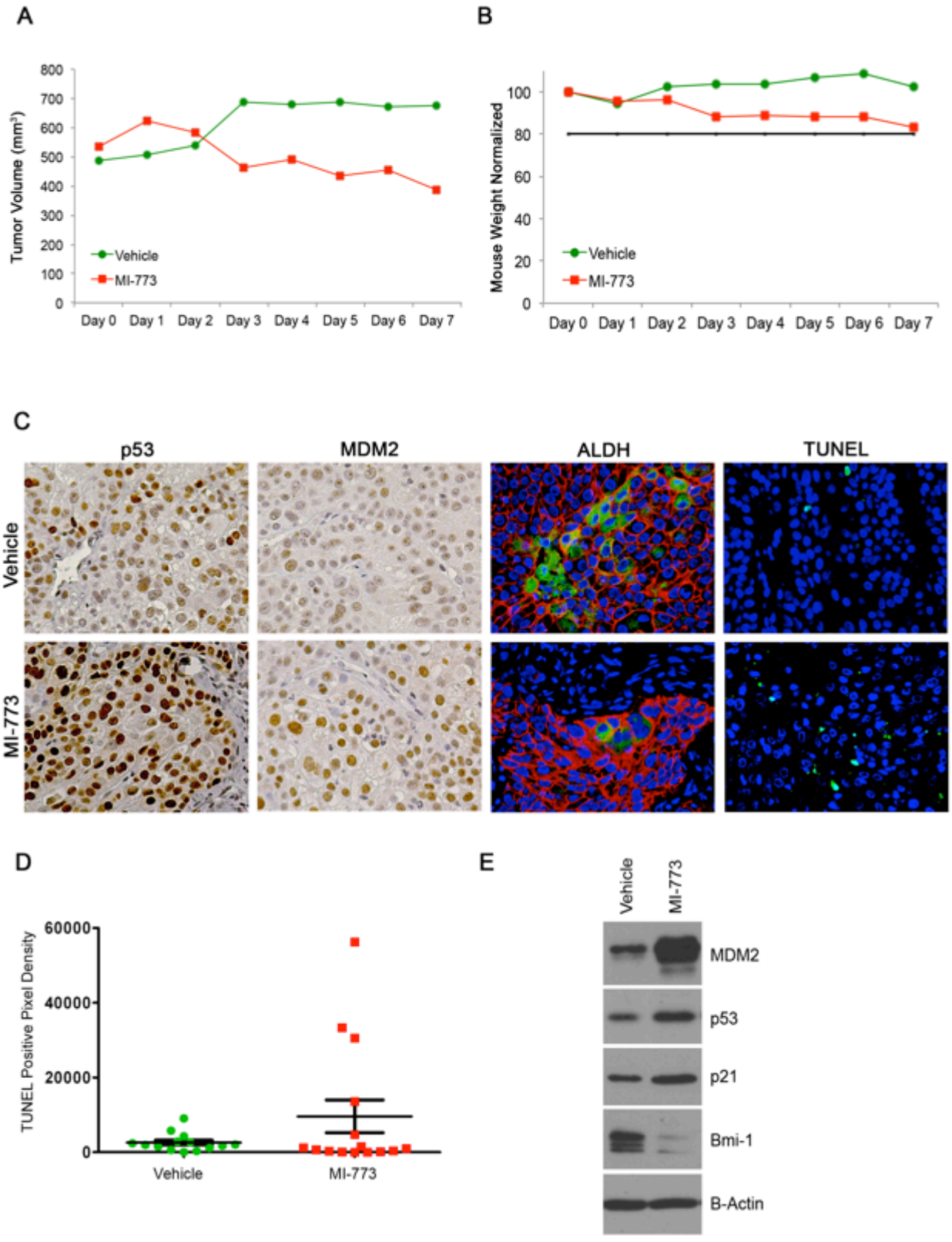
A
Tumor Volume (mm³)
800
700
600
500
400
300
200
100
0
Vehicle
MI-773
Day 0 Day 1 Day 2 Day 3 Day 4 Day 5 Day 6 Day 7
B
Mouse Weight Normalized
100
80
60
40
20
0
Vehicle
MI-773
Day 0 Day 1 Day 2 Day 3 Day 4 Day 5 Day 6 Day 7
C
p53
MDM2
ALDH
TUNEL
Vehicle
MI-773
D
TUNEL Positive Pixel Density
60000
40000
20000
0
Vehicle
MI-773
E
Vehicle
MI-773
MDM2
p53
p21
Bmi-1
B-Actin

Figure IV.7. Effect of 100mg/kg treatment of MI-773 on UM-HMC-3A cells. A, Graph depicting the tumor volume during 6 days of 100mg/kg treatment with MI-773. 600,000 UM-HMC-3A cells were co-implanted with 400,000 human endothelial cells (HDMEC) on biodegradable scaffolds in the subcutaneous space of SCID mice. Once tumor reached an average volume of 500mm^3, the mice were treated by daily oral gavage with 100mg/kg MI-773 or a vehicle control. **B,** Graph depicting the average mouse weight during the 6-day treatment sequence. **C,** Immunohistochemistry and immunofluorescence analysis of MI-773 or vehicle treated tumors. Immunohistochemistry and immunofluorescence images were taken at 200x. **D,** Graph depicting the pixel density per field of sections stained for TUNEL in MI-773 or vehicle treated tumors. Seven fields at 200X were taken per tumor section and quantified using the ImageJ software. Error bars indicated the standard error of the mean. **E,** Western blot analysis of MI-773 and vehicle treated tumors.

suggesting that p53 signaling was indeed activated (Figure IV.7C and 7E). We also observed an increased expression of p21 further confirming that p53 signaling pathways were indeed activated (Figure IV.7E). In addition to immunohistochemistry staining, we performed TUNEL staining to determine if 100mg/kg MI-773 was able to induce apoptosis in UM-HMC-3A tumors. Images of TUNEL staining showed an increased in the number of TUNEL positive cells in MI-773 treated tumors compared to vehicle treated tumors (Figure IV.7C). The pixel density of the images was quantitated and also showed an increase in the average pixel density per field in the treated versus control tumors (Figure IV.7D). Remaining tumor tissue was digested into a single cell suspension and stained for ALDH/CD44 to determine the percentage of cancer stem cells, however, no reduction was observed suggesting that this may be a dose dependent effect (data not shown). Immunofluorescence staining of ALDH/CD44 also revealed similar expression of both ALDH and CD44, however, western blot analysis does show a decreased expression of Bmi-1 suggesting some loss of stem cell associated functions (Figure IV.7C and 7E).

Overall our results confirm our findings *in-vivo* for UM-HMC-3A. We conclude that MI-773 is effective in reducing tumor volume and inducing p53 signaling thereby

initiating apoptosis in the UM-HMC-3A cells. We also conclude that MI-773 is an effective agent in reducing the cancer stem cell population in UM-HMC-3A cells when treated with low doses of the drug.

Effect of MDM2/p53 binding inhibition by MI-773 on cancer stem cells in UM-HMC-3B cells *in-vivo*

As the UM-HMC-3B cell line responded differently than the UM-HMC-3A cells *in-vitro* when treated with MI-773, we next sought to see if these results were consistent *in-vivo*. As UM-HMC-3B cells were so resistant to MI-773 *in-vitro*, we treated our *in-vivo* model with a higher treatment dose. Once again, we implanted 600,000 UM-HMC-3B cells with 400,000 HDMEC cells on biodegradable scaffolds and implanted them subcutaneously in SCID mice. We administered 100mg/kg MI-773 for six days by oral gavage. On the seventh day, the tumors were resected and analyzed. Overall, we saw little difference in tumor volume, again suggesting that these tumors are resistant to MI-773 treatments (Figure IV.8A). We monitored the mouse weight daily to identify any toxic effects but no decrease in mouse weight indicating that the mice tolerated the treatment (Figure IV.8B).

While there was little effect on overall tumor volume, we next were interested if the cancer stem cell population was affected despite the lack of tumor shrinkage. After the tumors were resected, we digested the tissue into a single cell suspension and stained for FACS analysis. Upon staining for ALDH activity and CD44 expression, we observed a drastic decrease in the $ALDH^{high}CD44^{high}$ cancer stem cell population in the MI-773 treated versus the vehicle treated (Figure IV.8C). We confirmed these results by ALDH/CD44 immunofluorescence staining in MI-773 treated tumors versus vehicle

treated tumors (Figure IV.8E). To determine if p53 was activated upon MI-773 treatment, we performed immunohistochemistry staining on drug treated and vehicle-

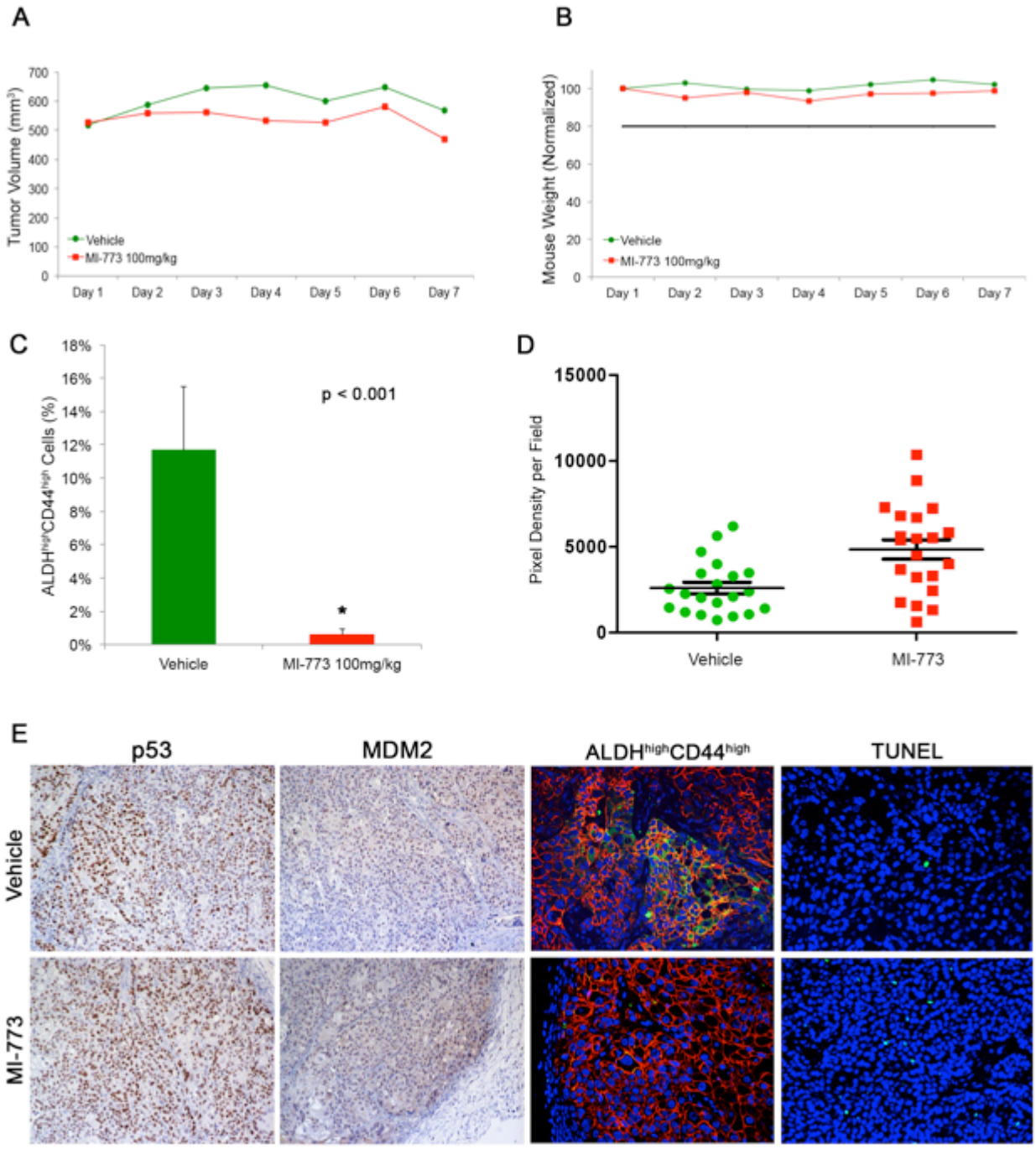

Figure IV.8. Effect of MDM2/p53 binding inhibition by MI-773 on cancer stem cells in UM-HMC-3B cells *in-vivo*. A, Graph depicting the tumor volume during 6 days of 100mg/kg treatment with MI-773. 600,000 UM-HMC-3B cells were co-implanted with 400,000 human endothelial cells (HDMEC) on biodegradable scaffolds in the subcutaneous space of SCID mice. Once tumor reached an average volume of 500mm^3, the mice were treated by daily oral

gavage with 100mg/kg MI-773 or a vehicle control. **B,** Graph depicting the average mouse weight during the 6-day treatment sequence. **C,** Graph depicting the percentage of $ALDH^{high}CD44^{high}$ cells in MI-773 treated tumors. After 6 days of treatment, the tumors were resected and digested into a single cells suspension. The cells were then stained and FACS analyzed. A t-test was used to test for significance. **D,** Graph depicting the pixel density per field of sections stained for TUNEL in MI-773 or vehicle treated tumors. Seven fields at 200X were taken per tumor section and quantified using the ImageJ software. Error bars indicated the standard error of the mean. **E,** Immunohistochemistry and immunofluorescence analysis of MI-773 or vehicle treated tumors. Immunohistochemistry images were taken at 100x and the immunofluorescence images were taken at 200X.

treated tumor sections and saw a slight increase in expression of both p53 and MDM2 (Figure IV.8E). To determine whether or not there was any induction of apoptosis in the tumors, we performed TUNEL staining and quantitated the images using ImageJ software. In the images, we observed an increased number of cells that were TUNEL-positive suggesting that MI-773 treatment induced apoptosis in UM-HMC-3B cells *in-vivo* (Figure IV.8D and 8E).Together these results suggest that MI-773 is a potent agent in reducing the cancer stem cells in UM-HMC-3B generated tumors. We also conclude that MI-773 is capable of inducing apoptosis of UM-HMC-3B.

To determine whether or not a higher dose of MI-773 would be more effective in reducing tumor volume, we implanted UM-HMC-3B cells as described above and treated the mice for 5 days with 200mg/kg MI-773 by daily oral gavage. After five days of treatment, the tumors were resected and analyzed. Over the five-day treatment cycle, we saw little reduction in overall tumor volume and saw a decrease in the MI-773-treated mouse weight suggesting the presence of toxic effects (Figure IV.9A and 9B). Interestingly we did see a greater accumulation of p53 and a decreased expression of G1 cell cycle associated proteins Cyclin A, Cyclin D1, Cyclin E, CDK2, CDK4, and CDK6 in the MI-773 treated tumors compared to the vehicle treated tumors

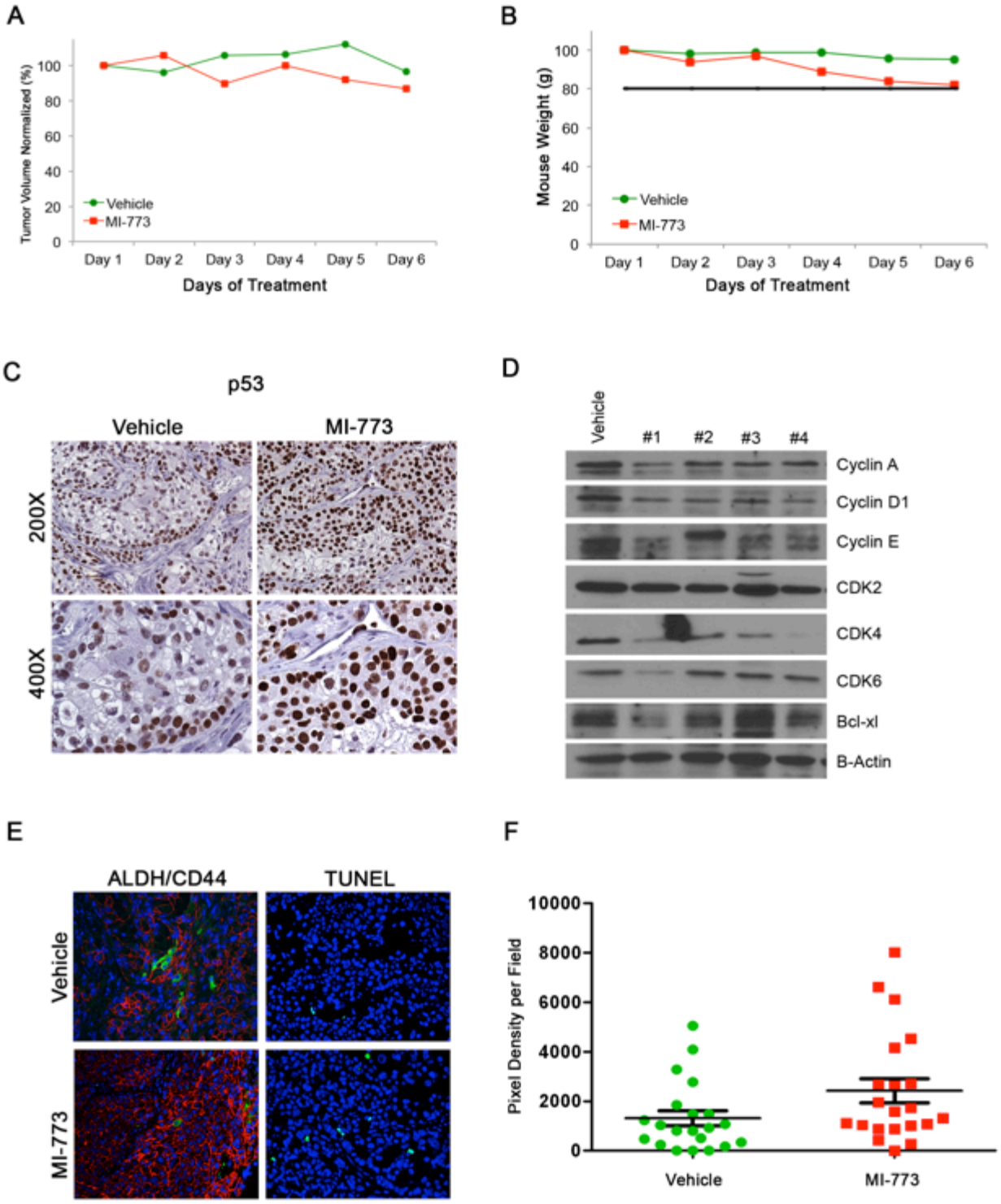

Figure IV.9. Effect of 200mg/kg treatment on UM-HMC-3B cells *in*-vivo. A, Graph depicting the tumor volume during 6 days of 100mg/kg treatment with MI-773. 600,000 UM-HMC-3A cells were co-implanted with 400,000 human endothelial cells (HDMEC) on biodegradable scaffolds in the subcutaneous space of SCID mice. Once tumor reached an average volume of 500mm^3, the mice were treated by daily oral gavage with 100mg/kg MI-773 or a vehicle control. **B,** Graph depicting the average mouse weight during the 6-day treatment sequence. **C,**

Immunohistochemistry staining for p53 in sections from the vehicle and MI-773 treated tumors. **D,** Western blot analysis of vehicle and MI-773 treated tumor tissues for G1 cells cycle-associated proteins. **E,** Immunofluorescence staining for ALDH/CD44 and TUNEL in vehicle and MI-773 treated tumors. **F,** Graph depicting the pixel density per field of sections stained for TUNEL in MI-773 or vehicle treated tumors. Seven fields at 200X were taken per tumor section and quantified using the ImageJ software. Error bars indicated the standard error of the mean.

(Figure IV.9C and 9D). These results suggest that we were able to activate p53 signaling and induce G1 cell cycle arrest in the tumors.

Once the tumor tissue were dissociated, we stained for ALDH activity and CD44 expression and saw a slight decrease in the $ALDH^{high}CD44^{high}$ population though the difference was not significant again suggesting that the effect on the cancer stem cell population is dose dependent (data not shown). We also performed immunofluorescence staining for ALDH/CD44 expression and once again observed a decrease in the number of $ALDH^{high}CD44^{high}$ cells (Figure IV.9E). To determine whether or not MI-773 treatment induced apoptosis, we performed TUNEL staining and quantitated the pixel density of the images. We did observe an increase in the number of TUNEL positive cells in the MI-773 treated tumors compared to the vehicle treated tumors (Figure IV.9E and 9F).

Together these results confirm our *in-vitro* findings that while UM-HMC-3B cells are more resistant to MI-773 treatment, this drug serves as an effective agent in reducing the cancer stem cells population. However, this effect appears to be more robust when mice are treated with lower doses of the drug. Interestingly, with 100mg/kg and 200mg/kg doses of MI-773 we did observe an induction of apoptosis suggesting the drug is more effective *in-vivo*.

Discussion

Resistance to chemotherapy and radiation treatments poses a clinical barrier to effectively treating patients with advanced stage mucoepidermoid carcinomas. Previous research indicates that cancer stem cells play a critical role in resistance to therapy and disease recurrence (12, 31-32). Studies from our laboratory identified cancer stem cells in salivary gland mucoepidermoid carcinoma (16). This aggressive subpopulation can be isolated using an $ALDH^{high}CD44^{high}$ marker combination. Importantly, we found that $ALDH^{high}CD44^{high}$ cells are uniquely tumorigenic compared to $ALDH^{low}CD44^{low}$ cells and are able to self renew and differentiate into non-cancer stem cells. Because of CSC resistance to treatment, novel therapies are needed to ablate this uniquely tumorigenic population of cancer stem cells. Already a great deal of research has been done in an effort to target stem cell associated pathways aiming to selectively eliminate the cancer stem cell population in other cancer types. Such pathways include Notch, Wnt, Hedgehog, IL-6, Her-2, and PI3K/AKT (33-36). For many of these pathways, lack of specific targeted agents poses a barrier to effective elimination of the cancer stem cell population.

Tumor-suppressor protein p53 plays a critical role in regulating the cell cycle and senescence as well as inducing apoptosis upon oncogenic stress. Importantly, research also suggests that p53 plays an important role in normal stem cell function by actively initiating or repressing several stem cell-associated proteins such as Nanog and Oct-4, making it an intriguing pathway to study in the context of cancer stem cells (37). Studies suggest that in the absence of p53, both normal and tumor cells acquire dedifferentiated phenotypes (20-25). MDM2, the main regulator of p53, functions as a E3 ubiquitin ligase

signaling p53 for degradation and can also bind p53 to block the transactivation domain of the protein. Inhibition of MDM2 binding to p53 prevents p53 degradation causing an accumulation of p53 in the cell. Many groups have sought to develop small molecule inhibitors to block MDM2/p53 binding interactions, however, most lack specificity to be effective therapeutically (38-42).

One promising molecule, MI-773, is significantly more specific and shows improved anti-tumor efficacy when compared to other MDM2 inhibitors (27). Upon treatment with MI-773 either *in-vitro* or *in-vivo*, Wang et al observed a significant induction of p53 signaling in a variety of different cancer types (27). Activation of p53 within these cells induced apoptosis, which in turn caused significant tumor shrinkage in *in-vivo* models (27). Importantly, in our studies, MI-773 showed significant therapeutic efficacy against both cancer stem cells and differentiated mucoepidermoid carcinoma cells. Upon treatment with low-dose MI-773, we observed a significant reduction of $ALDH^{high}CD44^{high}$ cancer stem cells in our HMC cells lines both *in-vitro* and *in-vivo*. Interesting, when we treated both $ALDH^{high}CD44^{high}$ and non-CSC cells with varying concentrations of MI-773, we saw no difference in the total cell density suggesting that the reduction in $ALDH^{high}CD44^{high}$ cells is due to differentiation rather then apoptosis or senescence. To further support this conclusion, we observed a drastic reduction in the self-renewal associated protein, Bmi-1, and a significant increase in differentiation-associated protein, p21.

In addition to inducing differentiation of cancer stem cells, our results show that MI-773 is able to induce both cell cycle arrest and apoptosis in the UM-HMC-1 and UM-HMC-3A cells *in-vivo* and *in-vitro* suggesting that this drug may be an efficacious

treatment for MEC patients. Interestingly, UM-HMC-3B cells were highly resistant to MI-773 induced apoptosis and cell cycle arrest but very susceptible to MI-773 ablation of the cancer stem cell population. A possible explanation is because MDM2 expression was higher in $ALDH^{high}CD44^{high}$ cells compared to non-CSC suggesting that the cancer stem cells may be more susceptible to MDM2 inhibition. Importantly, we also observed an increase in TUNEL-positive cells and a decrease in the expression of G1 cell cycle-associated proteins in our UM-HMC-3B *in-vivo* studies, suggesting that treatment with MI-773 could be more efficacious over longer time periods. In our mouse models, we co-implant the HMC cells with human endothelial cells to generate a supportive microenvironment. While outside the scope of this study, we hypothesize that some of the therapeutic effect in UM-HMC-3B cells upon treatment with MI-773 could also be due to the disruption of the vasculature within the tumors.

While little is known about the role of p53 and MDM2 in salivary gland mucoepidermoid carcinomas, several sequencing and immunohistochemistry studies suggest that p53 mutations and loss of heterozygosity are rare events (43-47). Interestingly, after performing PCR amplification and Sanger sequencing, we observed p53 mutations in our UM-HMC-1, UM-HMC-3A, and UM-HMC-3B cell lines. All three cell lines showed an A278P mutation which has also been seen in other cancer types. No studies have identified any functional deficiencies in p53 in cancer cells that have this mutation (48-49). UM-HMC-3A and UM-HMC-3B also showed a mutation at V157F, which studies suggest does structurally alter p53 (50). Interestingly, neither mutation occurs within the MDM2 binding region of p53. While MDM2 inhibitors were previously thought to be dependent on the presence of wild-type p53, studies suggest that MI-773

functions in cells containing mutant p53, depending on the mutation (28). In our experiments, UM-HMC-1 and UM-HMC-3A cells were susceptible to MI-773 treatment despite the presence of p53 mutations suggesting that the mutations are either non-interfering or that the mutations are heterozygous. Interestingly, while UM-HMC-3A and UM-HMC-3B cells have the same acquired mutations, only UM-HMC-3B cells were resistant, suggesting that UM-HMC-3B cells may have a homozygous mutation.

Collectively, this work demonstrates that inhibition of p53 and MDM2 binding effectively targets $ALDH^{high}CD44^{high}$ cancer stem cells in salivary gland mucoepidermoid carcinoma through activation of p53 and differentiation of the cells into non-cancer stem cells both *in-vitro* and *in-vivo*. Activation of p53 by inhibition of MDM2 binding also induces cells cycle arrest and apoptosis in mucoepidermoid carcinoma cells *in-vitro* and *in-vivo* leading to cell death and tumor shrinkage. These results suggests that patients with mucoepidermoid carcinomas may benefit from MDM2 inhibition therapies that target both the cancer stem cells and bulk cell populations.

References

1. Spiro RH. Salivary neoplasms: overview of a 35-year experience with 2807 patients. Head Neck Surg 1986;8:177–84.

2. Eversole LR, Sabes WR, Rovin S. Aggressive growth and neoplastic potential of odontogenic cysts: with special reference to central epidermoid and mucoepidermoid carcinomas. Cancer 1975;35:270–82.

3. Ezsias A, Sugar AW, Milling MA, Ashley KF. Central mucoepidermoid carcinoma in a child. J Oral Maxillofac Surg 1994;52:512–5.

4. Ellis GL, Auclair PL. Tumors of the salivary glands—Atlas of tumor pathology. In: Fascicle 17 Washington: Armed Forces Institute of, Pathology; 1996.

5. Gingell JC, Beckerman T, Levy BA, Snider LA. Central mucoepidermoid carcinoma. Review of the literature and report of a case associated with an apical periodontal cyst. Oral Surg Oral Med Oral Pathol 1984;57:436–40.

6. Ito FA, Ito K, Vargas PA, de Almeida OP, Lopes MA. Salivary gland tumors in a brazilian population: a retrospective study of 496 cases. Int J Oral Maxillofac Surg 2005;34:533–6.

7. Luna MA. Salivary mucoepidermoid carcinoma: revisited. Adv Anat Pathol 2006;13:293–307.

8. Pires FR, de Almeida OP, de Araujo VC, Kolawski LP. Prognostic factors in head and neck mucoepidermoid carcinoma. Arch Otolaryngol Head Neck Surg 2004;130:174–80.

9. Bell D, Holsinger CF, El-Naggar AK. CRTC1/MAML2 fusion transcript in central mucoepidermoid carcinoma of mandible–diagnostic and histogenetic implications. Ann Diagn Pathol 2010;14:396–401.

10. Chen AM, Granchi PJ, Garcia J, Bucci MK, Fu KK, Eisele DW. Local-regional recurrence after surgery without postoperative irradiation for carcinomas of the major salivary glands: impli- cations for adjuvant therapy. Int J Radiat Oncol Biol Phys 2007;67:982–7.

11. O'Neill ID. t(11;19) translocation and CRTC1–MAML2 fusion oncogene in mucoepidermoid carcinoma. Oral Oncol 2009;45:2–9.

12. Adams A, Warner K, Nör JE. Salivary gland cancer stem cells. Oral Oncol 2013;49:845-53.

13. Hambardzumyan D, Squatrito M, Holland EC. Radiation resistance and stem-like cells in brain tumors. Cancer Cell 2006;10:454-6.

14. Korkaya H, Paulson A, Charafe-Jauffret E, Ginestier C, Brown M, Dutcher J, et al. Regulation of mammary stem/progenitor cells by PTEN/Akt/beta- catenin signaling. PLoS Biol 2009; 7:e1000121.

15. Diehn M, Cho RW, Lobo NA, Kalisky T, Dorie MJ, Kulp AN, et al. Association of reactive oxygen species levels and radioresistance in cancer stem cells. Nature 2009;458:780-3.

16. Adams A, Warner K, Pearson AT, Zhang Z, Kim HS, Mochizuki D, et al. ALDH/CD44 identifies uniquely tumorigenic cancer stem cells in salivary gland mucoepidermoid carcinomas. Oncotarget 2015;6:26633-50.

17. Fridman JS, Lowe SW. Control of apoptosis by p53. Oncogene 2003;22:9030–40

18. Vogelstein B, Lane D, Levine AJ. Surfing the p53 network. Nature 2000;408:307–10

19. Vousden KH, Lu X. Live or let die: the cell's response to p53. Nat Rev Cancer 2000;2:594–604 .

20. Marión RM, Strati K, Li H, Murga M, Blanco R, Ortega S, et al. A p53-mediated DNA damage response limits reprogramming to ensure iPS cell genomic integrity. Nature 2009;460:1149-53.

21. Hong H, Takahashi K, Ichisaka T, Aoi T, Kanagawa O, Nakagawa M et al. Suppression of induced pluripotent stem cell generation by thep53-p21 pathway. Nature 2009;460:1132-5.

22. Utikal J, Polo JM, Stadtfeld M, Maherali N, Kulalert W, Walsh RM, et al. Immortalization eliminates a roadblock during cellular reprogramming into iPS cells. Nature 2009;460:1145-8.

23. Li H, Collado M, Villasante A, Strati K, Ortega S, Cañamero M, et al. The Ink4/Arf locus is a barrier for iPS cell reprogramming. Nature 2009;460:1136-9.

24. Kawamura T, Suzuki J, Wang YV, Menendez S, Morera LB, Raya A, et al. Linking the p53 tumour suppressor pathway to somatic cell reprogramming. Nature 2009;460:1140-4.

25. Tschaharganeh DF, Xue W, Calvisi DF, Evert M, Michurina TV, Dow LE, et al. p53-dependent Nestin regulation links tumor suppression to cellular plasticity in liver cancer. Cell 2014;158:579-92.

26. MomandJ, ZambettiGP. OlsonDC, GeorgeD, LevineAJ. Themdm-2 oncogene product forms a complex with the p53 protein and inhibits p53-mediated transactivation. Cell 1992;69:1237–45.

27. Wang S, Sun W, Zhao Y, McEachern D, Meaux I, Barrière C, et al. SAR405838: an

optimized inhibitor of MDM2-p53 interaction that induces complete and durable tumor regression. Cancer Res 2014;74:5855-65.

28. Hoffman-Luca CG, Yang CY, Lu J, Ziazadeh D, McEachern D, Debussche L, et al. Significant Differences in the Development of Acquired Resistance to the MDM2 Inhibitor SAR405838 between In Vitro and In Vivo Drug Treatment. PLoS One 2015;10:e0128807.

29. Warner KA, Adams A, Bernardi L, Nor C, Finkel KA, Zhang Z, et al. Characterization of tumorigenic cell lines from the recurrence and lymph node metastasis of a human salivary mucoepidermoid carcinoma. Oral Oncol 2013;49:1059-66.

30. Nör JE, Peters MC, Christensen JB, Sutorik MM, Linn S, Khan MK, Addison CL, Mooney DJ, Polverini PJ. Engineering and characterization of functional human microvessels in immunodef cient mice. Lab Invest 2001; 81: 453-463.

31. Hambardzumyan D, Squatrito M, Holland EC. Radiation resistance and stem-like cells in brain tumors. Cancer Cell 2006;10:454-6.

32. Shafee N, Smith CR, Wei S, Kim Y, Mills GB, Hortobagyi, et al. Cancer stem cells contribute to cisplatin resistance in Brca1/p53-mediated mouse mammary tumors. Cancer Res 2008;68:3243-50.

33. Takabe N, Harris PJ, Warren RQ, Ivy SP. Targeting cancer stem cells by inhibiting Wnt, Notch, and Hedgehog pathways. Nat Rev Clin Oncol 2011;8:97-106.

34. Krishnamurthy S, Warner KA, Dong Z, Imai A, Nör C, Ward BB, et al. Endothelial interleukin-6 de nes the tumorigenic potential of primary human cancer stem cells. Stem Cells 2014;32:2845-57.

35. Li X, Lewis MT, Huang J, Gutierrez C, Osborne CK, Wu MF, et al. Intrinsic resistance of tumorigenic breast cancer cells to chemotherapy. J Natl Cancer Inst 2008;100:672-9.

36. Kolev VN, Wright QG, Vidal CM, Ring JE, Shapiro IM, Ricono J, et al. PI3K/mTOR dual inhibitor VS-5584 preferentially targets cancer stem cells. Cancer Res 2015 ;75:446-55.

37. Kawamura T, Suzuki J, Wang YV, Menendez S, Morera LB, Raya A, et al. Linking the p53 tumour suppressor pathway to somatic cell reprogramming. Nature 2009;460:1140-4.

38. Vassilev LT, Vu BT, Graves B, Carvajal D, Podlaski F, Filipovic Z, et al. In vivo activation of the p53 pathway by small-molecule antagonists of MDM2. Science 2004;303:844–8.

39. Shangary S, Qin D, McEachern D, Liu M, Miller RS, Qiu S, et al. Temporal activation of p53 by a specific MDM2 inhibitor is selectively toxic to tumors and leads to complete tumor growth inhibition. Proc Natl Acad Sci U S A 2008;105:3933–8.

40. Vassilev LT. p53 Activation by small molecules: application in oncology. J Med Chem 2005;48:4491–9.

41. Vassilev LT. MDM2 inhibitors for cancer therapy. Trends Mol Med 2007;13:23–31.

42. Carry JC, Garcia-Echeverria C. Inhibitors of the p53/hdm2 protein-protein interaction- Path to the clinic. Bioorg Med Chem Letters 2013; 23:2480–5.

43. Gomes CC, Diniz MG, Orsine LA, Duarte AP, Fonseca-Silva T, Conn BI, et al. Assessment of TP53 mutations in benign and malignant salivary gland neoplasms. PLoS One 2012;7:e41261.

44. Augello C, Gregorio V, Bazan V, Cammareri P, Agnese V, Cascio S, et al. TP53 and p16INK4A, but not H-KI-Ras, are involved in tumorigenesis and progression of pleomorphic adenomas. J Cell Physiol 2006;207: 654–9.

45. Kishi M, Nakamura M, Nishimine M, Ikuta M, Kirita T, Konishi N. Genetic and epigenetic alteration profiles for multiple genes in salivary gland carcinomas. Oral Oncol 2005;41:161–9.

46. Kiyoshima T, Shima K, Kobayashi I, Matsuo K, Okamura K, Komatsu S, et al. Expression of p53 tumor suppressor gene in adenoid cystic and mucoepidermoid carcinomas of the salivary glands. Oral Oncol 2001;37:315–22.

47. Weber A, Langhanki L, Schutz A, Gerstner A, Bootz F, Wittekind C, et al. Expression profiles of p53, p63, and p73 in benign salivary gland tumors. Virchows Arch 2002;441:428–36.

48. Rehman A, Chahal MS, Tang X, Bruce JE, Pommier Y, Daoud SS. Proteomic identification of heat shock protein 90 as a candidate target for p53 mutation reactivation by PRIMA-1 in breast cancer cells. Breast Cancer Res 2005;7:R765-74.

49. Shi Y, Han Y, Xie F, Wang A, Feng X, Li N, et al. ASPP2 enhances oxaliplatin (L-OHP)-induced colorectal cancer cell apoptosis in a p53-independent manner by inhibiting cell autophagy. J Cell Mol Med 2015;19:535-43.

50. Calhoun S, Daggett V. Structural effects of the L145Q, V157F, and R282W cancer-associated mutations in the p53 DNA-binding core domain. Biochemistry 2011;50:5345-53.

CHAPTER V

Summary and Discussion

Introduction

Significant advancements have been made in the diagnosis and treatment of many types of cancer. While cancer still remains a significant clinical challenge worldwide, better therapies and diagnostic tools have helped reduce the impact of this disease. Sadly, little to no progress has been made in improving patient outcome of those diagnosed with salivary gland cancer. Importantly, salivary gland cancers are extremely heterogeneous and composed of many different subtypes making correct diagnosis of the tumor difficult. Due to the infrequency of salivary gland cancers and the difficulty in obtaining adequate research models, we have a poor understanding of the underlying biology that drives the persistent and relentless growth of these tumors.

Due to the generous donations of patients diagnosed with the most common from of salivary gland cancer, mucoepidermoid carcinoma, our laboratory has generated some of the first tumorigenic cell lines from tumor tissues resected from these patients (1). Using the cell lines, we have generated mouse xenograft models to better understand the biology of these tumors in an *in-vivo* model. Using these tools, we sought to better understand the biology driving the growth of aggressive and recurrent mucoepidermoid carcinomas. Below is summarized the chapters of this thesis detailing the observations and conclusions of our first projects studying mucoepidermoid

carcinoma. Chapter II consists of a review of the literature to give background for our overall hypothesis and specific aims found in chapters III and IV.

Summary of Chapters

CHAPTER II: The salivary glands play a critical role in the maintenance and function of the oral cavity. Both the major salivary and the minor salivary glands are essential for the lubrication and taste of food as well as proper speech. While rare, salivary gland tissue is susceptible to malignant cancerous growth. The most common form of salivary gland cancer, mucoepidermoid carcinoma, remains a significant threat to those who have been diagnosed (2). Of primary interest is the high level of recurrence seen within the patients and chemotherapy resistance of these tumors. Surgical resection and irradiation of less aggressive, low to intermediate-grade tumors is often successful. However, patients with aggressive high-grade tumors or patients with recurrent disease have few treatment options.

One hypothesis, the cancer stem cell hypothesis, has been used to explain the high rate of recurrence following chemotherapy and radiation treatments. Researchers have found a specific subpopulation of highly tumorigenic, stem-like cells that are not only capable of forming tumors using a low number of cells but also have the ability to differentiate and self-renew. These cancer stem cells are highly resistant to chemotherapy and radiation treatments.

Researchers identified cancer stem cell markers in head and neck squamous cell carcinoma using the ALDH/CD44 marker combination. Early studies identified both ALDH and CD44 individually as possible markers for cancer stem cells, however, combined sorting of $ALDH^{high}CD44^{high}$ staining cells isolated cells capable of forming

tumors in mice with as few as 1,000 cells whereas 10,000 $ALDH^{low}CD44^{low}$ cells were needed to form tumors (3). Importantly, studies have shown that $ALDH^{high}CD44^{high}$ cancer stem cells resided in perivascular niches rich in blood vessels and were supported by the surrounding endothelial cells.

Little research has been done to identify and isolate cancer stem cells in salivary gland mucoepidermoid carcinoma. However, researchers were able to isolate cancer stem cells in adenoid cystic carcinoma using high ALDH activity (4). $ALDH^{high}$ cells showed an increased ability to form spheres under low-attachment, serum-free conditions. As few as 100 $ALDH^{high}$ cells were capable of forming tumors *in-vivo* suggesting that this is indeed a population of cancer stem cells. Research is still needed to identify this population of cells in mucoepidermoid carcinoma.

Chapter III: To determine whether or not cancer stem cells exist within mucoepidermoid carcinoma, we first sought to determine the expression patterns of commonly used cancer stem cell markers (ALDH, CD10, CD24, CD44) in mucoepidermoid carcinoma patient samples using immunofluorescence imaging. We observed that ALDH and CD44 showed positive staining in almost all samples while CD10 and CD24 staining was variable. When normal salivary gland tissue was compared to less aggressive cystic and more aggressive solid tumor, we observed an increase in expression of all four markers suggesting that these proteins are associated with more aggressive disease.

To begin to functionally analyze these markers as stem cell markers, sorted UM-HMC-3A and UM-HMC-3B cells into ALDH/CD44, CD10/CD24, CD44/CD24, and CD10/CD24 and plated the different subpopulations in low-attachment, serum-free

conditions. We observed robust sphere formation in the $ALDH^{high}CD44^{high}$ cell population compared to the $ALDH^{low}CD44^{low}$ cells in both cell lines. Specific subpopulations of CD10/CD24, CD44/CD24, and CD10/CD24 sorted cells formed more salispheres, however, the outgrowing population was not the same between the two cell lines tested.

To determine the tumorigenic potential of the different subpopulations in the four marker combinations, we sorted UM-HMC-3A and UM-HMC-3B cells for $ALDH^{high}CD44^{high}$ and $ALDH^{low}CD44^{low}$ and implanted them *in-vivo*. Overall, we were able to generate tumors in 18 of the 36 scaffold implanted with 400 $ALDH^{high}CD44^{high}$ cells and only 1 of the 36 scaffolds implanted with 4,000 $ALDH^{low}CD44^{low}$ cells. Importantly, mice implanted with 5,000 $ALDH^{high}CD44^{high}$ cells reached palpability more quickly and grew tumors significantly faster then mice implanted with $ALDH^{low}CD44^{low}$ cells.

While cells sorted for CD10/CD24 and CD10/CD44 showed little tumorigenic potential in our mouse models, cells sorted for the four different CD44/CD24 subpopulations did show significant differences in tumorigenicity *in-vivo*. However, the differences observed were not repeatable in low-passage versus high-passage xenograft models suggesting that this marker combination does not identify and isolate a cancer stem cell population.

Together we conclude that $ALDH^{high}CD44^{high}$ marker combination identifies a population of cancer stem cells capable of self-renewal and differentiation as well as high tumorigenic potential.

CHAPTER IV: To determine if p53 plays a role in cancer stem cell biology and to determine if MDM2 inhibition is effective in therapeutically ablating the aggressive $ALDH^{high}CD44^{high}$ cancer stem cells, we treated UM-HMC-1, UM-HMC-3A, and UM-HMC-3B cells with 1uM MI-773 to bind MDM2 and prevent inhibition of p53 functioning in the cell. Upon 48, 72, and 96-hour treatments with MI-773, we observed a drastic reduction of $ALDH^{high}CD44^{high}$ cancer stem cells upon FACS analysis. Interestingly, when HMC cells were sorted for CSC and non-CSC then treated with MI-773, we observed no difference in the total number of CSC and non-CSC treated cells. This suggests that MI-773 primarily acts by causing differentiation of the $ALDH^{high}CD44^{high}$ cells rather than preferentially inducing apoptosis in the CSC versus non-CSC.

Importantly, treatment of HMC cells with MI-773 increased expression of p53, MDM2, and p21 indicating that p53 signaling is indeed activated. We also observed a dramatic decrease in Bmi-1 expression again indicating that activation the p53 reduces the stemness of the treated cells. In addition to activating p53 signaling and reducing the cancer stem cell population, we also observed an induction of cell cycle arrest and apoptosis in HMC cells *in-vitro* when treated with varying concentrations of MI-773.

To determine whether MI-773 treatment is effective in ablating cancer stem cells *in-vivo* we implanted UM-HMC-3A and UM-HMC-3B cells and treated the tumors with 50mg/kg or 100mg/kg respectively. Following six days of treatment, the tumors were excised and digested for FACS analysis. When compared to vehicle treated tumors, MI-773 treated tumors showed a dramatic reduction in the percentage of $ALDH^{high}CD44^{high}$ cancer stem cells, similar to the results we observed *in-vitro*. We also observed an increase in the number of TUNEL positive cells suggesting that MI-773 is also capable

of inducing apoptosis of HMC cells *in-vivo* through an activation of p53 signaling by the increase in expression of both MDM2 and p53.

Together, we conclude that MDM2 and p53 play a critical role in cancer stem cell biology. We also conclude that therapeutic inhibition of MDM2 binding to p53 is not only effective in inducing apoptosis and cell cycle arrest, but also in ablating cancer stem cells from the tumor both *in-vitro* and *in-vivo*.

Future Directions

While the research presented here elucidates some of the biology important to the growth of salivary gland mucoepidermoid carcinomas, many questions concerning pathobiology of this cancer type remain. Further research will be critical to bettering the outcome of patients diagnosed with this cancer, of particular interest is better understanding of $ALDH^{high}CD44^{high}$ cancer stem-like cells. While p53 appears to play an important role in inducing differentiation, other stem cell pathways such as PI3K/AKT also play an important role in mucoepidermoid carcinoma (5). Interestingly, we found this pathway to be activated in HMC cancer stem cells. Therapeutic targeting of these pathways could also be potentially effective in reducing cancer stem cells.

In our studies presented here, we identified p53 as an important protein in decreasing the $ALDH^{high}CD44^{high}$ cancer stem cells. While preliminary studies lead us to believe that this effect is due to p53 induced differentiation, further mechanistic investigation of p53 in MEC cancer stem cells is needed in order to more fully understand the role of p53 in cancer stem cell biology.

The primary purpose of studying the drug MI-773 was to observe the effect of MDM2 inhibition directly on the mucoepidermoid carcinoma cells. However, MDM2

inhibition could also have a drastic effect on the cells surrounding and supporting the cancer cells within the tumor. Tumors contain a heterogeneous population of cells that create a supportive microenvironment for the cancer cells to grow in. In our mouse models, we co-implanted HMC cancer cells with human endothelial cells to replicate the perivascular niche within tumors. As endothelial cells express wild-type p53 and MDM2, MI-773 could also be inducing apoptosis in these human and mouse endothelial cells thereby destroying the blood supply to the tumor environment.

Final Remarks

The cancer stem cell hypothesis was proposed many years ago, however, only within the last 15 years have we begun to identify and functionally characterize these cells (6-7). While most accept the concept of tumor heterogeneity, many do not believe stem cells to be the origin of cancer growth or that tumors grow in a hierarchical manner. Small populations of cancer stem cells have been identified in many solid malignancies, however, several have suggested that the use of immunodeficient mice and consequent lack of a human microenvironment is responsible for the difference in growth and tumor initiation (8-10). A previous study compared the growth of melanoma cells in NOD/SCID mice versus NOG mice and found that while only one in 100,000 cells were able to generate a tumor in the NOD/SCID mice while one in four cells was able to generate a tumor in the NOG mice suggesting that differences in surrounding microenvironment have a profound impact on the growth of the human cells (10). Unfortunately, full replication of the human microenviroment within a mouse model is complex. In our studies here, we co-implanted HMC cells with human endothelial cells

to create a more human derived microenvironment, however, we acknowledge that this is also a limitation of our study.

Another point of controversy within the cancer stem cell hypothesis is whether the cancer stem cells arise from actual tissue specific stem cells (11). The slow rate of division and longevity of stem cells within a tissue could lead to the accumulation of mutations, however, stem cells as the origin of cancer has not yet been definitively shown. It is important to note, that studies within this field do not directly identify the cell of origin within the different cancer types but instead remain a characterization of the heterogeneous growth of cancer cells within a particular population. In our studies, we do conclude that our identified cancer stem cells possess the properties of self-renewing and multipotency, however, we do not assert that the $ALDH^{high}CD44^{high}$ cells are derived from an actual salivary gland stem cell. While direct definition and categorization of these cells is still elusive, we maintain that overcoming cancer stem cell resistance to traditional therapies by targeting self-renewal and differentiation pathways remains an important area of study regardless of whether or not the cells are truly stem cells.

Collectively, this work demonstrates that salivary gland mucoepidermoid carcinomas exhibit a small sub-population of cells with uniquely high tumorigenic potential. These cells can be identified by high ALDH activity and CD44 expression. This work also demonstrates that inhibition of p53 and MDM2 binding effectively targets $ALDH^{high}CD44^{high}$ cancer stem cells in salivary gland mucoepidermoid carcinoma through activation of p53 and differentiation of the cells into non-cancer stem cells both *in-vitro* and *in-vivo*. Activation of p53 by inhibition of MDM2 binding also induces cells

cycle arrest and apoptosis in mucoepidermoid carcinoma cells *in-vitro* and *in-vivo* leading to cell death and tumor shrinkage. These results suggests that cancer stem cells play an important role in mucoepidermoid carcinoma and that patients with mucoepidermoid carcinomas may benefit from MDM2 inhibition therapies that target both the cancer stem cells and non-cancer stem cell populations.

References

1. Warner KA, Adams A, Bernardi L, Nor C, Finkel KA, Zhang Z, et al. Characterization of tumorigenic cell lines from the recurrence and lymph node metastasis of a human salivary mucoepidermoid carcinoma. Oral Oncol. 2013;49:1059-66.

2. Spiro RH. Salivary neoplasms: overview of a 35-year experience with 2807 patients. Head Neck Surg. 1986;8:177–84.

3. Krishnamurthy S, Dong Z, Vodopyanov D, Imai A, Helman JI, Prince ME, et al. Endothelial cell-initiated signaling promotes the survival and self-renewal of cancer stem cells. Cancer Res 2010;70:9969-78.

4. Sun S, Wang Z. ALDH high adenoid cystic carcinoma cells display cancer stem cell properties and are responsible for mediating metastasis. Biochem Biophys Res Commun. 2010;396:843-8.

5. Suzuki S, Dobashi Y, Minato H, Tajiri R, Yoshizaki T, Ooi A. EGFR and HER2-Akt-mTOR signaling pathways are activated in subgroups of salivary gland carcinomas. Virchows Arch. 2012;461:271-82.

6. Cohnheim J. Ueber entzundung und eiterung. Path Anat Physiol Kiln Med 1867;40:1–79.

7. Durante F. Nesso fisio-pathologico tra la struttura dei nei materni e la genesi di alcuni tumori maligni. Arch Memor Observ Chir Pract 1874;11:217-26.

8. Jones RJ. Controversies in cancer stem cells. J Mol Med (Berl). 2009 Nov;87:1077-8.

9. Kelly PN, Dakic A, Adams JM, Nutt SL, Strasser A. Tumor growth need not be driven by rare cancer stem cells. Science. 2007;317:337.

10. Quintana E, Shackleton M, Sabel MS, Fullen DR, Johnson TM, Morrison SJ. Efficient tumour formation by single human melanoma cells. Nature. 2008;456:593–8.

11. Gupta PB, Chaffer CL, Weinberg RA. Cancer stem cells: mirage or reality? Nat Med. 2009;15:1010-2.